doi: **10.12029/gc20160401**

夏林圻, 李向民, 余吉远, 等. 祁连山新元古代中—晚期至早古生代火山作用与构造演化[J]. 中国地质, 2016, 43(4): 1087−1138.

Xia Linqi, Li Xiangmin, Yu Jiyuan, et al. Mid−Late Neoproterozoic to Early Paleozoic volcanism and tectonic evolution of the Qilian Mountain[J]. Geology in China, 2016, 43(4): 1087−1138(in Chinese with English abstract).

祁连山新元古代中—晚期至早古生代火山作用与构造演化

夏林圻 李向民 余吉远 王国强

(中国地质调查局西安地质矿产研究所, 陕西 西安 710054)

提要: 祁连山地区的新元古代中—晚期至早古生代火山作用显示系统地时、空变化, 其乃是祁连山构造演化的火山响应。随着祁连山构造演化从Rodinia超大陆裂谷化—裂解, 经早古生代大洋打开、扩张、洋壳俯冲和弧后伸展, 直至洋盆闭合、弧−陆碰撞和陆−陆碰撞, 火山作用也逐渐从裂谷和大陆溢流玄武质喷发, 经大洋中脊型、岛弧和弧后盆地火山活动, 转变为碰撞后裂谷式喷发。850~604 Ma的大陆裂谷和大陆溢流熔岩主要分布于祁连和柴达木陆块。从大约550 Ma至446 Ma, 在北祁连和南祁连洋−沟−弧−盆系中广泛发育大洋中脊型、岛弧和弧后盆地型熔岩。与此同时, 在祁连陆块中部, 发育约522~442 Ma的陆内裂谷火山作用。早古生代洋盆于奥陶纪末(约446 Ma)闭合。随后, 从约445 Ma至约428 Ma, 于祁连陆块北缘发育碰撞后火山活动。此种时−空变异对形成祁连山的深部地球动力学过程提供了重要约束。该过程包括: (1)地幔柱或超级地幔柱上涌, 导致Rodinia超大陆发生裂谷化、裂解、早古生代大洋打开、扩张、俯冲, 并伴随岛弧形成; (2)俯冲的大洋板片回转, 致使弧后伸展, 进而形成弧后盆地; (3)洋盆闭合、板片断离, 继而发生软流圈上涌, 诱发碰撞后火山活动。晚志留世至早泥盆世(420~400 Ma), 先期俯冲的地壳物质折返, 发生强烈的造山活动。400 Ma后, 山体垮塌、岩石圈伸展, 相应发生碰撞后花岗质侵入活动。

关 键 词: 祁连山; 俯冲和碰撞; 新元古代中—晚期至早古生代火山作用; 大陆裂谷; 洋中脊玄武岩; 弧和弧后盆地; 构造演化

中图分类号: P511.3;P542.1 **文献标志码**: A **文章编号**: 1000−3657(2016)04−1087−52

Mid−Late Neoproterozoic to Early Paleozoic volcanism and tectonic evolution of the Qilian Mountain

XIA Lin−qi, LI Xiang−min, YU Ji−yuan, WANG Guo−qiang

(*Xi'an Institute of Geology and Mineral Resources, China Geological Survey, Xi'an* 710054*, Shaanxi, China*)

Abstract: Mid−Late Neoproterozoic to Early Paleozoic volcanism in the Qilian Mountain area, which shows systematic variations in space and time, seems to have been the volcanic response to the tectonic evolution of the Qilian Mountain. The volcanism gradually changed from rift−related and continental flood basaltic through MORB−type and island−arc and back−arc to post−

收稿日期:2016−05−09;**改回日期**:2016−06−06

基金项目:中国地质调查局综合研究项目(121201120133, 12120115070601, 12120101100015004)资助。

作者简介:夏林圻,男,1942年生,博士,研究员,博士生导师,主要研究方向:区域火山岩石学与地球动力学;E−mail: xlinqi@cgs.cn。

collisional rift−related eruptions along with the tectonic evolution of the Qilian Mountain shifting from rifting and break−up of Rodinia through opening and spreading of the Early Paleozoic oceans, subduction of the oceanic slabs and back−arc extension and ocean closure to arc−continent and continent−continent collision. The continental rift−related and flood lavas with ages of 850−604 Ma are distributed mainly on the Qilian and Qaidam Blocks. The widespread MORB−type and "island−arc−backarc"−type lavas were generated from about 550 to 446 Ma in both the North Qilian and the South Qilian ocean−trench−arc−basin systems. In the meantime, the intracontinental rift−related volcanism occurred in the central Qilian Block between about 522 and 442 Ma. The Early Paleozoic oceanic basins were closed at the end of Ordovician (about 446 Ma). Subsequent post−collisional volcanism occurred on the northern margin of the Qilian Block from about 445 to 428 Ma. Such spatial−temporal variations provide important constraints on the geodynamic processes that evolved at the depth to form the Qilian Mountain. These processes involved (1) upwelling of mantle plumes or a mantle superplume and subsequent rifting and break−up of Rodinia and subsequent opening, spreading and subduction of Early Paleozoic oceans followed by island−arc formation, (2) roll−back of the subducted oceanic slabs followed by back−arc extension and back−arc basin formation, (3) ocean closure and slab break−off followed by upwelling of asthenosphere and post−collisional volcanism. Intensive orogenic activities occurred in the Late Silurian and Early Devonian (about 420 to about 400 Ma) in response to the exhumation of the subducted crustal materials. Mountain collapse and lithosphere extension happened and formed post−collisional granitic intrusions at < 400 Ma.

Key words: Qilian Mountain; subduction and collision; Mid−Late Neoproterozoic to Early Paleozoic volcanism; continental rift; mid−ocean ridge basalt; arc and back−arc basin; tectonic evolution

About the first author: XIA Lin−Qi, male, born in 1942, doctor, professor; senior researcher, supervisor of doctor candidates, engages in the study of regional volcanic petrology and geodynamics; E−mail: xlinqi@cgs.cn.

Fund support: Supported by China Geological Survey Program (No. 121201120133, 12120115070601, 12120101100015004).

1 引 言

近年来, 有关地球上超大陆生长、演化和离散的历史, 尤其是大陆块汇聚和离散对于地幔动力学、岩浆作用、成矿作用、地表过程和生命演化的影响, 已经受到了极大地关注[1−3]。Rodinia超大陆在新元古代晚期碎裂, 尔后, 在早古生代末至晚古生代, 碎裂的陆块又逐渐地拼合到劳亚古陆(即古亚洲)[4], 该过程显示了一个全球性的Rodinia超大陆旋回。此超大陆旋回期地质事件也广泛地发育于中国的一个复合造山系之中, 这个造山系被称作"中央造山带"[5]。该复合造山系沿着中国的中央山链(包括昆仑山、祁连山和秦岭—大别山)自西向东延伸近5000 km(图1)。

祁连山在地理上位于中国中央山链的中部, 在地质构造上, 祁连山则是位于中国的3个主要构造块体(即华北克拉通、华南陆块和塔里木克拉通)之间的中心区域(图1), 这种格局限定了中国大陆的主体构造格架。祁连山在构造上是一个早古生代造山系, 自北向南, 由北祁连造山带、祁连陆块和柴北缘高压(HP)—超高压(UHP)变质带组成(图1)。该造山系的北、东、南部分别以阿拉善陆块、华北克拉通和柴达木陆块为界(图1)。其北西方向, 为世界上最大的走滑断裂系之一——阿尔金断裂系水平错断(图1)。

迄今为止, 对于古生代时期祁连山的构造演化已提出过若干种不同的假说。第一种意见认为: 北祁连造山带和柴北缘高压—超高压变质带是2个分别位于阿拉善陆块和祁连陆块之间、祁连陆块和柴达木陆块之间相互独立的俯冲带[6−8]。第二种意见推断: 北祁连俯冲带和柴北缘高压—超高压变质带是同一俯冲带中, 一种从大洋俯冲到大陆俯冲连续过程的产物, 并认为大洋型(即北祁连俯冲带)和大陆型(即柴北缘高压−超高压变质带)俯冲带最终没有被耦合在同一个构造带中, 是因为俯冲的洋壳和俯冲的陆壳具有不同的折返路径和折返机制[9, 10]。因此, 第二种意见推断, 柴北缘高压—超高压变质带并不是2个重要大陆块体的汇聚带[11]。此外, Gehrels et al. [12]还曾针对青藏高原北部早古生代构造演化, 提出过5种可能的模式。

由图2、图3和图4可见, 介于(北部)阿拉善陆块和(南部)祁连陆块间的北祁连造山带, 自南向北, 由仰冲的新元古代晚期—寒武纪(550~497 Ma, 表1)洋壳残片(蛇绿岩套, 代表了北祁连洋盆的残骸)、俯冲杂岩带(包括有高压变质岩(含有榴辉岩的蓝片岩, 表2)和混杂岩)、中寒武世—奥陶纪(503~446 Ma)弧

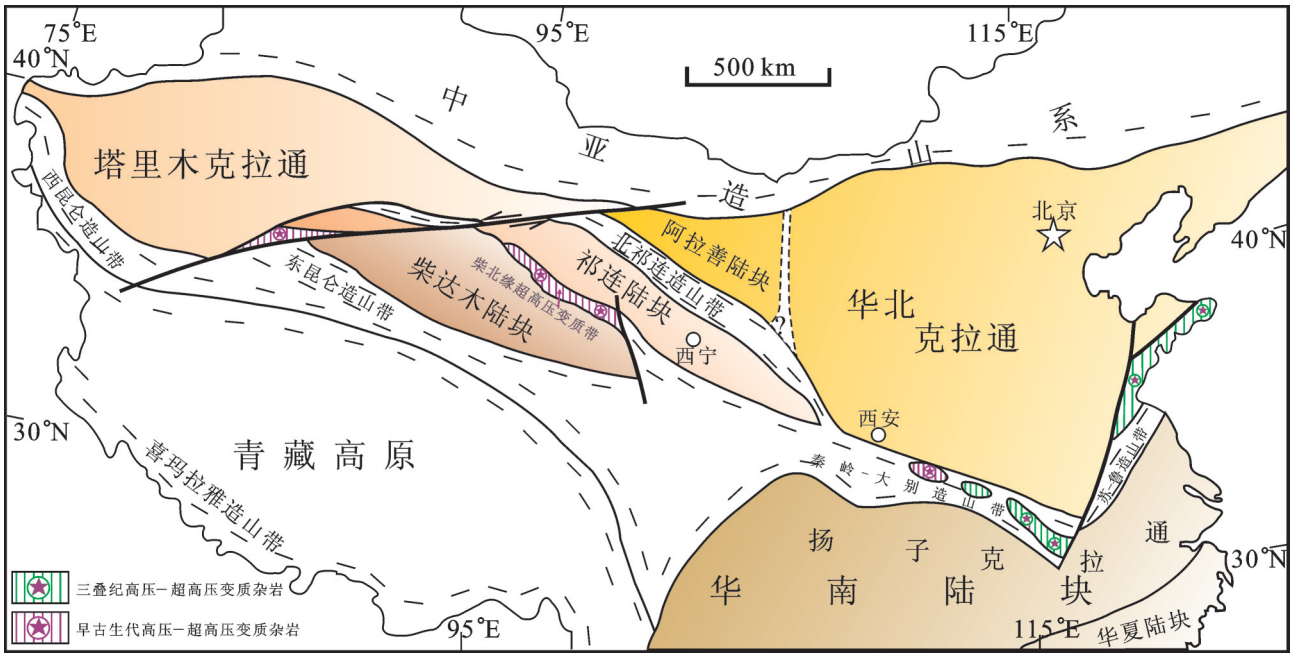

图1 中国大地构造格架简图(示主要前寒武纪克拉通、陆块和显生宙造山带)

Fig. 1 Tectonic framework of China illustrating the major Precambrian cratons and blocks and younger orogens

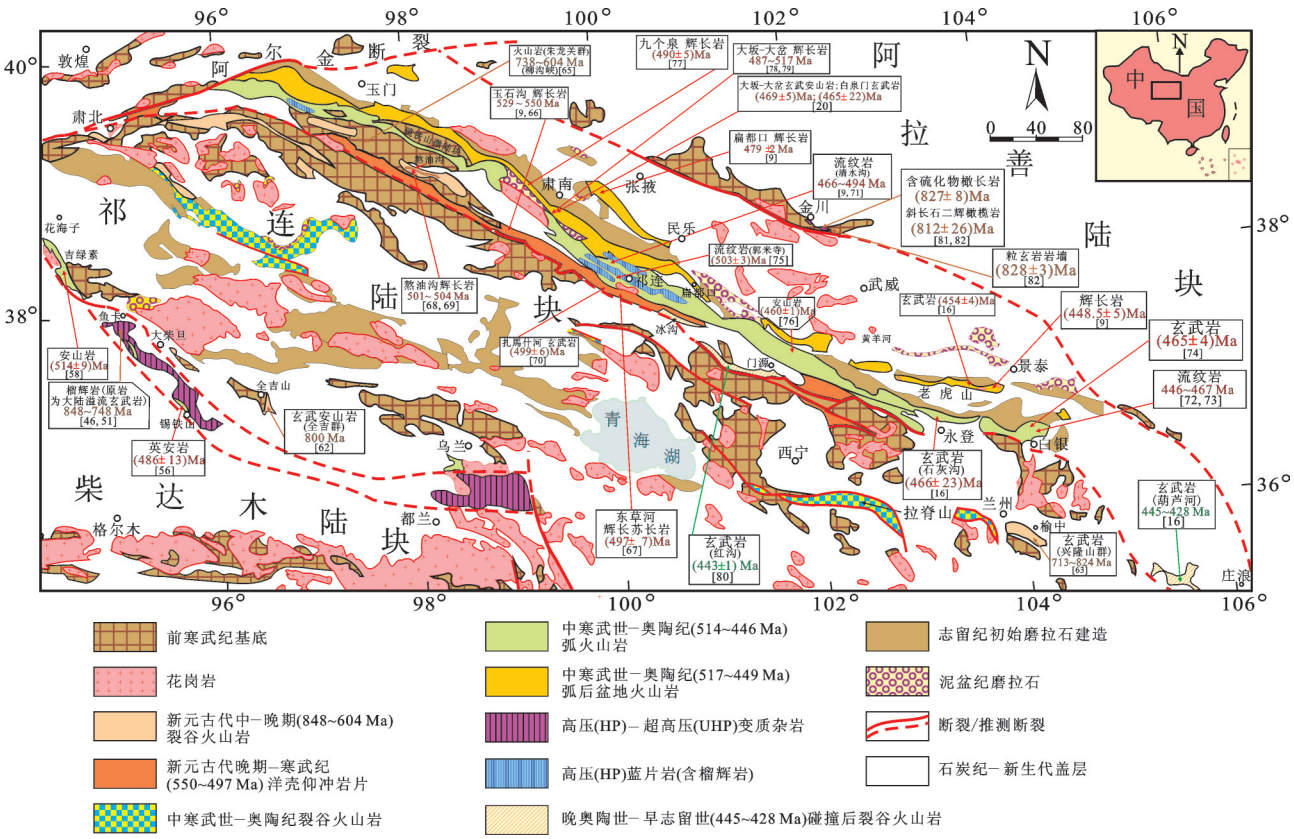

图2 祁连山地质略图 (兼示主要火山岩带位置及其年龄)

Fig. 2 Geological sketch map of the Qilian Mountain with localities of major volcanic rocks and their ages

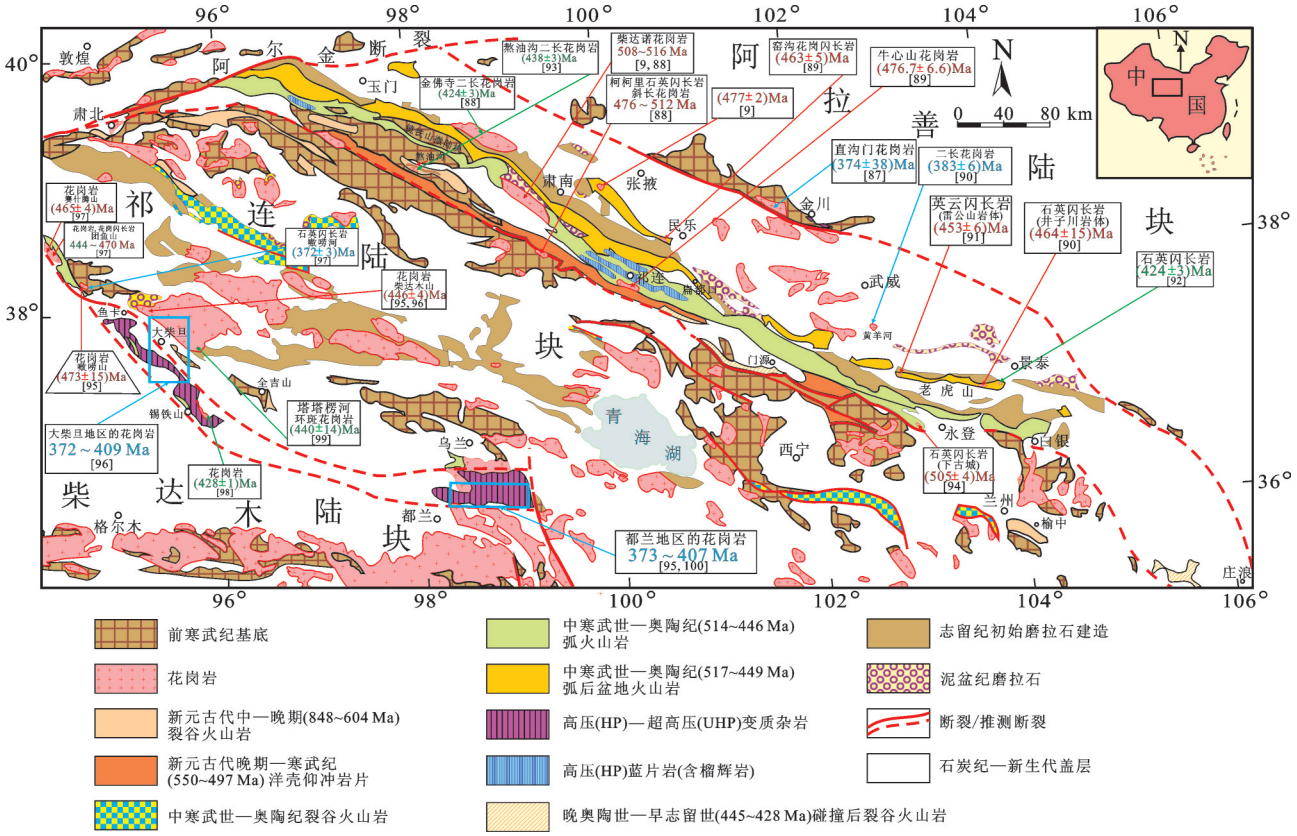

图3 祁连山地质略图 (兼示主要花岗岩体及其年龄)

Fig. 3 Geological sketch map of the Qilian Mountain, showing major granitic plutons and their ages

火山岩和花岗岩带(表1,表3)、中寒武世—奥陶纪(517~449 Ma)弧后盆地火山岩和花岗岩带(表1,表3)、志留纪初始磨拉石建造和泥盆纪磨拉石构成。

上述北祁连造山带中的早古生代洋-沟-弧-盆体系分布态势和向南-南西方向逆冲的韧性剪切构造暗示: 北祁连早古生代洋盆是向北—北东方向俯冲到阿拉善陆块之下[6-8, 11, 13-19, 20-22]。

自20世纪90年代以来, 许多研究者对于祁连陆块和柴达木陆块间鱼卡—大柴旦—锡铁山—都兰地区所发育的柴北缘高压—超高压变质带已进行了大量卓有成效的研究工作[6, 7, 10, 11, 23-55] (图2~图4)。该高压—超高压变质带主要由花岗质片麻岩和粗屑/泥质片麻岩构成, 它们的原岩岩性为大陆壳岩石, 上述片麻岩中常夹含有数量不等的榴辉岩和超镁铁岩质岩石的岩块。片麻岩、榴辉岩和超镁铁质岩石中所含锆石的定年研究揭示, 这些岩石曾经受了早期(476~445 Ma)柯石英稳定域之下的高压变质作用和晚期(440~421 Ma)超高压变质作用(T= 630~790°C; P= 2.3~3.2 GPa (相当于76~106 km深处的静岩压力))。前者的锆石中含有石榴子石-绿辉石-金红石-石英包裹体, 后者表现为锆石中含有柯石英和金刚石(表4; 详情读者可参阅Song et al. [10]及其参考文献)。此外, 新近的一些研究[31, 32, 36, 39, 40, 44, 55]报道: 在该高压—超高压变质带中, 产出有一些受到超高压变质的蛇绿岩岩块, 包括: 蛇纹石化方辉橄榄岩、条带状超镁铁质到辉长质堆晶岩(包括有橄榄石辉石岩、石榴子石辉石岩和蓝晶石榴辉岩)和原岩岩性为MORB(洋脊玄武岩)的榴辉岩。辉长质蓝晶石榴辉岩的原岩结晶年龄为550~500 Ma[39, 40]。这些受到超高压变质的蛇绿岩岩块代表了大陆俯冲之前先期俯冲的南祁连洋盆的残骸。柴北缘高压—超高压变质带应当是代表了被折返保存下来的早期俯冲洋壳和晚期俯冲陆壳。因此, 前述475 Ma到445 Ma的早期高压变质阶段可以被解释成是大洋俯冲的时间, 而440 Ma到421 Ma的晚期超高压变质阶段则是大陆俯冲的时间。所以, 柴北缘高压—超高

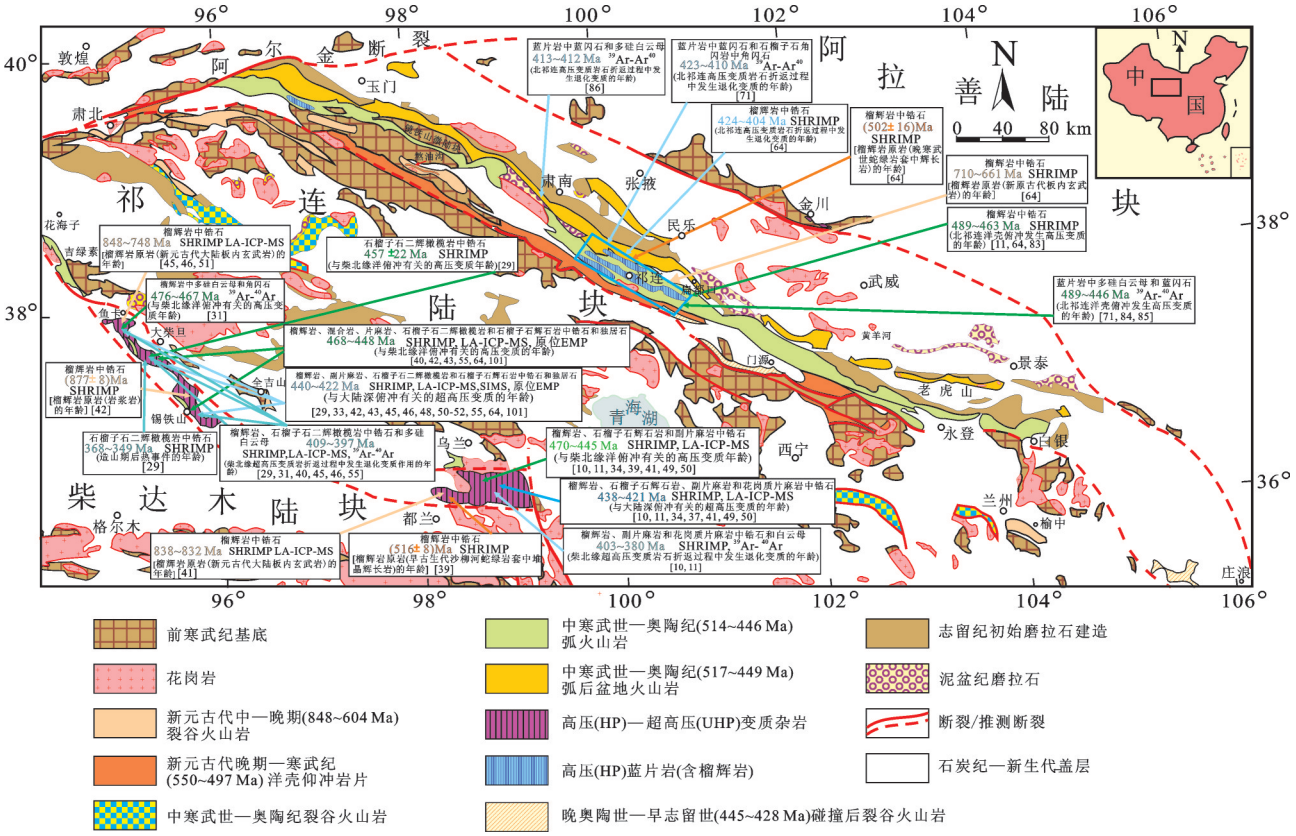

图4 祁连山超高压变质岩和高压变质岩的同位素年龄

Fig.4 Isotopic ages of the ultrahigh pressure metamorphic rocks and high pressure metamorphic rocks in the Qilian Mountains

压变质带记录了一个从大洋俯冲到大陆俯冲的完整的历史[10]。

以往的研究还揭示, 沿着上述柴北缘高压—超高压变质带及其以北地区, 还断断续续近于平行地分布着一条早古生代(542~486 Ma)滩涧山群弧火山岩带[56-58](表1, 图2)。这种高压—超高压变质带和弧火山岩套间近于平行的分布, 暗示着在柴达木陆块和祁连陆块之间也应当存在有一条造山带(即柴北缘俯冲带或缝合带)。本文中, 笔者采纳Xu et al. [8]的意见, 认为柴北缘滩涧山群弧火山岩应为南祁连洋盆向北俯冲诱发的弧火山作用的产物。

应当指出, 分别位于阿尔金走滑断裂两侧的祁连陆块和阿尔金陆块具有相似的构造、建造年龄和组成[8](图1)。尤其是, 北祁连高压变质带和柴北缘高压—超高压变质带可以分别和北阿尔金高压变质带和南阿尔金高压—超高压变质带相对比[59, 60]。这种对比揭示, 阿尔金走滑断裂带的北西盘, 至少被左旋偏移了大约400 km [61]。

前面已经提及, 中、外研究者曾对于古生代时期祁连山的构造演化提出过多种不同的认识。本文拟着重聚焦于祁连山地区广泛发育的新元古代中—晚期到早古生代火山岩系, 对其分布、性质、测年和岩石地球化学数据进行综合整理。尔后, 基于对火山岩研究数据和其他地质信息的综合分析, 推断和重建祁连山新元古代中—晚期到早古生代的构造演化历史。

2 地质背景

如前所述, 祁连山造山系由北祁连造山带、祁连陆块和柴北缘造山带(包括柴北缘岛弧-弧后盆地和柴北缘高压—超高压变质带)构成, 该造山系北、东、南、西分别以阿拉善陆块、华北克拉通、柴达木陆块和塔里木克拉通为界(图1)。

2.1 阿拉善陆块

阿拉善陆块外观呈三角形, 长期以来一直被当做是华北克拉通的西部组成[102, 103]。该陆块以断裂

表 1 祁连山新元古代—早古生代火山岩、蛇绿岩和超镁铁质岩的年龄数据

Table 1 Compiled age data of Neoproterozoic−Early Paleozoic volcanic rocks, ophiolites and ultramafic rocks in the Qilian Mountain

岩石类型	位置	年龄/Ma	方法	资料来源
新元古代火山岩				
玄武安山岩	全吉群, 全吉山	800	锆石 U−Pb TIMS	[62]
榴辉岩(原岩为大陆溢流玄武岩)	鱼卡, 柴达木陆块北缘	847~848	锆石 U−Pb SHRIMP	[51]
玄武岩	兴隆山群, 榆中县	713~824	锆石 U−Pb LA−ICP−MS	[63]
榴辉岩(原岩为板内玄武岩)	上香子沟, 祁连县	710~661	锆石 U−Pb SHRIMP	[64]
榴辉岩(原岩为板内玄武岩)	鱼卡, 柴达木陆块北缘	795~748	锆石 U−Pb LA−ICP−MS	[45, 46]
榴辉岩(原岩为板内岩浆岩)	锡铁山, 柴达木陆块北缘	877 ± 8	锆石 U−Pb SHRIMP	[42]
火山岩	朱龙关群, 柳沟峡	604~738	锆石 U−Pb TIMS	[65]
新元古代晚期— 寒武纪洋壳的仰冲岩片(蛇绿岩)				
辉长岩	玉石沟蛇绿岩套	550 ± 17	锆石 U−Pb SHRIMP	[66]
辉长岩	玉石沟蛇绿岩套	548 ± 9	锆石 U−Pb SHRIMP	[9]
辉长岩	玉石沟蛇绿岩套	529 ± 9	锆石 U−Pb SHRIMP	[9]
辉长苏长岩	东草河蛇绿岩套	497 ± 7	锆石 U−Pb SHRIMP	[67]
辉长岩	熬油沟蛇绿岩套	504 ± 6	锆石 U−Pb SHRIMP	[68]
辉长岩	熬油沟蛇绿岩套	501.4 ± 4.3	锆石 U−Pb SHRIMP	[69]
枕状玄武岩(细碧岩)	扎麻什河(东沟)蛇绿岩套	499.3 ± 6.2	锆石 U−Pb LA−ICP−MS	[70]
中寒武世 — 奥陶纪火山岩				
英安岩	滩间山群, 锡铁山地区	486 ± 13	锆石 U−Pb TIMS	[56]
安山岩	滩间山群, 吉绿素地区	514 ± 8.5	锆石 U−Pb LA−ICP−MS	[58]
玄武岩	滩间山群, 绿梁山地区	542 ± 13	锆石, U−Pb TIMS	[57]
长英质熔岩	清水沟, 祁连县	466 ± 9	锆石, U−Pb TIMS	[71]
		481 ± 18		
流纹岩	清水沟, 祁连县	494 ± 6	锆石 U−Pb LA−ICP−MS	[9]
流纹岩	白银地区	446 ± 3	锆石 U−Pb SHIRIMP	[72]
流纹岩(石英角斑岩)	白银地区	467.3 ± 2.9	锆石 U−Pb LA−ICP−MS	[73]
		467.1 ± 2.2		
玄武岩(细碧岩)	白银地区	465.0 ± 3.7	锆石 U−Pb LA−ICP−MS	[74]
玄武岩(辉石细碧岩)	石灰沟, 永登县	465.7 ± 23	Sm−Nd 等时线	[16]
流纹岩	郭米寺, 祁连县	503 ± 3	锆石 U−Pb LA−ICP−MS	[75]
安山岩	银灿, 门源县	460.17 ± 0.92	锆石 U−Pb LA−ICP−MS	[76]
中寒武世 — 奥陶纪弧后盆地火山岩和蛇绿岩				
玄武岩(辉石细碧岩)	老虎山, 景泰县	453.6 ± 4.4	Sm−Nd 等时线	[16]
辉长岩	老虎山蛇绿岩套, 景泰县	448.5 ± 4.7	锆石 U−Pb SHRIMP	[9]
玄武岩	白泉门, 肃南县	464.6 ± 21.9	Sm−Nd 等时线	[20]
辉长岩	扁都口蛇绿岩套, 民乐县	479 ± 2	锆石 U−Pb LA−ICP−MS	[9]
玄武安山岩	大坂 — 大岔, 肃南县	468.9 ± 4.6	Sm−Nd 等时线	[20]
辉长岩	九个泉蛇绿岩套, 肃南县	490 ± 5	锆石 U−Pb SHRIMP	[77]
辉长岩	大坂 — 大岔蛇绿岩套, 肃南县	487 ± 9	锆石 U−Pb SHRIMP	[78]
		517 ± 4		
辉长岩	大坂—大岔蛇绿岩套, 肃南县	505 ± 8	锆石 U−Pb SHRIMP	[79]
晚奥陶世 — 早志留世被动陆缘裂谷火山岩				
玄武岩(细碧岩)	红沟, 门源县	443.2 ± 1.2	锆石 U−Pb LA−ICP−MS	[80]
玄武岩(细碧玢岩)	葫芦河, 庄浪县	445~428	Sm−Nd 等时线	[16]
超镁铁质侵入体				
含硫化物橄长岩	金川侵入体, 阿拉善陆块	827 ± 8	锆石 U−Pb SHRIMP	[81]
斜长石二辉橄榄岩	金川侵入体, 阿拉善陆块	812 ± 26	斜锆石 U−Pb SHRIMP	[82]
粒玄岩脉	金川侵入体, 阿拉善陆块	828 ± 3	锆石 U−Pb SHRIMP	[82]

为边界, 绝大部分为沙漠覆盖。该陆块具有由2.3~1.9 Ga英云闪长岩−花岗片麻岩构成的早前寒武纪基底[104], 其上为寒武系—中奥陶统盖层覆盖[105]。该陆块东北部出露有约2.7 Ga角闪岩[106], 一些变沉积岩系中发现有2.5~3.5 Ga的碎屑锆石[107, 108]。在龙首山地区发育有828~812 Ma金川超镁铁质侵入体[81, 82](图2, 表1)和971~845 Ma片理化花岗岩体[109, 110], 金川岩体中产出有储量位居全球第3位的Cu−Ni硫化

表 2 北祁连山高压变质带中高压变质岩石的年龄数据

Table 2 Compiled age data of HPM rocks in the North Qilian Mountains

位置	岩石	测试矿物	年龄/Ma	方法	年龄描述	资料来源
百经寺	榴辉岩	锆石	468 ± 13	U–Pb SHRIMP	榴辉岩相变质年龄; 相当于北祁连洋壳俯冲发生高压变质的年龄	[83]
上香子沟	榴辉岩	锆石	464 ± 6; 463 ± 6	U–Pb SHRIMP	榴辉岩相变质年龄	[11, 83]
百经寺	榴辉岩	锆石	502 ± 16	U–Pb SHRIMP	榴辉岩原岩(晚寒武世蛇绿岩套中辉长岩)的年龄	[64]
上香子沟	榴辉岩	锆石	710~661 489 ± 7; 477 ± 16 404~424	U–Pb SHRIMP	榴辉岩原岩(新元古代板内玄武岩)的年龄; 榴辉岩相变质年龄; 北祁连高压变质岩石折返过程中发生退化变质的年龄	[64]
清水沟	蓝片岩	多硅白云母	448 ± 11	^{39}Ar–^{40}Ar 坪	蓝片岩相变质年龄	[84]
清水沟	蓝片岩	多硅白云母	445.7 ± 8.9; 447.4 ± 3.5; 450.9 ± 4.0; 453.9 ± 9.2	^{39}Ar–^{40}Ar 坪	蓝片岩相变质年龄	[85]
清水沟	蓝片岩	蓝闪石	489.3 ± 16.2; 448.6 ± 11 422.89 ± 7.07; 410.9 ± 4.1	^{39}Ar– ^{40}Ar	蓝片岩相变质年龄 北祁连高压变质岩石折返过程中发生退化变质的年龄	[71]
百经寺	蓝片岩	多硅白云母	459.7 ± 4.4; 462 ± 1.3; 455.1 ± 9.9	^{39}Ar–^{40}Ar 等时线 ^{39}Ar– ^{40}Ar 坪	北祁连高压变质岩石折返过程中发生退化变质的年龄 蓝片岩相变质年龄	[71]
瓦窑河 鱼儿沟	石榴子石角闪岩	角闪石	412.4 ± 0.9	^{39}Ar–^{40}Ar 坪	北祁连高压变质岩石折返过程中发生退化变质的年龄	[71]
九个泉	(1)绿帘石蓝片岩 (2)硬柱石蓝片岩	蓝闪石 多硅白云母	(1) 413 ± 5; (2) 415 ± 7	^{39}Ar–^{40}Ar 等时线	北祁连高压变质岩石折返过程中发生退化变质的年龄	[86]

物矿床。这些新元古代侵入体的发育表明, 阿拉善陆块很可能并不是华北克拉通的西部组成, 而是一块碎裂后的Rodinia超大陆的碎块, 具有与其南面祁连陆块相似的构造属性[9, 10, 111]。

2.2 祁连陆块

祁连陆块是一个具有古生代沉积岩系盖层和前寒武系基底的叠瓦状逆冲带(图2)。该陆块西南部大柴旦地区出露有由古元古代花岗片麻岩(2.47~ 2.2 Ga)、淡色花岗岩(1.96~1.91 Ga)和环斑花岗岩(1.77~1.76 Ga)组成的前寒武纪杂岩[47, 112, 113]。在西宁地区北部的片麻岩中还发现产出有940~880 Ma花岗质侵入体[109, 114, 115]。此外, 以往的研究[19, 62, 63, 65, 69, 116]还揭示, 在祁连陆块上发育有兴龙山群裂谷火山岩(824~713 Ma)、全吉群裂谷火山岩(800 Ma)和朱龙关群大陆溢流火山岩(738~604 Ma)等新元古代中—晚期裂谷火山岩系(图2,表1)。上述地质事实导致研究者们一致认为祁连陆块具有与扬子克拉通相似的构造属性[10, 12, 47, 109, 117]。

2.3 柴达木陆块

柴达木陆块是一个具有前寒武纪结晶基底和巨厚沉积盖层的中—新生代内陆盆地。王惠初等[118]曾证明柴达木陆块南部泥质和花岗质片麻岩中发育有格林威尔期(1074~988 Ma)变质作用和深熔作用, 以及2.6~2.4 Ga和少量3.2 Ga的碎屑锆石。Chen et al. [45, 46]和Song et al. [51]曾报道: 产于柴达木陆块北缘的鱼卡榴辉岩具有848~748 Ma的原岩年龄, 而且其原岩岩性与大多数具地幔柱成因的大陆溢流玄武岩相似。因此, Song et al. [10]推断柴达木陆块也具有与扬子克拉通相似的构造属性。

2.4 塔里木克拉通

由于塔里木克拉通上遍布巨厚的古生界盖层, 因而对于该克拉通的大部分前寒武纪基底知之甚少。只是在塔里木克拉通的北部, 新元古代基底岩石才有较广泛的出露。在库鲁克塔格地区, 新元古界的中—上部地层不整合覆盖在新元古界下部的帕尔岗塔格群之上; 在阿克苏—柯坪地区, 下寒武统地层不整合盖在阿克苏群之上[119−122]。

研究[119−126]揭示: 在新元古界中−上部至下寒武统地层中分布有裂谷火山岩系。这套火山岩系在库鲁克塔格地区发育最为完全, 自下而上共有4个火山岩单元: 即贝义西单元(新元古代早中期)、扎摩

表3 祁连山古生代花岗岩类年龄数据

Table 3 Compiled age data on Paleozoic granites in the Qilian Mountain

岩石类型	位置	年龄/Ma	方法	资料来源
阿拉善陆块花岗岩体				
花岗岩	直沟门岩体	374 ± 38	锆石 U-Pb TIMS	[87]
北祁连花岗岩类				
二长花岗岩	金佛寺岩体	424.1 ± 3.3	锆石 U-Pb SHRIMP	[88]
花岗闪长岩	窑沟岩体	463.2 ± 4.7	锆石 U-Pb SHRIMP	[89]
花岗岩	柴达诺岩体	508.3 ± 4.6	锆石 U-Pb SHRIMP	[88]
		516 ± 4		[9]
花岗岩	牛心山岩体	476.7 ± 6.6	锆石 U-Pb SHRIMP	[89]
二长花岗岩	黄羊河岩体	383 ± 6	锆石 U-Pb SHRIMP	[90]
英云闪长岩	雷公山岩体	453.4 ± 5.6	锆石 U-Pb SHRIMP	[91]
石英闪长岩	井子川岩体	464 ± 15	锆石 U-Pb SHRIMP	[90]
石英闪长岩	老虎山岩体	423.5 ± 2.8	锆石 U-Pb TIMS	[92]
奥长花岗岩	熬油沟岩体	438 ± 3	锆石 U-Pb SHRIMP	[93]
石英闪长岩, 斜长花岗岩	柯柯里岩体	500.7 ± 4.6	锆石 U-Pb SHRIMP	[88]
		475.6 ± 5.9		
		512.4 ± 1.8		
石英闪长岩	下古城岩体	505.4 ± 4	锆石 LA-ICP-MS	[94]
南祁连(柴达木陆块北缘)花岗岩类				
花岗岩	嗷唠山岩体	473 ± 15	锆石 U-Pb SHRIMP	[95]
花岗岩	野马滩岩体, 都兰县	397 ± 4.2	锆石 U-Pb SHRIMP	[95]
花岗岩	柴达木山岩体	446 ± 10	锆石 U-Pb SHRIMP	[95]
花岗岩	柴达木山, 大柴旦地区	446.3 ± 3.9	锆石 U-Pb SHRIMP	[96]
花岗岩	绿梁山岩体(北部), 大柴旦地区	408.6 ± 4.4	锆石 U-Pb SHRIMP	[96]
花岗闪长岩	绿梁山岩体(南部), 大柴旦地区	403.3 ± 3.8	锆石 U-Pb SHRIMP	[96]
花岗闪长岩	依克达木湖, 大柴旦地区	402 ± 3	锆石 U-Pb SHRIMP	[96]
花岗岩	巴嘎柴达木湖南, 大柴旦地区	374.5 ± 1.6	锆石 U-Pb SHRIMP	[96]
花岗闪长岩	大头羊沟, 大柴旦地区	372.0 ± 2.7	锆石 U-Pb SHRIMP	[96]
花岗闪长岩	团鱼山, 柴北缘西段	469.7 ± 4.6	锆石 U-Pb SHRIMP	[97]
花岗岩	赛什腾山, 柴北缘西段	465.4 ± 3.5	锆石 U-Pb SHRIMP	[97]
花岗岩	团鱼山, 柴北缘西段	443.5 ± 3.5	锆石 U-Pb SHRIMP	[97]
石英闪长岩	嗷唠河, 柴北缘西段	372.1 ± 2.6	锆石 U-Pb SHRIMP	[97]
花岗岩	三岔沟岩体, 柴北缘西段	271.2 ± 1.5	锆石 U-Pb SHRIMP	[97]
花岗岩	三岔沟岩体, 柴北缘西段	260.4 ± 2.3	锆石 U-Pb SHRIMP	[97]
花岗岩	锡铁山岩体	428 ± 1	锆石 U-Pb TIMS	[98]
环斑花岗岩	塔塔楞河岩体	440 ± 14	锆石 U-Pb SHRIMP	[99]
花岗岩	野马滩东, 都兰县	406.6 ± 3.5	锆石 U-Pb SHRIMP	[100]
花岗闪长岩	巴立给哈滩西, 都兰县	407.3 ± 8.3	锆石 U-Pb SHRIMP	[100]
花岗岩	巴立给哈滩西, 都兰县	397.0 ± 6.0	锆石 U-Pb SHRIMP	[100]
花岗闪长岩	水文站北, 都兰县	404.5 ± 4.0	锆石 U-Pb SHRIMP	[100]
花岗岩	水文站北, 都兰县	397.0 ± 3.7	锆石 U-Pb SHRIMP	[100]
石英闪长岩	水文站南, 都兰县	380.5 ± 5.0	锆石 U-Pb SHRIMP	[100]
花岗岩	察察公麻西, 都兰县	382.5 ± 3.6	锆石 U-Pb SHRIMP	[100]
花岗闪长岩	察察公麻西, 都兰县	372.5 ± 2.8	锆石 U-Pb SHRIMP	[100]

克提单元(新元古代中晚期)、水泉沟单元(新元古代晚期)和西山布拉克单元(早寒武世)[123-125]。所有研究[122-127]均认为这套火山岩系产生于大陆板内环境,其形成与Rodinia超大陆裂解过程中的地幔柱活动和大陆裂谷化有关。现已发表了4个有关贝义西单元的地质年代学数据,它们是:1个Pb-Pb年龄(773 Ma)[128]和3个锆石U-Pb SHRIMP年龄:755 Ma[122]、740 Ma和725 Ma [129]。此外,朱杰辰和孙文鹏[130]还曾获得过阿克苏—柯坪地区苏盖特布拉克组的锆石U-Pb年龄(TIMS法,740 Ma);Xu et al. [129]则曾获得库鲁克塔格地区扎摩克提火山岩单元的锆石U-Pb SHRIMP年龄(615 Ma)。

除了上述新元古代双峰式裂谷火山岩外,据报道,在塔里木克拉通中还发育有3类新元古代侵入体,它们是:824~630 Ma镁铁质岩墙群[131-133]、833~760 Ma超镁铁质-镁铁质侵入体[134-136]和820~744 Ma碱性花岗岩[135, 137]。塔里木克拉通记录的这些新元古代(840~630 Ma)火成事件也均被解释为与Rodinia超大陆裂解过程中的地幔柱活动有关[132, 133, 135, 136]。Zhang et al. [137] 最近还报道,在塔里木克拉通的南缘也分布有与新元古代裂谷化有关的镁铁质岩墙(锆石U-Pb SHRIMP年龄:(802±9) Ma)和玄武岩。

上述数据表明,塔里木克拉通也应当曾经是Rodinia超大陆的组成单元[126]。塔里木克拉通的东端曾被阿尔金断裂系平移错断。阿尔金断裂系两侧相对应的高压和超高压变质带表明,该断裂系东部的柴达木陆块和祁连陆块曾被向北东方向水平位移了约400 km(图1)。因此,Song et al.[53]推断,在阿尔金断裂系因响应欧-亚碰撞发生左旋移动之前,塔里木克拉通和柴达木—祁连陆块有可能曾经是联结在一起的一个单一的大陆块。

2.5 华南陆块

华南陆块通常被认为是由扬子克拉通和华夏陆块拼合而成(图1)。然而,对于扬子克拉通和华夏陆块相互碰撞的年龄却有着新元古代早期(大约为1.0~0.9 Ga)[139-145]和新元古代中期(大约为850~840 Ma)[146-149]等2种不同的推断。

崆岭杂岩是扬子克拉通中最古老的岩石单元,它由太古宙至古元古代高级变质英云闪长质片麻岩、奥长花岗岩质片麻岩、花岗闪长岩质片麻岩、角闪岩和变质表壳岩组成[150]。虽然从元古宙或更年轻的多种岩石中曾鉴别出存在有太古宙继承性碎屑锆石,但华夏陆块中已知最古老的结晶基底乃是浙江省西南部和福建省西北部的1.8 Ga花岗质岩石[151, 152]。

新元古代中期(827~746 Ma)双峰式(基性-酸性)裂谷火山岩系广泛地分布于华南陆块之中(详见文献[126]及其参考文献)。这些火山岩系不整合于新元古代早—中期基底之上,并为新元古代晚期地层所覆盖。同位素地质年代学数据揭示,华南陆块中新元古代中期火山作用的年龄下限应当小于830 Ma,其年龄上限大约为740 Ma。根据华南和塔里木等2个陆块中均发育新元古代岩浆活动,研究者们已经意识到这2个陆块可能具有相似的构造属性[53, 126]。

综上所述,祁连古陆块及与其相邻的其他古陆块(包括有:阿拉善陆块、塔里木克拉通、柴达木陆块和华南陆块)可能均曾经是Rodinia超大陆的组成单元。

3 祁连山地区的新元古代中—晚期至早古生代火山作用

就时、空分布而言,笔者的综合研究识别出祁连山地区主要发育有6套火山岩:(1)祁连陆块中的新元古代中—晚期(848~604 Ma)裂谷火山岩,主要分布于祁连陆块的北部,包括有分布于祁连陆块西北部的朱龙关群和多若诺尔群火山岩系(738~604 Ma)、分布于祁连陆块东部的兴隆山群火山岩(824~713 Ma)和少量分布于祁连陆块南部的全吉群火山岩(~800 Ma);(2)北祁连新元古代晚期至寒武纪(550~497 Ma)洋壳(即蛇绿岩)仰冲岩片中的洋脊玄武岩(MORB)型火山岩;(3)北祁连山和南祁连山的寒武纪至奥陶纪弧火山岩,包括有沿北祁连造山带主构造线连续分布的503~446 Ma北祁连弧火山岩带和在祁连陆块南缘呈断续状分布滩涧山群弧火山岩带(542~486 Ma),后者主要出露于吉绿素、绿梁山、锡铁山和乌兰等地区;(4)分布于北祁连弧火山岩带后方(即东北方向)的北祁连寒武纪至奥陶纪(517~449 Ma)弧后盆地火山岩带;(5)分布于祁连陆块中部的寒武纪至奥陶纪拉脊山裂谷火山岩带;(6)出露于祁连陆块北缘冰沟、红沟和葫芦河等地的晚奥陶世至早志留世(445~428 Ma)碰撞后裂谷火山岩(图2~图4)。

3.1 祁连陆块及邻区新元古代中—晚期(848~604 Ma)裂谷火山岩

如图2所示,新元古代中—晚期朱龙关群和多

表 4 柴北缘高压、超高压变质带中高压、超高压变质岩石的年龄数据

Table 4 Compiled age data on HPM–UHPM rocks of the Northern Qaidam HPM–UHPM belt

位置	岩石	测试矿物	年龄/Ma	方法	年龄描述	资料来源
鱼卡	榴辉岩	多硅白云母、角闪石	(1) 476 ± 6; 466.7 ± 1.2; (2) 409 ± 1	$^{39}Ar-^{40}Ar$ 坪 $^{39}Ar-^{40}Ar$ 坪	与早期大洋俯冲有关的高压变质的年龄; 柴北缘超高压变质岩折返过程中发生退化变质作用的年龄	[31]
鱼卡	含石榴子石白云母-角闪石-钠长石片麻岩 含蓝晶石石榴子石-云母片岩	锆石	431 ± 3; 432 ± 19	U-Pb LA-ICP-MS	与大陆深俯冲有关的超高压变质的年龄	[48]
鱼卡	榴辉岩	锆石	(1) 748~795; (2) 431 ± 4; 436 ± 3; (3) 409 ± 4	U-Pb LA-ICP-MS	榴辉岩原岩 (新元古代板内玄武岩) 的年龄; 与大陆深俯冲有关的超高压变质的年龄; 柴北缘超高压变质岩折返过程中发生退化变质作用的年龄	[45, 46]
鱼卡	榴辉岩	锆石	(1) 847 ±10; 848 ± 15; (2) 433 ± 20	U-Pb SHRIMP U-Pb SIMS	榴辉岩原岩(新元古代大陆溢流玄武岩)的年龄; 与大陆深俯冲有关的超高压变质的年龄	[51]
鱼卡	花岗片麻岩	锆石	941 ± 21; 976 ± 21	U-Pb LA-ICP-MS	新元古代格林威尔造山(岩浆)事件的年龄	[53]
鱼卡	泥质片麻岩	锆石	426.5 ± 2.4	U-Pb LA-ICP-MS	峰期超高压变质作用的年龄	[10]
绿梁山	石榴子石二辉橄榄岩	锆石	(1) 457 ± 22; (2) 423 ± 5; (3) 397 ± 6; (4) 368~349	U-Pb SHRIMP	与早期大洋俯冲有关的高压变质作用的年龄; 与大陆深俯冲有关的超高压变质的年龄; 柴北缘超高压变质岩折返过程中发生退化变质作用的年龄; 造山期后热事件的年龄	[29]
绿梁山, 胜利口	长英质片麻岩	锆石	427.2 ± 4.5	U-Pb LA-ICP-MS	与大陆深俯冲有关的超高压变质作用的年龄	[33]
绿梁山, 胜利口	混合岩、片麻岩、石榴子石二辉橄榄岩 石榴子石辉石岩	锆石	(1) 468 ± 4 (2) 430 ± 5; 427 ± 3; 429 ± 3	U-Pb LA-ICP-MS	与早期大洋俯冲有关的高压变质作用的年龄; 与大陆深俯冲有关的超高压变质作用的年龄	[101]
绿梁山	退变榴辉岩	锆石	448 ± 3 427 ± 5	U-Pb SHRIMP	与早期大洋俯冲有关的高压变质年龄; 与大陆深俯冲有关的超高压变质年龄	[64]
锡铁山	退变榴辉岩 (变基性岩、石榴子石-蓝晶石片麻岩, 石榴子石-矽线石片麻岩)	锆石	(1) 461 ± 8; 452 ± 12; 451 ± 6; (2) 430 ± 4; 423 ± 12; (3) 409 ± 12	U-Pb SHRIMP	与早期大洋俯冲有关的高压变质的年龄; 与大陆深俯冲有关的超高压变质作用的年龄; 柴北缘超高压变质岩折返过程中发生退化变质作用的年龄	[40, 55]
锡铁山	榴辉岩	锆石	(1) 877 ± 8; (2) 461 ± 4; (3) 440 ± 5; 439 ± 8	U-Pb SHRIMP	榴辉岩原岩(岩浆岩)的年龄; 与早期大洋俯冲有关的高压变质作用的年龄; 与大陆深俯冲有关的超高压变质作用的年龄	[42]
锡铁山	榴辉岩	锆石	432.7 ± 3.1	U-Pb SIMS	与大陆深俯冲有关的超高压变质的年龄	[52]
锡铁山	花岗片麻岩 石榴子石-蓝晶石片麻岩	锆石	951 ± 24, 942 ± 16 916 ± 7	U-Pb LA-ICP-MS U-Pb SIMS	新元古代格林威尔造山(岩浆)事件的年龄; 新元古代格林威尔造山(岩浆)事件的年龄	[53]
锡铁山	石榴子石-蓝晶石片麻岩 石榴子石-蓝晶石片麻岩	锆石 独居石	(1) 945 ± 7, 938 ± 23; (2) 460~455; (3) 425~422	U-Pb SHRIMP U-Th-Pb 原位 EMP	新元古代格林威尔造山(岩浆)事件的年龄; 与早期大洋俯冲有关的高压变质作用的年龄; 峰期超高压变质作用的年龄	[53]

续表4

位置	岩石	测试矿物	年龄/Ma	方法	年龄描述	资料来源
都兰县, 野马滩	正片麻岩	锆石	927 ± 7, 921 ± 7	U-Pb SHRIMP	新元古代格林威尔造山(岩浆)事件的年龄	[35]
都兰县, 野马滩	花岗片麻岩	锆石	932 ± 18, 907 ± 18	U-Pb SHRIMP	新元古代格林威尔造山(岩浆)事件的年龄	[53]
都兰县, 野马滩	榴辉岩 泥质片 麻岩中含柯石英包裹体	锆石	(1) 457 ± 7; (2) 423 ± 6; (3) 403 ± 9	U-Pb SHRIMP	与早期大洋俯冲有关的高压变质作用的年龄; 与大陆深俯冲有关的超高压变质作用的年龄; 柴北缘超高压变质岩折返过程中发生退化变质作用的年龄	[11]
都兰县, 野马滩	榴辉岩	锆石	(1) 452 ± 4; 442 ± 4; (2) 432.5 ± 5; 423 ± 4	U-Pb SHRIMP	与早期大洋俯冲有关的高压变质作用的年龄; 与大陆深俯冲有关的超高压变质作用的年龄	[34]
都兰县, 野马滩	副片麻岩	锆石	431 ± 5; 426 ± 4	U-Pb SHRIMP	与大陆深俯冲有关的超高压变质作用的年龄	[37]
都兰县, 野马滩	副片麻岩	锆石	(1) 458 ± 6; (2) 421 ± 6.5	U-Pb LA-ICP-MS	与早期大洋俯冲有关的高压变质作用的年龄; 与大陆深俯冲有关的超高压变质作用的年龄	[49, 50]
都兰县, 野马滩	榴辉岩	锆石	(1) 462 ± 13; (2) 424 ± 13; (3) 400~380	U-Pb SHRIMP	与大洋俯冲有关的高压变质年龄; 超高压变质作用的年龄; 退化变质作用的年龄	[10]
都兰县, 野马滩	花岗质片麻岩中白云母	白云母	401.5 ± 1.6	$^{39}Ar-^{40}Ar$ 坪	柴北缘超高压变质岩折返过程中发生退化变质作用的年龄	[11]
都兰县, 阿尔茨托山	含柯石英榴辉	锆石	(1) 838~832; (2) 446 ± 3; (3) 438 ± 2, 430 ± 4	U-Pb SHRIMP U-Pb LA-ICP-MS	榴辉岩原岩 (新元古代板内玄武岩) 的年龄; 与大洋俯冲有关的高压变质年龄; 超高压变质作用的年龄	[41]
都兰县, 沙柳河(变)蛇绿岩套	蓝晶石榴辉岩(堆晶辉长岩)	锆石	(1)516 ± 8; (2)470~449, 450 ± 11, 445 ± 7; (3) 426 ± 13, 425 ± 8	U-Pb SHRIMP	榴辉岩原岩(早古生代沙柳河蛇绿岩套中的堆晶辉长岩)的年龄; 与早期大洋俯冲有关的高压变质年龄; 超高压变质作用年龄	[10, 39]
	石榴子石辉石岩(超镁铁质堆晶岩)	锆石	(1) 450 ± 11; (2) 425 ± 9	U-Pb SHRIMP	与大洋俯冲有关的高压变质年龄; 峰期超高压变质作用年龄	[10]

若诺尔群、全吉群、兴隆山群火山岩分别分布于祁连陆块西北部、祁连陆块南部的全吉山地区和祁连陆块东部的兴龙山地区。地质年代学研究已经报道了一系列有关上述火山岩系的同位素年龄数据, 如: 朱龙关群火山岩的锆石U-Pb TIMS年龄: 736~604 Ma[65]; 全吉群火山岩的锆石U-Pb TIMS年龄: 800 Ma[62]; 兴隆山群火山岩的锆石U-Pb LA-ICP-MS年龄: 824~713 Ma[63](图5-a; 表1)。上述朱龙关群、全吉群和兴隆山群火山岩系分别不整合覆盖在上元古界下部的北大河群、马衔山群和达肯大坂群之上, 其上部又为上元古界上部和古生界地层所覆盖(图5)。

此外, 过往的研究还查明: (1)北祁连高压蓝片岩带中的上香子沟榴辉岩具有710~661 Ma的原岩年龄(U-Pb SHRIMP锆石年龄), 其原岩与板内玄武岩相似[64](表1, 表2; 图4); (2)柴北缘高压—超高压变质带中的鱼卡榴辉岩具有848~748 Ma的原岩年龄(U-Pb SHRIMP和LA-ICP-MS锆石年龄), 其原岩与大陆溢流玄武岩相似[45, 46, 51](表1, 表4; 图2, 图4); (3)柴北缘高压—超高压变质带中的都兰榴辉岩具有838~832 Ma的原岩年龄, 其原岩与板内玄武岩相似[41](表4; 图4); (4)柴北缘高压—超高压变质带中的锡铁山榴辉岩具有(877±8)Ma的原岩年龄(U-Pb SHRIMP锆石年龄), 其原岩与板内岩浆岩相似[42](表1, 表4; 图4); (5)含超大型Cu-Ni硫化物矿床的新元古代中期(828~812 Ma)金川镁铁质-超镁铁质侵入体产出于阿拉善陆块南部的龙首山地区[81, 82](表1; 图2)。

笔者的综合研究揭示祁连陆块中的新元古代中—晚期火山岩具有下述重要特点:

(1)新元古代中—晚期火山岩主要分布于祁连陆块的西北部, 包括有朱龙关群[19, 65, 69, 116]和多若诺尔群[153]火山岩; 还有少量新元古代中—晚期火山岩分布于祁连陆块的东部(兴隆山群)[63]和南部(全吉群)[62]。新元古代中—晚期火山岩主要由玄武质(包括玄武质和玄武安山质; 图7)熔岩组成, 火山碎屑岩次之。包含拉斑和碱性等2个岩石系列(图7)。这些新元古代中—晚期大陆裂谷(和大陆溢流)玄武质火山岩系在熬油沟地区出露最为完整: 下部为枕状拉斑玄武质熔岩夹白云岩, 中部为浅变质细碎屑岩含铁矿层, 上部为白云岩、碱性玄武质熔岩和基

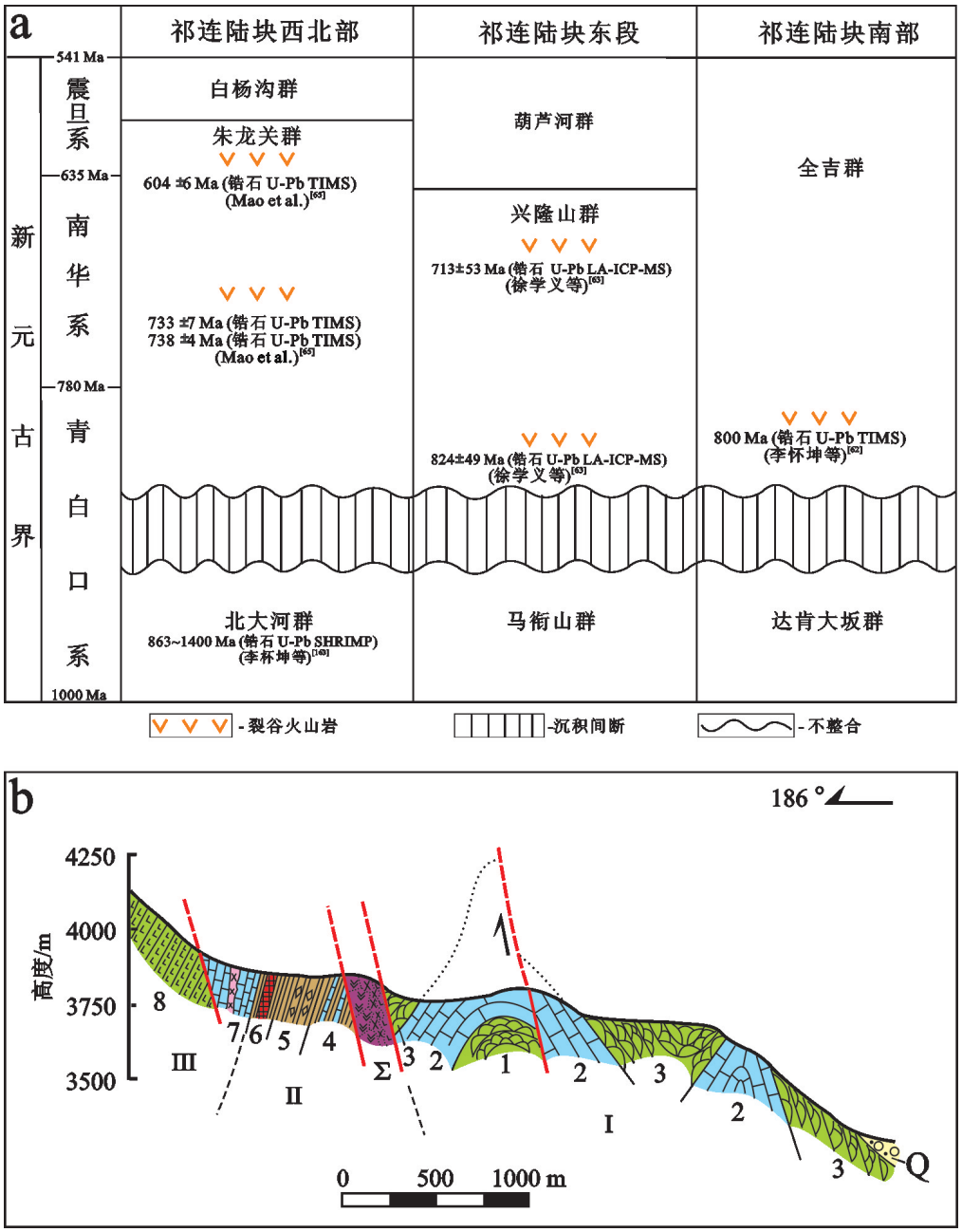

图5 a—祁连山地区祁连陆块中新元古界地层划分和对比; b—肃南县熬油沟朱龙关群剖面

(据文献[116]修编)

I—龙关群下部岩系: 1—枕状辉石玄武岩; 2—含石英白云岩及白云岩; 3—枕状辉石玄武岩(有辉绿岩脉侵入); II—朱龙关群中部岩系: 4—砂泥质板岩夹灰岩; 5—含砾(有火山岩砾)泥质板岩; 6—硅质板岩夹菱铁矿-赤铁矿层。III— 朱龙关群上部岩系: 7—含石英白云岩(有辉长岩脉侵入); 8—辉石玄武岩。Q—第四系; Σ—熬油沟蛇绿岩岩片(由被肢解的蛇纹岩、辉长岩、块状玄武岩和枕状玄武岩构成)

Fig.5 a−Stratigraphic division and correlation of Neoproterozoic strata in the Qilian Block from the Qilian Mountain; b−Geological section of the Zhulongguan Group from Aoyougou area of Sunan County (modified after reference [116])

I−The lower part of the Zhulongguan Group: 1−Pillow pyroxene−basalt; 2−Quartz−bearing dolomite and dolomite; 3−Pillow pyroxene−basalt into which diabase veins intruded. II−The middle part of the Zhulongguan Group: 4−Sand−argillaceous slate with limestone; 5−Gravel−bearing argillaceous slate (with gravels of volcanic rock); 6−Siliceous slate with siderite−hematite bed. III−The upper part of the Zhulongguan Group: 7−Quartz−bearing dolomite into which gabbro veins intruded; 8−Pyroxene−basalt. Q− Quaternary sediments; Σ−Aoyougou ophiolite slice (consisting of dismembered serpentinite, gabbro, and massive and pillow−like basalts)

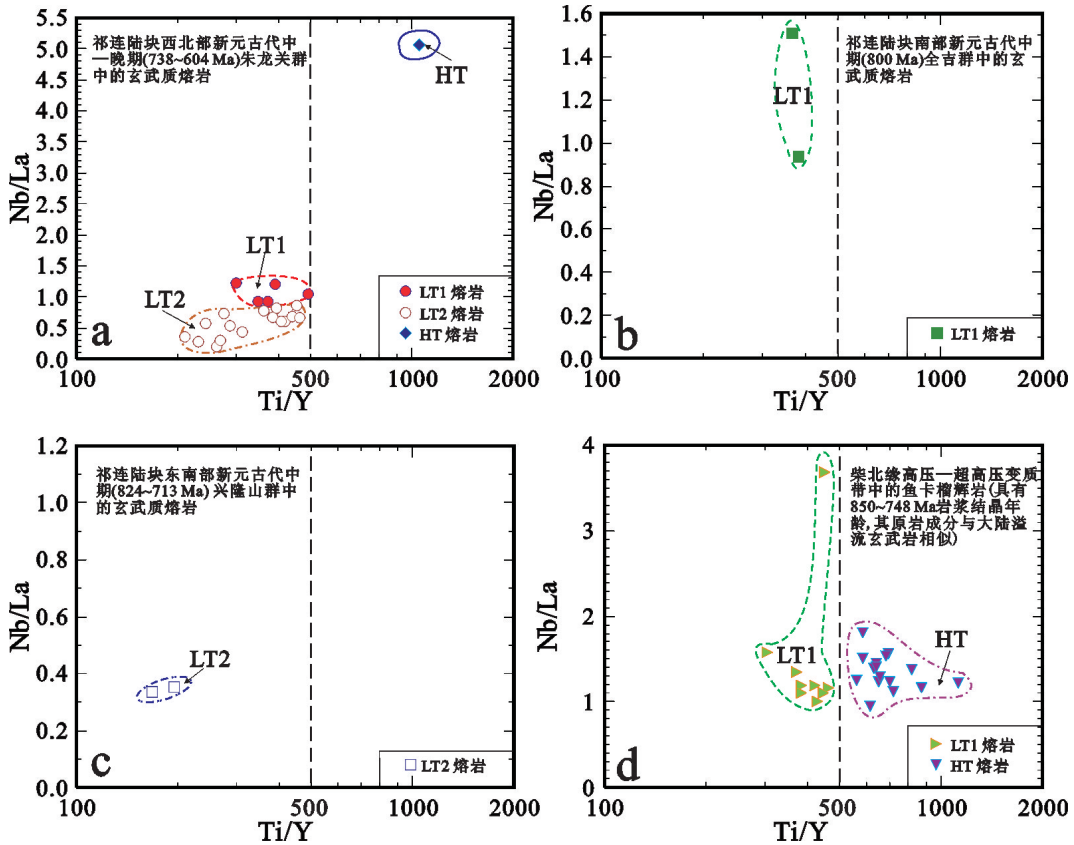

图6 a—祁连陆块西北部朱龙关群玄武质熔岩, b—祁连陆块南部全吉群玄武质熔岩, c—祁连陆块东部兴隆山群玄武质熔岩和d—柴达木陆块北缘高压—超高压变质带中鱼卡榴辉岩(原岩与大陆溢流玄武岩相似)的Ti/Y–Nb/La分类图解

(数据来源: (a): [19, 69, 116]; (b): [62]; (c): [63]; (d): [46, 51])

Fig.6 Classification of Mid−Late Neoproterozoic rift−related basaltic lavas of a−Zhulongguan Group in the northwestern Qilian Block, b−Quanji Group in the southern Qilian Block, c−Xinglongshan Group in the southeastern Qilian Block, and d−Yuka eclogites (protoliths similar to continental flood basalts) in the HPM−UHPM belt from northern margin of the Qaidam Block in terms of Ti/Y versus Nb/La

(Data sources: (a): [19, 69, 116]; (b): [62]; (c): [63]; (d): [46, 51])

性火山碎屑岩[116](图5−b, 图7−a, b)。在此应当特别指出: 分布于祁连陆块西北部的朱龙关群大陆溢流玄武岩系与熬油沟蛇绿岩乃是2个组成、时代与构造性质全然不同的地质体, 不能将二者混为一谈。前者为大陆溢流玄武岩系, 是Rodinia超大陆裂谷化—裂解作用的产物[19, 69, 116]; 后者则是北祁连早古生代洋盆闭合时, 仰冲在祁连陆块北缘上的北祁连早古生代洋壳的残片。

(2)从图7−e, f可见, 产出于柴北缘高压−超高压变质带中具有848~748 Ma原岩年龄的鱼卡榴辉岩[46, 51]具有与玄武岩相似的原岩岩性, 包含拉斑和碱性等2个岩石系列, Song et al.[51]将其定性为大陆溢流玄武岩。这套榴辉岩的原岩(大陆溢流玄武岩)应当是发育于柴达木陆块上。

(3)根据Ti/Y比值, 上述新元古代中—晚期玄武质熔岩可以被划分为高Ti/Y (HT, Ti/Y ≥ 500)和低Ti/Y (LT, Ti/Y < 500)等2个岩浆类型(图6)。根据Nb/La比值, LT熔岩又可以进一步被划分为LT1熔岩和LT2熔岩等2个亚类。HT和LT1熔岩为没有遭受岩石圈混染的(具地幔柱成因)大陆玄武质熔岩[164, 165], 具有Nb/La比值相对较高(0.91~5.07)和“大隆起式”似洋岛玄武岩(OIB)不相容微量元素原始地幔标准化分配型式, 无Nb、Ta、P、Zr、Hf和Ti的负异常(图8−a, c, e, f)。HT和LT1熔岩总体上具有与洋岛玄武岩相重叠的(OIB)元素比值(图8−g)。相反, 其余的玄武质熔岩(也就是LT2熔岩)总体上属于拉

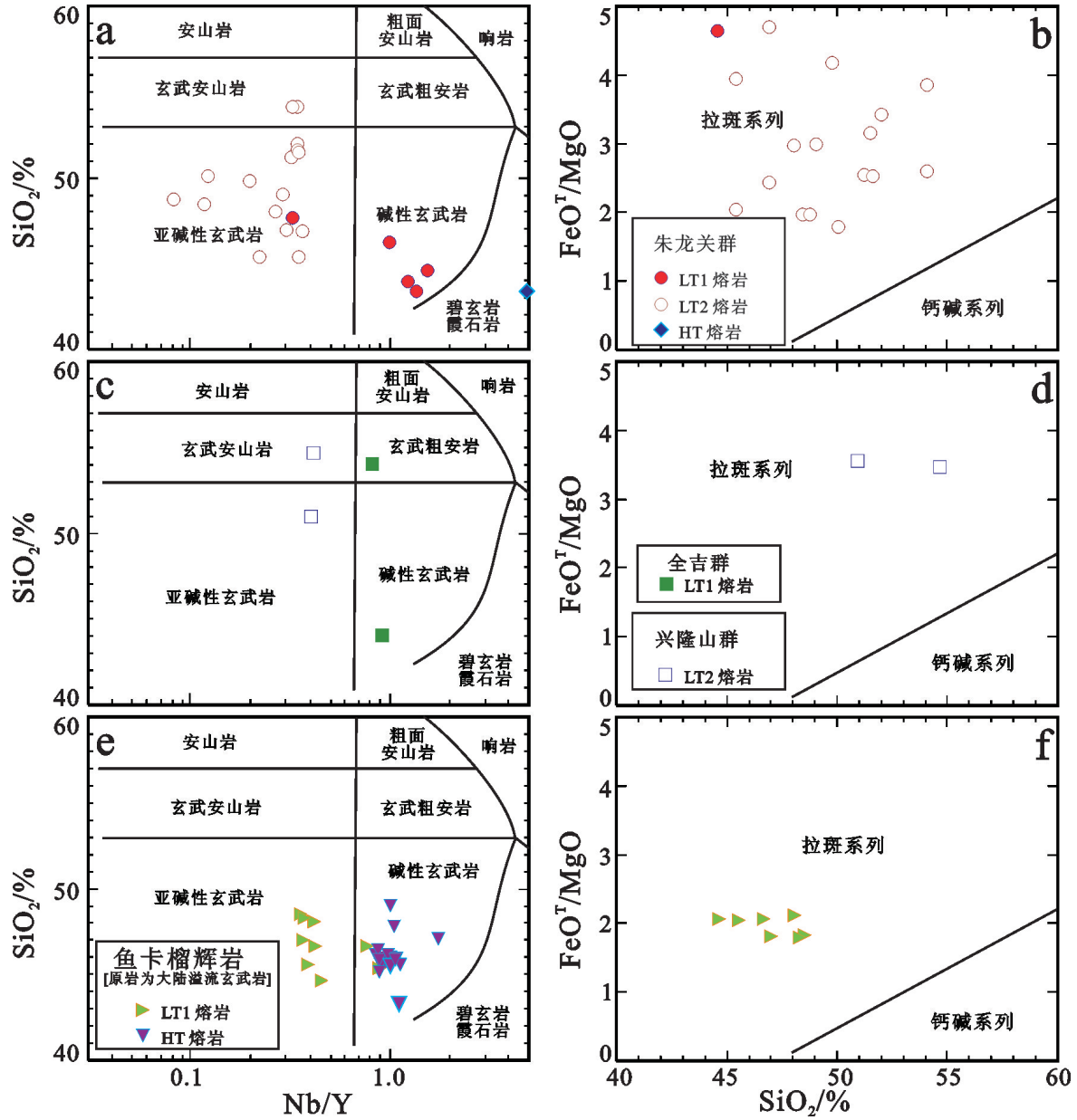

图7 祁连山新元古代中—晚期裂谷玄武质熔岩a, c, e—SiO_2−Nb/Y 图解 (据[154])和b, d, f—FeOT/MgO − SiO_2图解 (据[155])

图7–b, d, f分别适用于图7–a, c, e中的亚碱性火山岩;数据来源同图6

Fig.7 a, c, e−SiO_2 versus Nb/Y diagrams (after reference [154]) and b, d, f−FeOT/MgO versus SiO_2 diagrams (after freference [155]) for Mid−Late Neoproterozoic rift−related basaltic lavas from the Qilian Mountain

Fig. 7–b, d, f show the sub−alkaline volcanic rocks as plotted in Fig. 7–a, c, e respectively; Data sources as for Fig. 6

斑系列(图7−b, d), 具有低的Nb/La比值(0.88~0.18), 明显亏损Nb, Ta, P, Zr, Hf和Ti(图8−b, d), 但它们的不相容微量元素的浓度却明显的高于消减带玄武岩(图8−b, d)。LT2熔岩的主体具有较洋岛玄武岩(OIB)较高的La/Nb和较低La/Ba比值(图8−g), 表明此类熔岩曾遭受地壳或/和陆下岩石圈组分的影响。因此, LT2熔岩乃是遭受了地壳或/和陆下岩石圈混染的大陆玄武岩[164, 165]。

(4)新元古代中—晚期玄武质熔岩的$\varepsilon_{Nd}(t)$值的变化与岩石遭受大陆地壳或大陆岩石圈混染的程度紧密相关。图8−h显示:①没有受到混染的样品(即HT和LT1熔岩)恒定地具有正的$\varepsilon_{Nd}(t)$值(+1至+

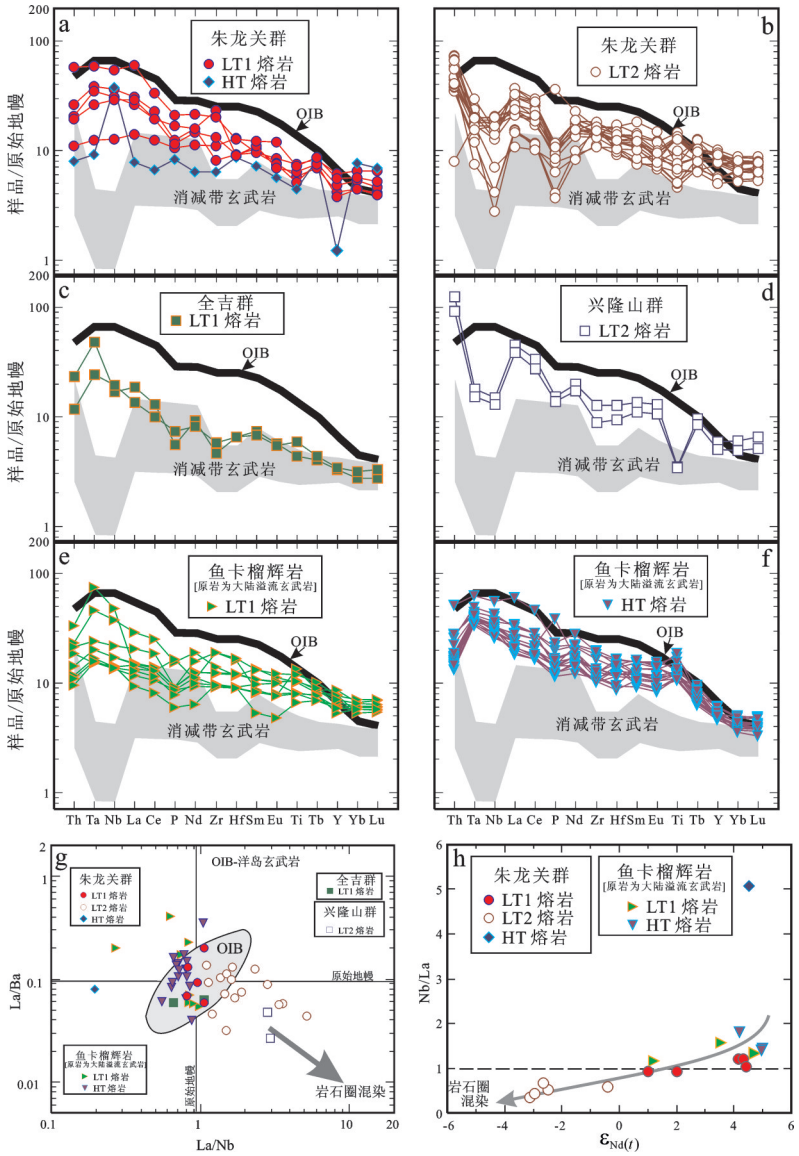

图8 a, b—祁连陆块西北部朱龙关群, c—祁连陆块南部全吉群, d—祁连陆块南部兴龙山群新元古代中晚期玄武质熔岩, e, f—柴达木陆块北缘高压-超高压变质带中鱼卡榴辉岩(原岩与大陆溢流玄武岩相似)的不相容微量元素原始地幔(据[156])标准化蛛网图; g—朱龙关群、全吉群、兴龙山群新元古代中晚期裂谷玄武质熔岩和鱼卡榴辉岩(原岩与大陆溢流玄武岩相似)的La/Ba-La/Nb图解; h—朱龙关群新元古代中晚期裂谷玄武质熔岩和鱼卡榴辉岩(原岩与大陆溢流玄武岩相似)的Nb/La-$\varepsilon Nd(t)$图解

图8-a~f中, 洋岛玄武岩(OIB)据[156]; 图中阴影区表示消减带玄武岩的成分范围, 其上限和下限分别由高-K玄武岩和低-K玄武岩的平均值(据[157])限定; 图8-g中, 岩石圈混染效应导致成分点向高La/Nb和低La/Ba方向迁移; 洋岛玄武岩(OIB)的成分范围据[158, 159]数据来源同图6

Fig. 8 Primitive mantle (after reference [156]) normalized incompatible trace-element spider diagrams for Mid-Late Neoproterozoic basaltic lavas of a, b-Zhulongguan Group in the northwestern Qilian Block, c-Quanji Group in the southern Qilian Block, d-Xinglongshan Group in the southeastern Qilian Block, and e, f-Yuka eclogites (protoliths similar to continental flood basalts) in the HPM-UHPM belt from northern margin of the Qaidam Block; g-La/Ba versus La/Nb plots for Mid-Late Neoproterozoic rift-related basaltic lavas of Zhulongguan Group, Quanji Group, Xinglongshan Group and Yuka eclogites (protoliths similar to continental flood basalts); h-Nb/La versus $\varepsilon Nd(t)$ diagram for Mid-Late Neoproterozoic rift-related basaltic lavas of Zhulongguan Group and Yuka eclogites (protoliths similar to continental flood basalts)

In Fig. 8-a-f, patterns for oceanic island basalts (OIB) are from [156]. The shaded area shows the range for subduction-zone basalts, with the lower and upper limits being defined by "average" low-K and high-K basalts, respectively (after [157]). In Fig. 8-g, the dispersion to higher La/Nb and lower La/Ba may represent the effects of lithospheric contamination. Field for oceanic island basalts (OIB) after reference [158, 159]; data sources as for Fig. 6

5);②遭受混染的样品(即LT2熔岩)则以具有负的$\varepsilon_{Nd}(t)$值为特征(−3.1 至 −0.4)。负ε_{Nd}(t)值的产生应当是与其受到古老大陆岩石圈混染有关[165]。特别应当强调指出: 虽然古老大陆岩石圈混染作用和俯冲板片源流体和/或熔体都可以导致玄武质岩石的Nb/La比值降低, 但是, 只有前一种作用才能导致产生明显的负$\varepsilon_{Nd}(t)$值[165]。

(5)当我们利用不采用Nb、Ta或Ti等作为判别因子的Zr/Y−Zr构造环境地球化学判别图解时, 可以发现所有新元古代中—晚期玄武质熔岩的成分点全部落在板内玄武岩(WPB)成分域内(图9−a)。相反, 当利用一些采用Nb、Ta或Ti等作为判别因子的构造环境地球化学判别图解时(图9−b~d), 则会发现没有受到混染的样品(也就是HT和LT1熔岩)成分点仍然落在板内玄武岩(WPB)成分域内, 但是, 所有其他遭受了岩石圈混染的样品(也就是LT2熔岩)成分点, 全都向低Nb、低Ta或低Ti的方向迁移, 落入岛弧(或活动陆缘)玄武岩成分域。在这种情况下, 我们绝不能将LT2熔岩当作是弧玄武质岩石。如前所述, LT2熔岩的不相容微量元素的浓度明显高于消减带玄武岩的不相容微量元素的浓度, 而且LT2熔岩具有负的$\varepsilon_{Nd}(t)$值(值得注意的是, 弧玄武质岩石的$\varepsilon_{Nd}(t)$总是为正值[165])。因此, LT2熔岩乃是遭受了古老大陆岩石圈混染的大陆玄武质岩石。

(6) Condie[166, 167]提出, 可以用4个不活泼的高场强(HFSE)元素比值: Nb/Th、Zr/Nb、Zr/Y和Nb/Y对某些同位素地幔库加以特征化。这些高场强元素比值的优点在于, 它们既不会像同位素比值那样随着时间发生改变, 也不会受到次生蚀变作用的影响。如Condie[167]所指, Zr−Y−Nb关系(图9−e)能够将地幔柱源和非地幔柱源玄武岩加以区分。

由图9−e清楚可见, 所有新元古代中—晚期没有受到地壳或岩石圈混染的LT1和HT玄武岩的成分点全部落在ΔNb线上方由深部亏损地幔柱组分(DEP)和原始地幔组分(PM)所界定的地幔柱域之中。这与前述借用主量元素和微量元素和同位素地球化学证据证明LT1和HT熔岩为地幔柱源玄武岩也是一致的。

图9−e还显示, LT2熔岩的成分点则落在富集组分(EN)所限定的区域内, 它们代表了受到大陆地壳或(和)陆下岩石圈混染的地幔柱源玄武岩。这与前述由主量元素、微量元素和同位素地球化学研究获得的结论也是一致的。

综上所述, 前述发育于祁连陆块和柴达木陆块之上的新元古代中−晚期没有受到混染和遭受了混染的玄武质熔岩的确是喷发于陆内裂谷环境, 成因上可能与地幔柱活动有关。

应当指出, 发生于中国一些前寒武纪陆块上的新元古代中—晚期陆内裂谷火山作用, 完全可以和地球上其他一些Rodinia大陆块(包括有澳大利亚、劳仑、南韩、印度和塞舍尔等)上同时期的裂谷火山作用进行对比(文献[126]及其参考文献)。这一全球性板内火山作用通常被认为是与导致Rodinia超大陆裂谷化和最终裂解的地幔柱或超级地幔柱活动有关(文献[126]及其参考文献)。

现有资料揭示(文献[126]及本研究), 中国的新元古代中—晚期裂谷火山和岩浆活动可以被划分为2个阶段: 第一阶段为大约877 Ma至604 Ma, 主要发育于阿拉善、祁连、柴达木、华南及相邻的陆块中, 第二阶段为大约773 Ma至540 Ma, 主要育于塔里木克拉通及相邻陆块中。

与第一阶段祁连、柴达木、华南等古陆块上裂谷火山岩系同时代的火山岩系, 同样也发现于澳大利亚[168, 169]、印度[170]、喀拉哈里(南非)[171]、阿拉伯—努比亚地体[172, 173]和劳仑[174, 175, 176]等古陆块上。Li et al. [177]提出: Rodinia超大陆的西半部, 在大约750 Ma前, 可能开始裂离(图10)。第一阶段末期的火山活动可以解释为是代表了Rodinia超大陆的西半部的裂解和一个广阔大洋的打开, 这一阶段的裂解, 首先是发生于澳大利亚—东南极古陆和华南古陆之间, 尔后是发生于华南古陆和劳仑古陆之间[126]。

第二阶段的裂谷火山岩系中, 塔里木克拉通西北部的早寒武世基性火山岩单元可以和澳大利亚中部和北部的早寒武世Kalkarindji玄武岩相对比[178, 179], 这一时期发育的裂谷火山作用, 可以解释为代表了澳大利亚古陆和塔里木古陆间的裂离[126]。

综上所述, 可以发现, Rodinia超大陆的裂解是穿时发生的[177]。中国若干古陆块上发生的新元古代中—晚期火山作用(和岩浆作用)乃是Rodinia超大陆裂谷化和裂解作用的响应, 它同时也是全球性早古生代大洋开启的先兆[126]。北祁连洋和南祁连洋可能就是全球性早古生代大洋的2个分支。

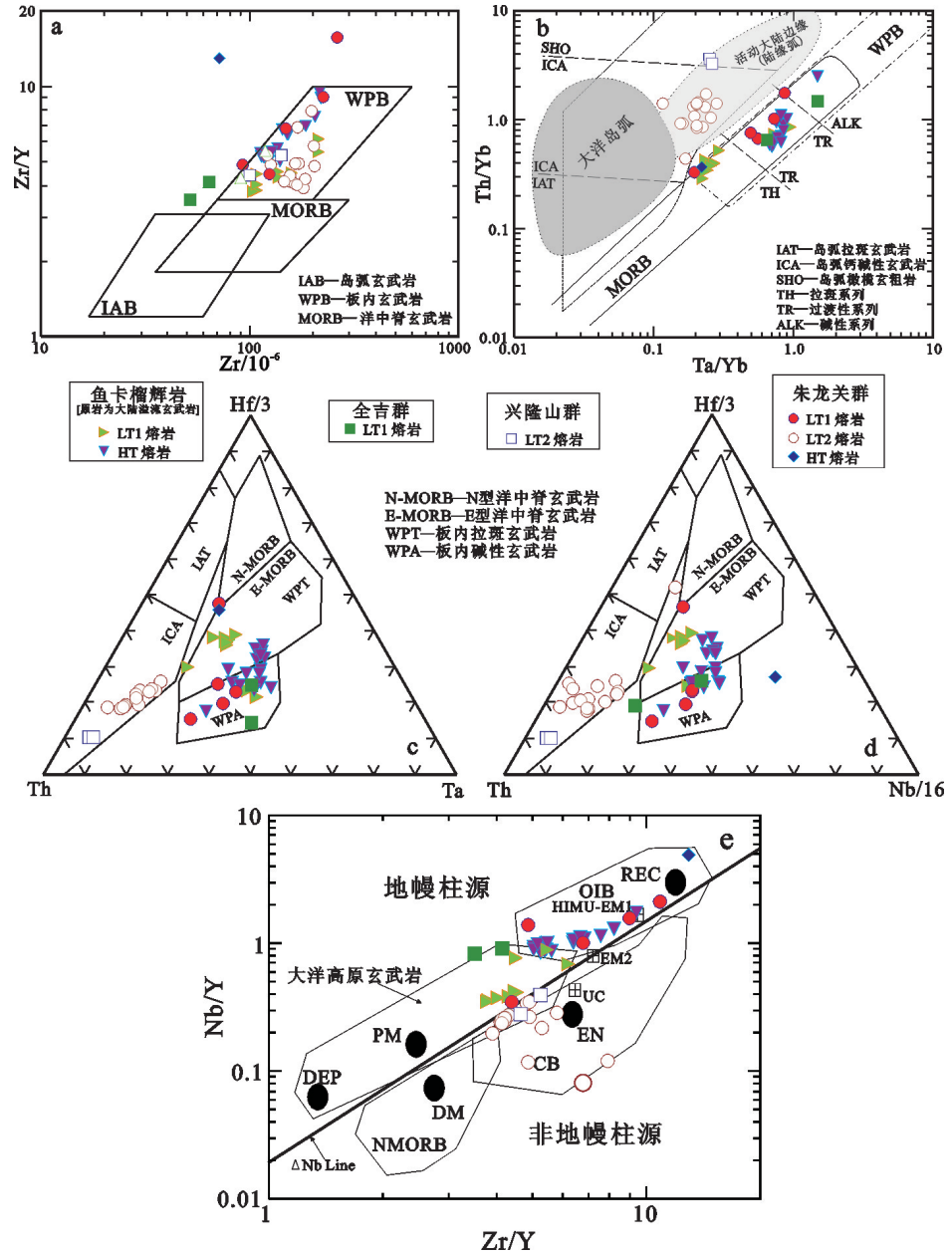

图9 祁连山新元古代中—晚期裂谷玄武质熔岩形成的构造环境判别图解

a—Zr/Y−Zr图解 (据[160]); b—Th/Yb−Ta/Yb图解 (据[161]); c—Hf/3–Th–Ta 图解 (据 [162]); d—Hf/3–Th–Nb/16 图解 (据 [162]); e—祁连山新元古代中−晚期裂谷玄武质熔岩的Zr/Y − Nb/Y 图解(据[167])

缩写符: UC—上部陆壳; CB—受到大陆壳或/和大陆岩石圈混染的大陆玄武岩; PM—原始地幔; DM—浅部亏损地幔; HIMU—高−μ (U/Pb)源; EM1 和EM2 富集地幔源; OIB—洋岛玄武岩; DEP—深部亏损地幔; EN—富集组分; REC—再循环组分

数据来源同图6

Fig. 9 Tectonic setting of Mid−Late Neoproterozoic rift−related basaltic lavas from the Qilian Mountain

a−Zr/Y versus Zr diagram (after [160]); b−Th/Yb versus Ta/Yb diagram (after [161]); c−Hf/3–Th–Ta diagram (after [162]); d−Hf/3–Th–Nb/16 diagram (after reference [162]); e−Zr/Y versus Nb/Y diagram (after reference [167]) for Mid−Late Neoproterozoic rift−related basaltic lavas from the Qilian Mountain

Abbreviations: UC − Upper continental crust; CB − Contaminated (by continental crust or/and subcontinental lithosphere) basalts; PM − Primitive mantle; DM − Shallow depleted mantle; HIMU − High−μ (U/Pb) source; EM1 and EM2 − Enriched mantle sources; OIB − Oceanic island basalt; DEP − Deep depleted mantle; EN − Enriched component; REC − Recycled component

Data sources as for Fig. 6

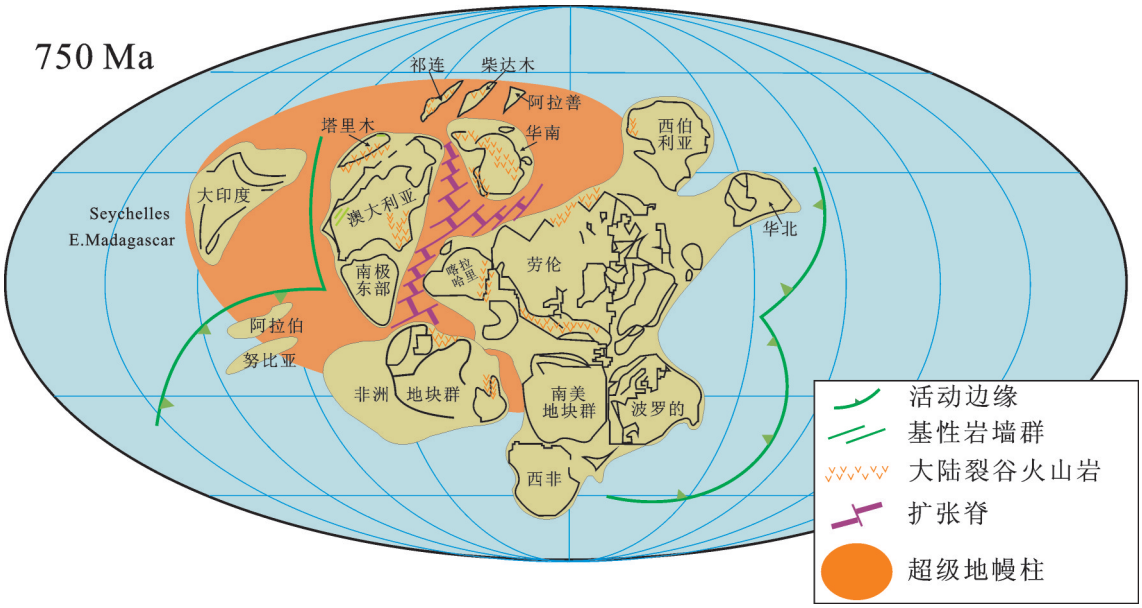

图10 大约750 Ma前Rodinia超大陆裂解状态复原图 (据[177]修编)

Fig. 10 Cartoon diagram showing the breakup of Rodinia at. ca. 750 Ma (modified after reference [177])

3.2 新元古代晚期至寒武纪(550~497 Ma)洋中脊玄武岩(MORB)

新元古代晚期至寒武纪洋中脊玄武岩发育于仰冲到祁连陆块北缘上的北祁连洋壳残片之中(图2)。该仰冲岩片是北祁连大洋板块的组成部分, 其之所以逃脱了在消减带被毁灭的命运, 是由于在洋盆闭合的最后阶段, 这很小的一部分洋壳被仰冲到了被碰撞大陆的前陆之上, 从而以仰冲洋壳残片——蛇绿岩套(ophiolite suite)的形式被保存在大陆造山带的山体之中[13−20, 116]。地质年代学研究已经报道了该洋壳残片的一系列同位素年龄数据, 如: 玉石沟蛇绿岩套中辉长岩的SHRIMP U−Pb锆石年龄: 550~529 Ma[9, 66]; 熬油沟蛇绿岩套中辉长岩的SHRIMP U−Pb锆石年龄: 504~501 Ma[68, 69]; 东草河蛇绿岩套中辉长苏长岩的SHRIMP U−Pb锆石年龄: 497 Ma[67]; 扎马什河蛇绿岩套中枕状玄武岩的U−Pb LA−ICP−MS锆石年龄: 499 Ma[70](图2; 表1)。此外, Zhang et al. [64]还报道了北祁连高压蓝片岩带中百经寺榴辉岩(原岩岩性与蛇绿岩套中的辉长岩相似)的原岩年龄(SHRIMP U−Pb锆石年龄)为502 Ma(表2; 图4)。

该新元古代晚期至寒武纪洋中脊玄武岩实际上为具有完整和不完整假层序的蛇绿岩套的组成部分。具有完整蛇绿岩假层序的蛇绿岩套(如玉石沟蛇绿岩套、东草河蛇绿岩套和扎马什河蛇绿岩套等)自下而上由蛇纹石化方辉橄榄岩、辉长质堆晶岩、枕状玄武岩和辉绿岩墙及沉积岩系(包括有玄武质凝灰岩和硅质岩)[9, 14, 16, 66, 67, 70, 180, 181]等组成。具有不完整假层序的蛇绿岩套(如熬油沟蛇绿岩套)的特点是其原始的蛇绿岩假层序已不复存在, 目前由被肢解的蛇纹岩、辉长岩、块状玄武岩和枕状玄武岩的岩块组成[19, 68, 69, 116]。

此外, 在柴北缘高压—超高压变质带中, 也发现有一些经历了超高压变质的蛇绿岩岩块, 它们系由蛇纹石化方辉橄榄岩、条带状超镁铁质到辉长质堆晶岩(包括有橄榄石−辉石岩、石榴子石−辉石岩和蓝晶石−榴辉岩)和具有MORB原岩岩性的榴辉岩组成, 它们被认为是代表了俯冲的南祁连洋壳的残骸[31, 32, 36, 39, 40, 44, 182]。据报道, 辉长质蓝晶石−榴辉岩的原岩年龄(SHRIMP U−Pb锆石年龄)为550~500 Ma[39, 40](表4; 图4)。

我们的综合研究揭示, 产于仰冲的北祁连洋壳岩片中的新元古代晚期至寒武纪洋脊玄武岩具有下述重要特点:

(1)它们仅由玄武岩组成(图11−a), 均属于拉斑系列(图11−b)。在原始地幔标准化不相容微量元素

蛛网图中, 玉石沟蛇绿岩套和扎马什河蛇绿岩套的所有玄武岩均显示与现今E−MORB相似的不相容微量元素分配型式(图12−a, b); 而其他东草河蛇绿岩套和熬油沟蛇绿岩套中的玄武岩样品, 却具有与现今N−MORB相似的不相容微量元素分配型式(图12−c)。

(2)在各种构造环境地球化学判别图解中, 仰冲的北祁连洋壳岩片中所有玄武质岩石样品的成分点, 均无一例外地落入洋脊玄武岩(MORB)成分域中(图13−a~c)。

(3)随着玄武岩样品的$^{87}Sr/^{86}Sr_{(t)}$比值不断增加(0.705→0.70568), 但其$\varepsilon_{Nd}(t)$值仍保持相对恒定[181](6.8~6.3; 图13−d), 这种现像的产生, 可能是与洋脊玄武岩水下喷发过程中与海水相互作用或受到碳酸盐岩壳混染有关[186]。

(4)在北祁连550~497 Ma洋脊型蛇绿岩套中产出有洋脊型Cu−Zn块状硫化物矿床[17]。

(5)一些研究者[181, 187]认为北祁连洋属于原特提斯洋(proto−Tethyan Ocean)体系。此类提法值得商榷。因为, 特提斯构造域按其原始的定义, 指的是三叠纪时由于冈瓦纳古陆裂解, 在劳亚古陆和冈瓦纳古陆之间形成的一个洋域体系[188, 189]。如前所述, 北祁连洋和南祁连洋实际上应当是由于Rodinia超大陆裂解而产生的全球性早古生代大洋的组成部分(图10)。

3.3 寒武纪—奥陶纪弧和弧后盆地火山岩

3.3.1 北祁连中寒武世—奥陶纪(503~446 Ma)岛弧火山岩

野外填图和系统的地质研究业已查明: 寒武纪至奥陶纪俯冲杂岩带、岛弧火山岩带和弧后盆地火山岩带被完好地保存于北祁连造山带中[13−20, 116](图2)。

代表北祁连山早古生代古海沟俯冲部位的俯冲杂岩带, 迄今为止共发现2条。第一条规模较大, 西起鹰咀山地区, 向东南经玉门镇南昌马地区、石油沟, 再向东南经边马沟—清水沟—百经寺, 直至景阳岭, 发育于托莱山北坡前述仰冲洋壳岩片的北东侧, 东西延展已超过400 km[19]。它是由于大洋板块俯冲、铲刨, 不断在弧前增生而形成的楔形俯冲杂岩增生地体, 包括有含榴辉岩的高级蓝片岩带(具有典型石榴子石 + 多硅白云母 + 蓝闪石 + 绿帘石矿物组合[203, 204])、镁铁质−超镁铁质岩块、火山岩岩片、混杂堆积岩、放射虫硅质岩残片, 以及由滑塌堆积、浊流沉积及复理石组成的增生楔[21]。第二条俯冲杂岩带规模很小, 仅出露于白泉门以西至九个泉一带, 是北祁连寒武−奥陶纪弧后盆地发展演化过程中发育的次级俯冲带[19]。

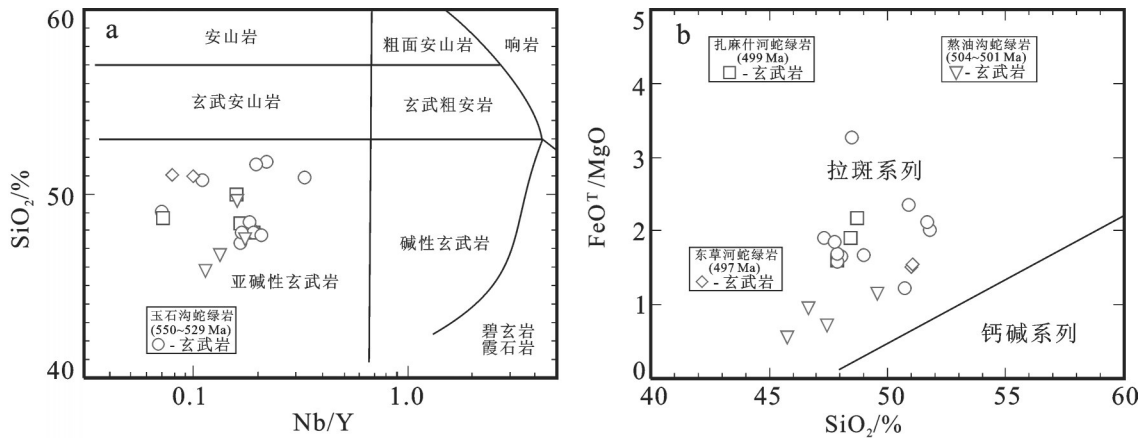

图11 北祁连山仰冲的新元古代晚期—寒武纪洋壳(蛇绿岩)残片中玄武岩的a—SiO_2 − Nb/Y图解 (据[154]) 和b—$FeO^T/MgO-SiO_2$图解 (据 [155])

图11−b适用于图11−a中的亚碱性火山岩;数据来源: [14, 16−18, 66, 67, 69, 70, 81]

Fig.11 a−SiO_2 versus Nb/Y diagrams (after reference [154]) and b−FeO^T/MgO versus SiO_2 diagrams (after reference [155]) for basalts in the obducted slices of Late Neoproterozoic−Cambrian ocean−crust (ophiolites) from the North Qilian Mountain

Fig. 11−b shows the sub−alkaline volcanic rocks as plotted in Fig. 11−a; Data sources: [14, 16−18, 66, 67, 69, 70, 81]

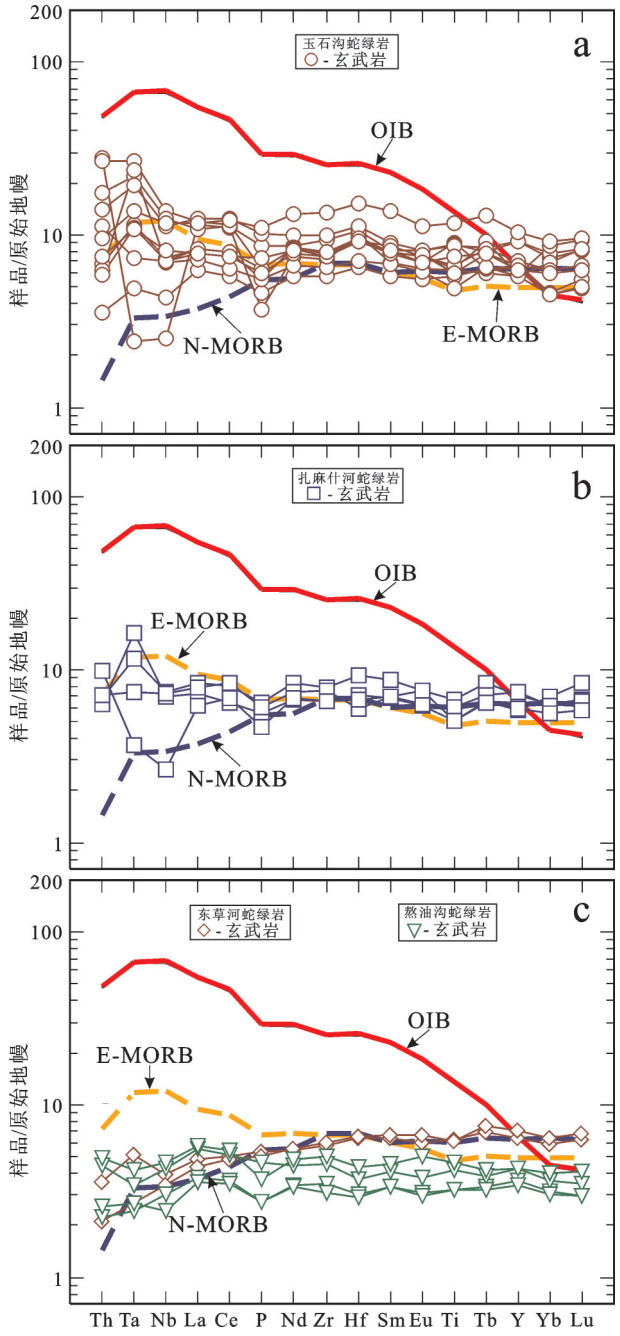

图12北祁连山仰冲的新元古代晚期—寒武纪洋壳(蛇绿岩)残片中玄武岩的不相容微量元素原始地幔(据[156])标准化蛛网图

洋岛玄武岩(OIB)、E型洋脊玄武岩(E-MORB)和N型洋脊玄武岩(N-MORB)据[156]

数据来源同图11

Fig. 12 Primitive mantle (after reference [156]) normalized incompatible trace-element spider diagrams for basalts in the obducted slices of Late Neoproterozoic-Cambrian ocean-crust (ophiolites) from the North Qilian Mountain

Patterns for oceanic island basalts (OIB), E-type mid-ocean ridge basalts (E-MORB) and N-type mid-ocean ridge basalts (N-MORB) after reference [156]

Data sources as for Fig. 11

北祁连中寒武世—奥陶纪岛弧火山岩带位于前述俯冲杂岩带的北东侧[9, 13, 14, 16, 71-76]。研究查明, 北祁连早古生代岛弧火山作用具有中心式喷发和裂隙式喷发等2种产态[13-19]。

我们的综合研究揭示, 北祁连中寒武世—奥陶纪岛弧火山岩具有下述重要特点:

(1)出露于永登县石灰沟地区的岛弧火山岩系(图2), 下部属拉斑岩系, 中部属钙碱系列, 上部为橄榄玄粗岩系列(shoshonitic series)(图14-a, b)。岛弧火山岩系上部层位中橄榄玄粗岩系(包括有粗面玄武岩、白榴碱玄岩、白榴方沸岩和白榴粗面斑岩等)的出现, 是北祁连古岛弧体系在晚奥陶世已达到成熟阶段的重要标志[13-20]。区域岩石学研究查明, 北祁连早古生代岛弧火山岩系中, 石灰沟式岛弧火山岩系为裂隙式火山喷发的产物[13-16]。此类裂隙式岛弧火山岩系, 在门源县银灿地区也有发育[76](图2, 图14-g, h; 表1)。该裂隙式岛弧火山岩系主要由中性熔岩, 其次为玄武质岩石和火山碎屑岩组成。

(2)北祁连山东部的白银地区, 发育有典型的双峰式(由长英质熔岩、玄武质熔岩及同质火山碎屑岩构成)岛弧裂谷型火山岩套(图14-c, d)。研究查明, 此类双峰式火山岩套通常为岛弧裂谷环境下中心式喷发的产物[19, 20]。典型的白银式Cu-Pb-Zn块状硫化物矿床就赋存于该岛弧裂谷型双峰式火山岩套的长英质火山岩石之中[17, 19]。此外, 在北祁连岛弧火山岩带的中部(祁连县地区)和西部(边马沟地区)(图2)也发育有由酸性火山岩和基性火山岩构成的岛弧裂谷型双峰式火山岩套[19, 20](图14-e, f)。

(3)上述中寒武世—奥陶纪岛弧火山岩系中的玄武质熔岩具有岛弧系玄武岩的典型地球化学特点: ①除了橄榄玄粗岩系外, 其余的玄武质熔岩均具有很低的(与消减带玄武岩相似的)不相容微量元素浓度和明显的Nb, Ta和Ti负异常(图15-a, c, e, g); ②所有玄武质熔岩的成分点均落入弧(包括大洋弧和大陆弧)玄武岩的成分域内(图15-b, d, f, h)。

(4)北祁连弧火山岩样品中, Sr、Nd同位素成分的变化很大(图16)。边马沟地区的岛弧熔岩显示随着 $^{87}Sr/^{86}Sr_{(t)}$ 比值增高(0.707→0.712)$\varepsilon_{Nd}(t)$ 值却保持相对恒定(3.1~4.1)的特点[191](图16-a), 这种Sr、Nd同位素成分的变化特点可能是与这套岛弧熔岩系水下喷发有关, 反映了水下喷发的熔岩与海水相互

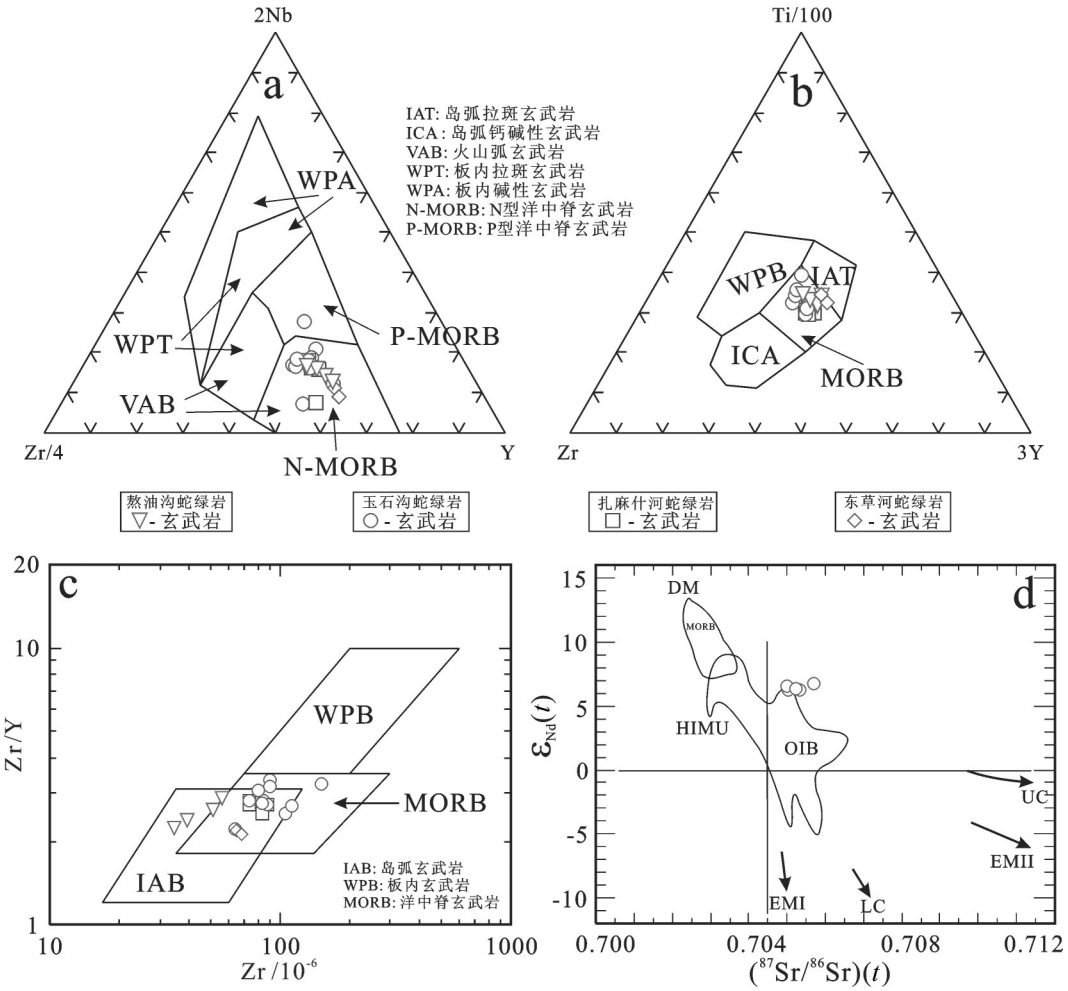

图13 北祁连山仰冲的新元古代晚期—寒武纪洋壳(蛇绿岩)残片中玄武岩的构造环境判别图解

a—2Nb−Zr/4−Y 图解 (据 [183]); b—Ti/100–Zr–3Y 图解 (据 [184]); c—Zr/Y − Zr 图解 (据 [160]); d—玉石沟蛇绿岩中玄武岩的 $\varepsilon Nd(t) - {}^{87}Sr/{}^{86}Sr(t)$图解 (据[185])

UC—上地壳; LC—下地壳; EM I和EM II—富集地幔源I和II; HIMU—高μ地幔源; DM—亏损地幔源

数据来源同图11

Fig. 13 Tectonic setting of basalts in the obducted slices of Late Neoproterozoic−Cambrian ocean−crust (ophiolites) from the North Qilian Mountain

a−2Nb−Zr/4−Y diagram (after reference [183]); b−Ti/100−Zr−3Y diagram (after reference [184]); c−Zr/Y vesus Zr diagram (after reference [160]); d −εNd(t) versus $^{87}Sr/^{86}Sr(t)$ diagram for the basalts in the Yushigou ophiolite (after reference [185])

UC − Upper crust; LC − Lower crust; EM I and EM II − Enriched mantle I and II sources; HIMU − High−μ mantle source; DM − Depleted mantle source

Data sources as for Fig. 11

作用或是受到了碳酸盐壳的混染[186]。图16−b显示, 石灰沟地区和白银地区的岛弧玄武岩具有较高的 $^{87}Sr/^{86}Sr_{(t)}$ 比值 (0.7055~0.7075)和较低的$\varepsilon_{Nd}(t)$ 值 (−1.2 ~ +4.4), 同一地区的长英质熔岩, 却具有较低的 $^{87}Sr/^{86}Sr_{(t)}$ 比值(0.7044~0.7077)和较高的 $\varepsilon_{Nd}(t)$ 值 (+4.6 ~ +8)[16, 72]。

(5)在北祁连造山带中, 广泛地发育有同时代的火山弧花岗岩类侵入体(图3)。地质年代学研究揭示: 它们形成于北祁连洋壳俯冲的时代[9, 88−91, 94](从520 Ma至446 Ma, 表3)。其中, 有一些较大的花岗岩类侵入体研究得较为深入, 它们是: ①柯柯里石英闪长岩−斜长花岗岩体[88] (512~476 Ma; 表3), ②柴达诺花岗岩体 [9, 88] (516~508 Ma; 表3), ③牛心山花岗岩体[89] (477 Ma; 表3), ④窑沟花岗闪长岩体[89] (463

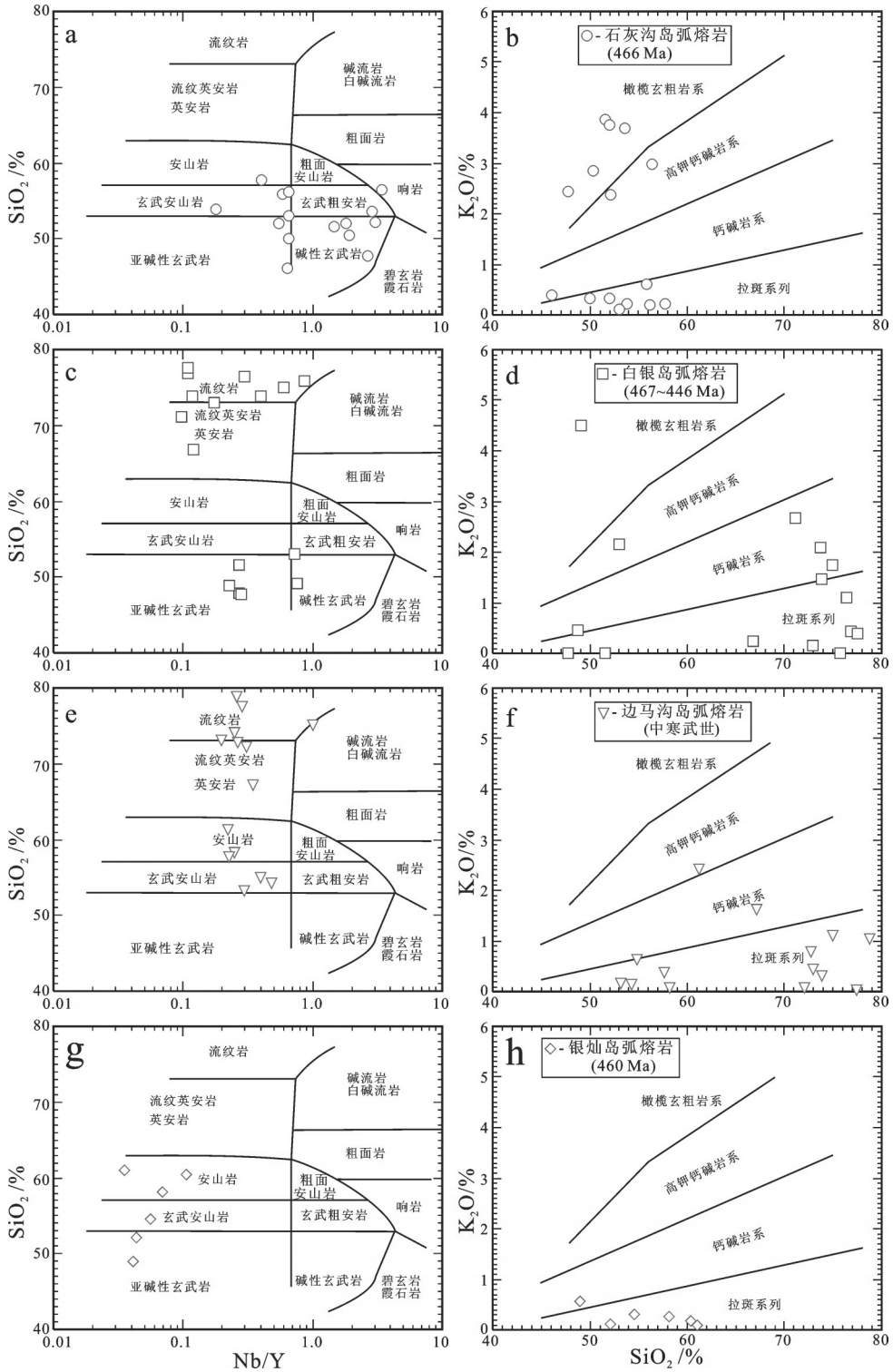

图14 北祁连山中寒武世—奥陶纪弧火山岩的a, c, e, g—SiO_2 − Nb/Y 图解 (据[154])和b, d, f, h—K_2O − SiO_2图解 (据 [190])
数据来源: (a, b): [13, 14, 16, 17, 20]; (c, d): [14, 16, 17, 72]; (e, f); [19, 20, 191]; (g, h): [76]

Fig. 14 a, c, e, g−SiO_2 versus Nb/Y diagrams (after reference [154]) and b, d, f, h−K2O versus SiO_2 diagrams (after reference [190]) for Middle Cambrian-Ordovician arc−related volcanic rocks from the North Qilian Mountain
Data sources: (a, b): [13, 14, 16, 17, 20]; (c, d): [14, 16, 17, 72]; (e, f): [19, 20, 191; (g, h): [76]

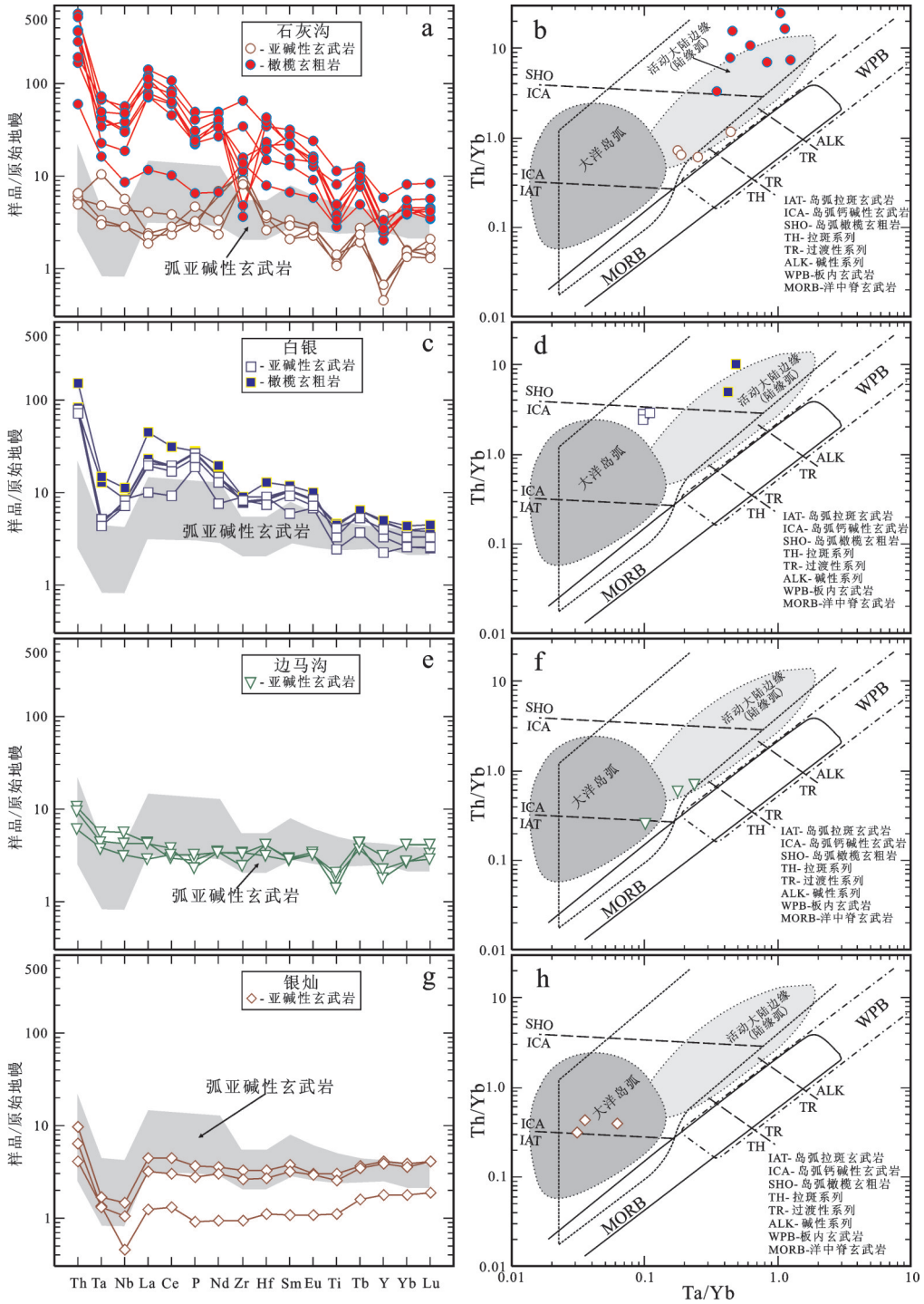

图15 北祁连山中寒武世—奥陶纪弧火山岩的a, c, e, g—不相容微量元素原始地幔 (据[156]) 标准化蛛网图和b, d, f, h—Th/Yb−Ta/Yb图解(据 [161])

图中阴影区表示弧亚碱性玄武岩的成分范围, 其下限和上限分别由低–K 玄武岩和高–K 玄武岩的平均值(据 [157])限定

数据来源同图14

Fig. 15 a, c, e, g−Primitive mantle (after reference [156]) normalized incompatible trace−element spider diagrams and b, d, f, h −Th/Yb versus Ta/Yb diagrams (after reference [161]) for Middle Cambrian−Ordovician arc−related volcanic rocks from the North Qilian Mountain

The shaded area shows the range for arc sub−alkaline basalts, with the lower and upper limits being defined by “average” low−K and high−K basalts, respectively (after reference [157])

Data sources as for Fig. 14

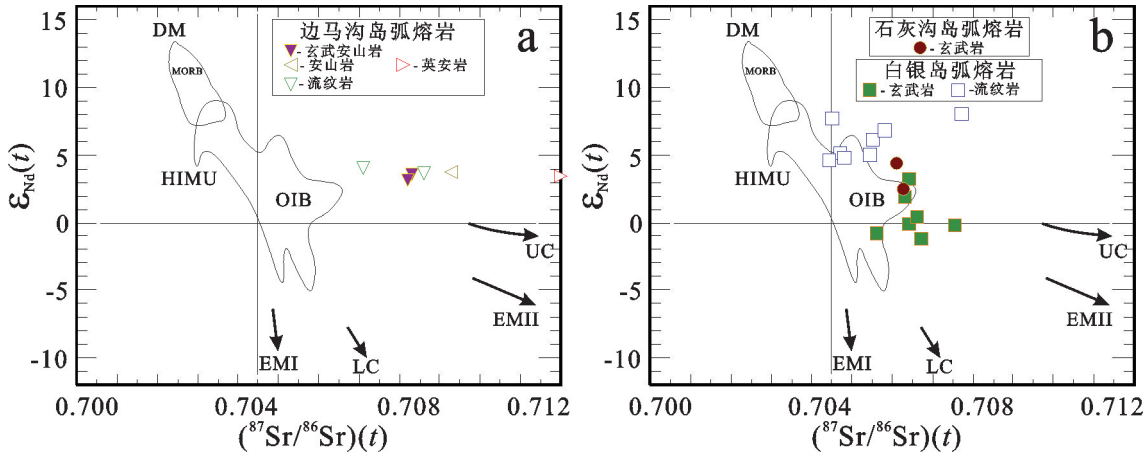

图16 a, b—北祁连山中寒武世—奥陶纪弧火山岩的$\varepsilon_{Nd}(t)$ −$^{87}Sr/^{86}Sr(t)$ 图解(据[185])

UC—上地壳; LC—下地壳; EM I和EM II—富集地幔源I和II; HIMU—高μ地幔源; DM—亏损地幔源

数据来源同图14

Fig.16 a, b−Plots of $\varepsilon_{Nd}(t)$ versus $^{87}Sr/^{86}Sr(t)$ for Middle Cambrian−Ordovician arc−related volcanic rocks from the North Qilian Mountain (diagram after [185])

UC−Upper crust; LC − Lower crust; EM I and EM II−Enriched mantle I and II sources; HIMU−High−μ mantle source; DM − Depleted mantle source

Data sources as for Fig. 14

Ma; 表3), ⑤雷公山英云闪长岩体[91] (453 Ma; 表3)。

应当指出, 对于北祁连早古生代洋盆的俯冲方向一直存在争议。第一种意见认为是向北俯冲[7−9, 11, 13−16, 19, 20, 22]。第二种意见推断是向南俯冲[187, 196−199]。第三种意见则主张为双向俯冲[88, 200]。在“引言”一节中已经提及, 区域尺度(规模)上, 北祁连造山带中, 自南向北, 从中寒武世—奥陶纪俯冲杂岩带, 经岛弧火山岩带, 至弧后盆地火山岩带, 3个岩带间近乎平行地分布(图2), 明确无误地意味着: 早古生代北祁连大洋岩石圈是向北俯冲, 不是向南俯冲。岛弧火山岩的年龄数据(503~446 Ma; 表1)和北祁连大洋岩石圈俯冲过程中峰期高压变质作用(即前进变质作用)的年龄(489~446 Ma; 表2)表明: 自503 Ma至446 Ma的年龄范围可能恰恰是反映了北祁连洋壳俯冲的时限。

3.3.2 北祁连寒武纪至奥陶纪(517~449 Ma)弧后盆地火山岩

北祁连寒武纪至奥陶纪(517~449 Ma; 表1)弧后盆地带位于岛弧带的后方(即东北侧)(图2)。以往的研究查明: 强烈的弧后海底扩张发生于弧后盆地带的东部(老虎山地区)和西部(大坂—大岔和卡马尔沟—九个泉地区), 导致形成弧后扩张脊型蛇绿岩套。此类弧后扩张脊型蛇绿岩套的上部枕状熔岩中, 产出有塞浦路斯型Cu−Zn块状硫化物矿床[16, 19, 20](图2, 图17)。弧后扩张脊型蛇绿岩套乃是仰冲的弧后盆地海底。以往的研究揭示, 在北祁连山东部, 志留系和更年轻的地层覆盖在岛弧和弧后盆地带之上, 但观察不到岛弧和弧后盆地带二者之间的接触关系(为更为年轻的沉积地层所覆盖)。然而, 在北祁连山西部, 自边马沟到白泉门(即从南向北), 可以观察到, 岛弧和弧后盆地对火山岩系连续出露, 提供了十分完整的从岛弧向弧后盆地发展的岛弧→弧后盆地演化序列[19, 20](图2, 图17)。

野外填图揭示, 边马沟到肃南地区, 自南向北存在有3个主要地质单元, 即: “岛弧单元”、“弧后盆地单元”和“志留纪前陆盆地单元”(图17)。3个单元之间为断层接触。岛弧单元主要由双峰式火山岩组成, 实为岛弧裂谷单元[20]。弧后盆地单元由2种具有不同蛇绿岩序列的火山−沉积岩系组成。一些地方可以见到, 弧后盆地单元被由浅海相到陆相砾岩、砂岩和灰岩组成的泥盆纪磨拉石建造不整合上覆。前陆盆地单元系由志留纪初始磨拉石组成(包括有页岩、板岩、砂岩、和砾岩, 图17)。

我们的综合研究揭示, 北祁连寒武纪至奥陶纪弧后盆地火山岩具有下述重要特点:

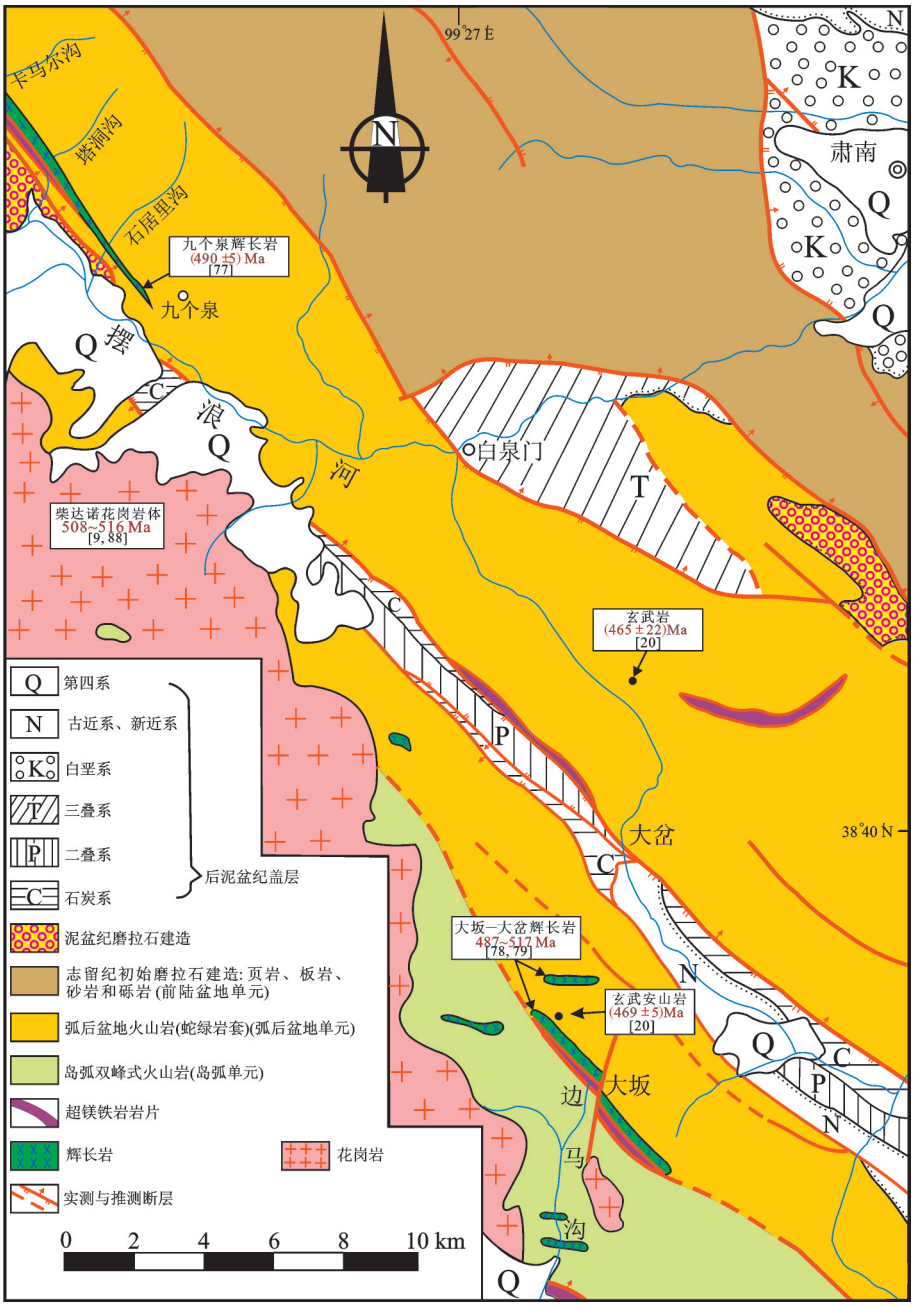

图 17 北祁连山边马沟—肃南地区早古生代岛弧和弧后盆地地质略图(据[20]修编)

Fig.17 Geological sketch map of the early Paleozoic island arc and back-arc basins in the Bianmagou-Sunan area of the North Qilian Mountain (modified after reference [20])

(1)北祁连山西段边马沟至大坂一带的岛弧裂谷单元(图17)系由流纹英安岩-流纹岩和玄武安山岩-安山岩组成的双峰式岩套构成(图14-e, f), 系为弧后盆地形成早期阶段岛弧裂谷化的产物[19, 20]。

(2)弧后盆地单元南部(从大坂到大岔一带)(图17), 弧后盆地熔岩为弧后盆地蛇绿岩套的组成部分, 该蛇绿岩套自底部到顶部, 系由蛇纹石化方辉橄榄岩、辉长岩(具有517~487 Ma的锆石SHRIMP U-Pb年龄[78, 79]; 表1)、辉绿岩墙(具钠长花岗闪长岩脉)、枕状熔岩、块状玄武岩和凝灰岩组成。前述辉绿岩墙清楚地植根于辉长岩中, 它们起着为上覆玄武岩提供熔岩补给的补给通道的作用[19, 20]。弧后盆

地熔岩由玄武岩、玄武安山岩(具有469 Ma的Sm−Nd等时线年龄[20]; 表1)和安山岩组成(图18−a, b)。根据其元素地球化学特点, 中性熔岩具有玻安岩(Boninite)的地球化学图谱: 高SiO_2 (55%~61%)、高MgO (5%~17%)、高相容微量元素含量(Ni = 80×10^{-6}~420 ×10^{-6}, Cr = 300×10^{-6}~1250×10^{-6})、TiO_2含量很低(< 0.35%)(图22−a~d)。Crawford et al. [202]曾指出玻安岩系列岩浆可能是在弧火山作用停止、弧后扩张开始的情况下产生。

(3)弧后盆地单元南部的弧后盆地玄武岩显示强烈的弧的信号(图19− a, b), 它们同时具有似MORB和似弧的双重特点(图19−a, b)。产生这种似MORB + 似弧的双重地球化学特点, 是由于这里的初始弧后盆地是通过岛弧裂谷化产生, 此过程中, 被消减作用改造的地幔组分必然会卷入到弧后盆地岩浆的生成过程之中, 因而造成弧后扩张中心玄武岩具有向弧玄武岩过渡的地球化学特点。因此, 北祁连山早古生代弧后盆地单元南部的构造演化, 极为生动地描述了经岛弧裂谷化诞生弧后盆地的过程。其成因上显然是与岛弧裂谷化导致最早期弧后盆地的打开有关[20]。

(4)弧后盆地单元的北部是以弧后扩张脊型玄武质熔岩为特征, 此类弧后扩张脊型玄武岩构成了该处弧后盆地蛇绿岩套的重要组成部分。弧后盆地单元北部的弧后盆地蛇绿岩套自底部向顶部由蛇纹石化方辉橄榄岩、辉长岩(具有490 Ma的 锆石SHRIMP U−Pb年龄[77]; 表1)、辉绿岩墙、枕状玄武岩(具有465 Ma的Sm−Nd等时线年龄[20]; 表1)、凝灰

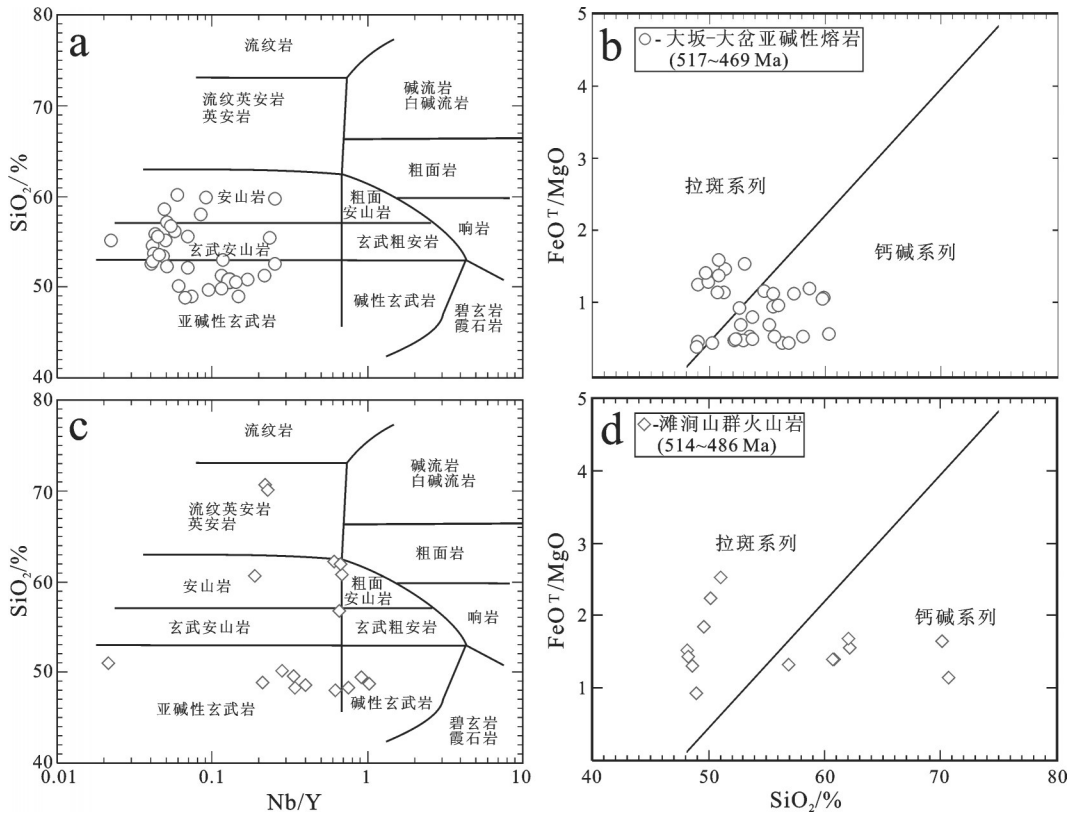

图18 a, b—北祁连山大坂—大岔地区火山岩(517~469 Ma)和c, d—柴北缘滩涧山群火山岩(514~486 Ma)的SiO_2−Nb/Y图解(图解据 [154])和$FeO^T/MgO-SiO_2$ 图解 (图解据[155])

图b, d分别适用于图a, c中的亚碱性火山岩;数据来源: (a, b): [16−19, 78, 79, 192]; (c, d): [57, 58]

Fig.18 SiO_2 versus Nb/Y diagrams (after reference [154]) and FeO^T/MgO versus SiO_2 diagrams (after reference [155]) for a, b− Volcanic rocks (517−469 Ma) in the Daban−Dacha area of the North Qilian Mountain and c, d− Tanjianshan Group volcanic rocks (514−486 Ma) from the North Qaidam

Fig. 18−b, d show the sub−alkaline volcanic rocks as plotted in Fig 18−a, c;Data sources: (a, b): [16−19, 78, 79, 192]; (c, d): [57, 58]

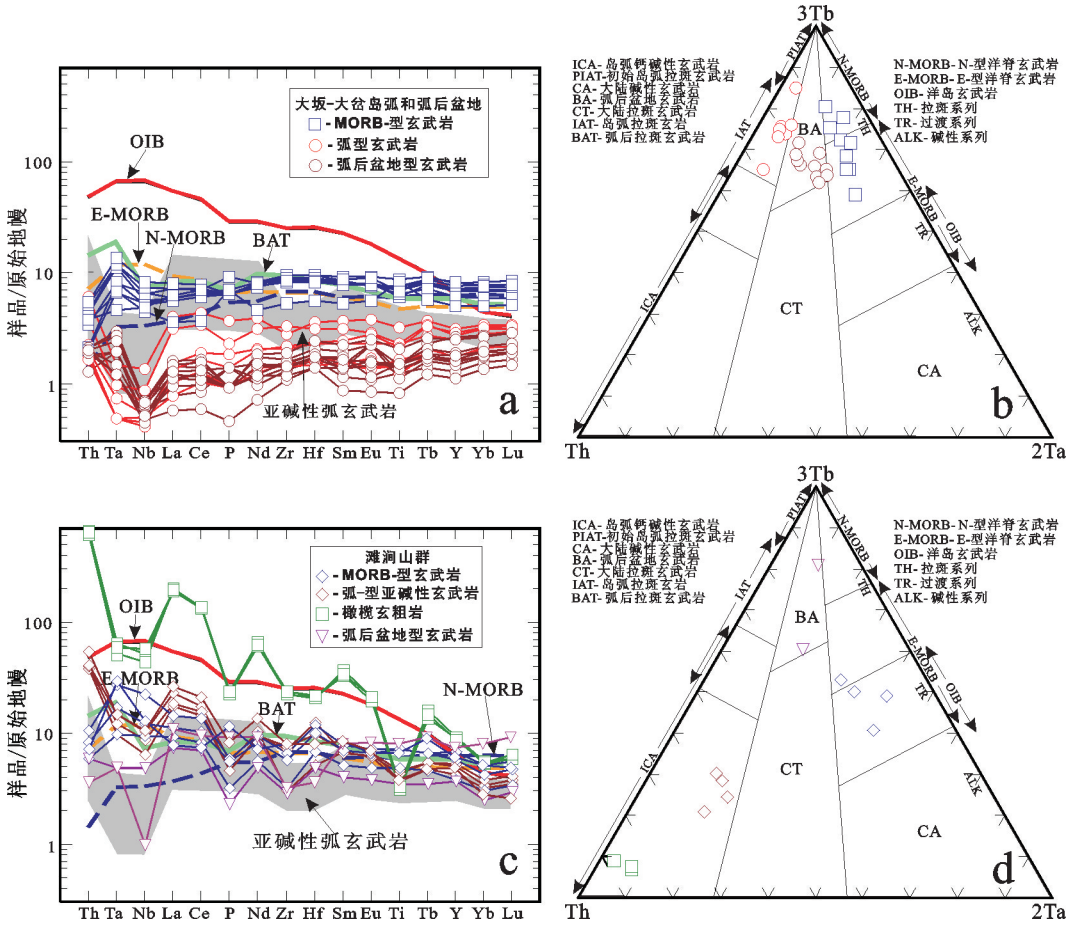

图19 北祁连山大坂—大岔地区火山岩(517~469 Ma)和柴北缘滩涧山群火山岩(514~486 Ma)的 a, c—不相容微量元素原始地幔 (据[156]) 标准化蛛网图和b, d—3Tb−Th−2Ta 图解 (据 [193])

洋岛玄武岩(OIB)、E型洋脊玄武岩(E−MORB)和N型洋脊玄武岩(N−MORB)据[156]; 弧后拉斑玄武岩(BAT)据[194]

数据来源同图18

Fig. 19 a, c−Primitive mantle (after reference [156]) normalized incompatible trace−element spider diagrams and b, d−3Tb−Th−2Ta diagrams (after reference [193]) for the volcanic rocks (517~469 Ma) in the Daban−Dacha area of the North Qilian Mountain and the Tanjianshan Group volcanic rocks (514~486 Ma) from the North Qaidam

Patterns for oceanic island basalts (OIB), E−type mid−ocean ridge basalts (E−MORB) and N−type mid−ocean ridge basalts (N−MORB) after reference [156]. Patterns for back−arc tholeiites (BAT) after reference [194]

Data sources as for Fig. 18

质板岩、枕状玄武岩、玄武岩、玄武质凝灰岩和硅质岩组成。此类弧后盆地蛇绿岩套的产出乃是该地区曾经发生弧后海底扩张的标志, 它代表了被保存于造山带中的弧后盆地的仰冲海底[14−20]。此类弧后扩张脊型蛇绿岩套出露于北祁连山的西部(沿摆浪河, 从九个泉经石居里沟、卡马尔沟至塔洞沟一带)和东部(老虎山地区)[19, 20](图2, 图17)。

(5)弧后扩张脊型熔岩主要由属拉斑系列的玄武质熔岩组成(图20−a~d)。虽然弧后盆地南部和弧后盆地北部的玄武岩在地质产状和岩石学特点上十分相似, 但是弧后盆地北部的玄武岩具有更为强烈的MORB特征(图21−a~d)。十分明显, 从弧后盆地的南部向着弧后盆地的北部, 弧后盆地火山岩的性质也反映出弧后扩张作用逐渐地越来越成熟。也就是说, 最年轻的岛弧裂谷化的产物是发育于南部(表现为弧后盆地南部的玄武岩具有强烈的消减带信号, 图19−a, b), 而弧后扩张作用相对成熟阶段的产物则分布于北部(表现为弧后盆地北部的玄武岩具有更为强烈的MORB习性, 图21−a~d)[19, 20]。

(6)北祁连弧后盆地带的中段(如扁都口地区)未

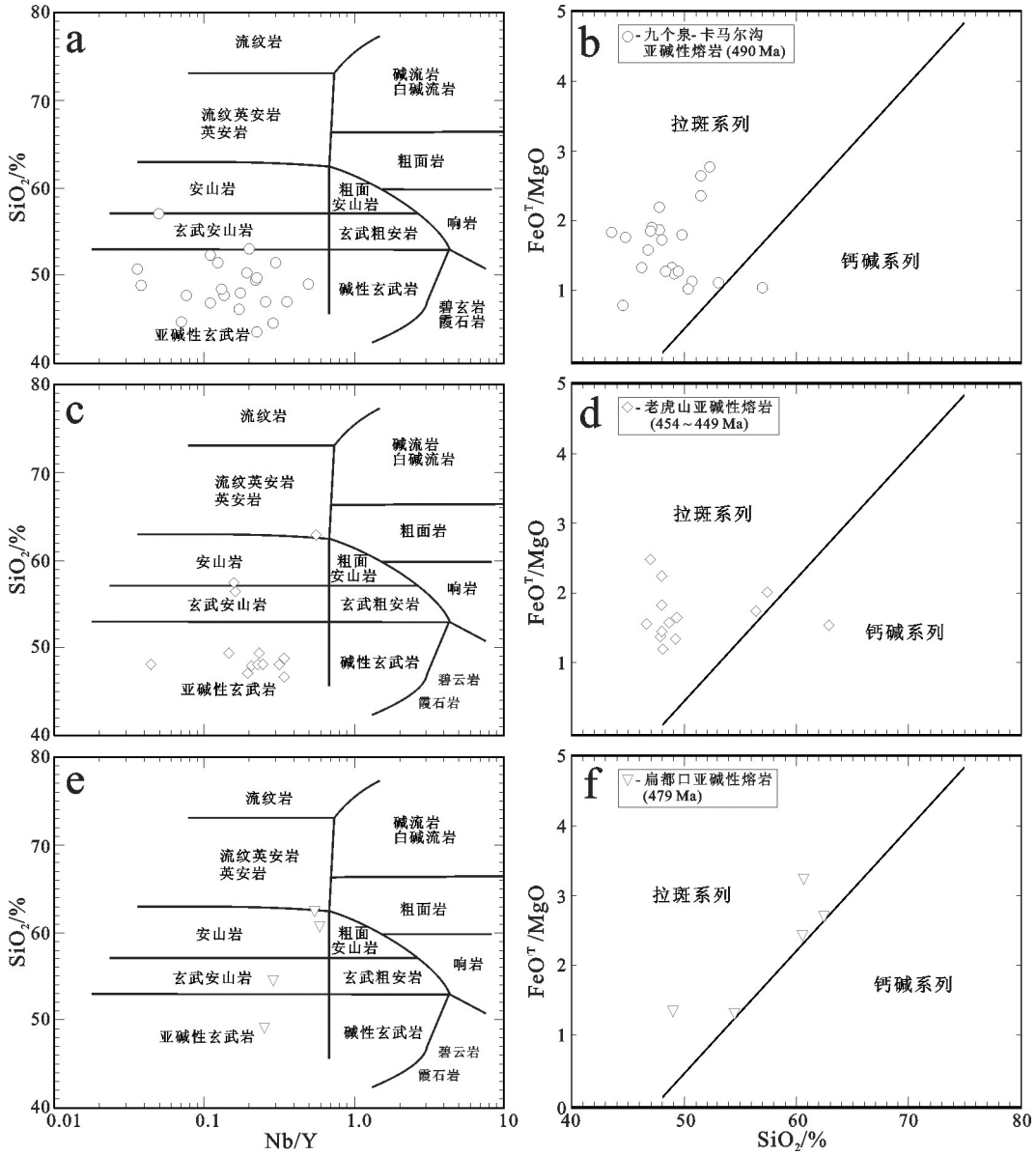

图20 北祁连山弧后盆地火山岩(490~449 Ma)的a, c, e—SiO_2 − Nb/Y图解(图解据 [154])和b, d, f—FeO^T/MgO − SiO_2 图解(图解据[155])

图b, d, f分别适用于图a, c, e中的亚碱性火山岩;数据来源: (a, b): [16−20, 77, 191]; (c, d): [16−20, 195]; (e, f): [16−18]

Fig. 20 a, c, e−SiO_2 versus Nb/Y diagrams (after Winchester and Floyd, 1977) and b, d, f−FeO^T/MgO versus SiO_2 diagrams (after Miyashiro, 1975) for the volcanic rocks (490−449 Ma) in the back−arc basins from the North Qilian Mountain

Fig. 20 b, d, f show the sub−alkaline volcanic rocks as plotted in Fig. 20 a, c, e

Data sources: (a, b): [16−20, 77, 191]; (c, d): [16−20, 195]; (e, f): [16−18]

发现蛇绿岩套[19, 20]。扁都口地区的弧后盆地熔岩由玄武岩、玄武安山岩和安山岩构成, 属拉斑系列(图20−e, f)。扁都口地区的玄武质熔岩仅仅具有弧后盆地玄武岩(BAB)的习性, 没有显示任何弧玄武岩或洋脊玄武岩(MORB)的特性(图21−e, f)。所有上述特点, 意味着在北祁连弧后盆地带的中段, 并没有发生过强烈弧后海底扩张, 弧后盆地的海底没有露出[19, 20]。

(7)宽度200~500 m的NW向低级蓝片岩(具有典型方柱石 + 绿纤石 + 蓝闪石 + 文石矿物组合[203, 204])

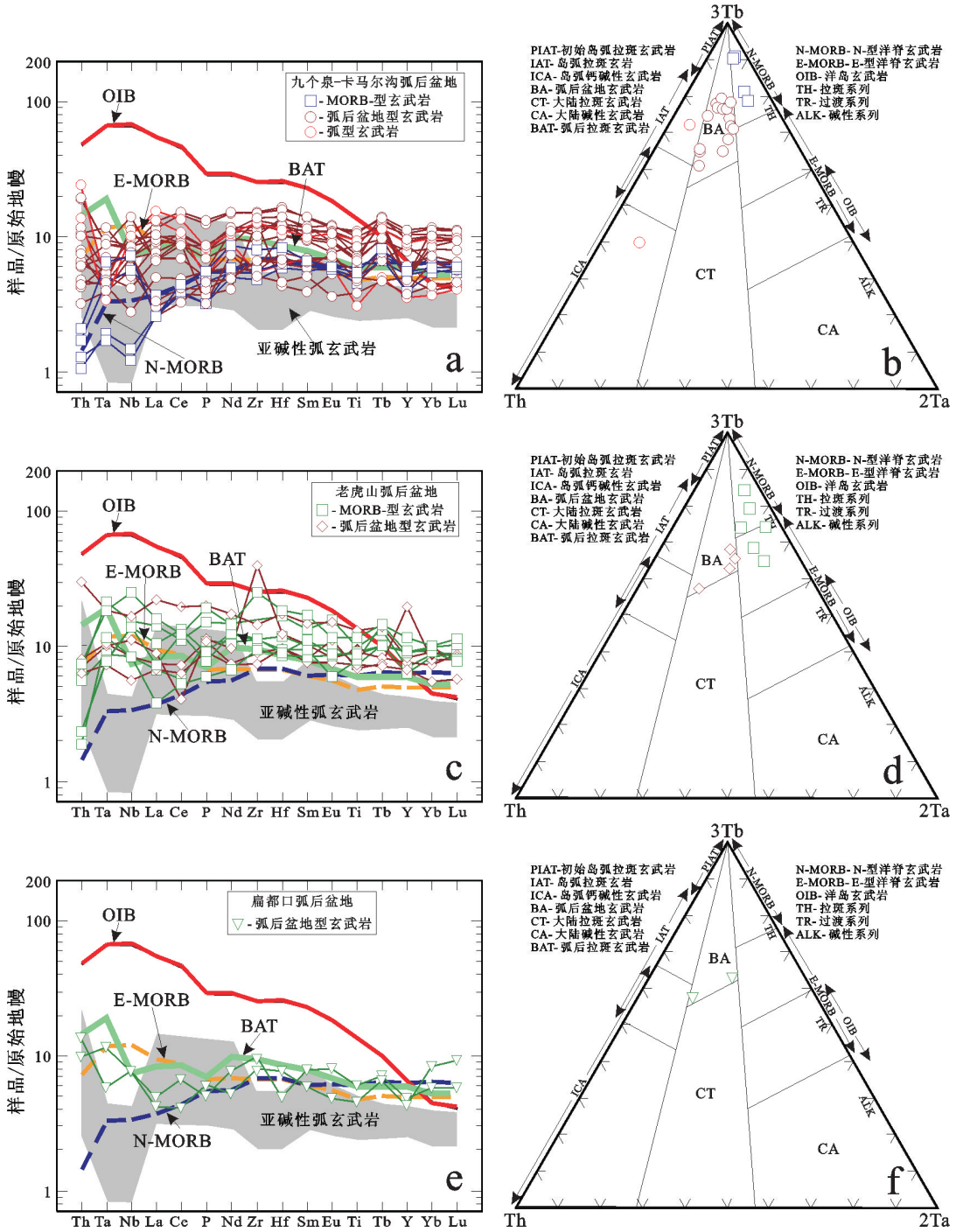

图21 北祁连山弧后盆地玄武质熔岩(490~449 Ma)的a, c, e—不相容微量元素原始地幔 (据[156]) 标准化蛛网图和b, d, f—3Tb−Th−2Ta 图解 (据 [193])

洋岛玄武岩(OIB)、E型洋脊玄武岩(E−MORB)和N型洋脊玄武岩(N−MORB)据[156]; 弧后拉斑玄武岩(BAT)据[194]

数据来源同图20

Fig.21−a, c, e−Primitive mantle (after reference [156]) normalized incompatible trace−element spider diagrams and b, d, f−3Tb−Th−2Ta diagrams (after reference [193]) for the basaltic lavas (490−449 Ma) in the Back−arc basins from the North Qilian Mountain

Patterns for oceanic island basalts (OIB), E−type mid−ocean ridge basalts (E−MORB) and N−type mid−ocean ridge basalts (N−MORB) after reference [156]. Patterns for back−arc tholeiites (BAT) after reference [194]

Data sources as for Fig. 20

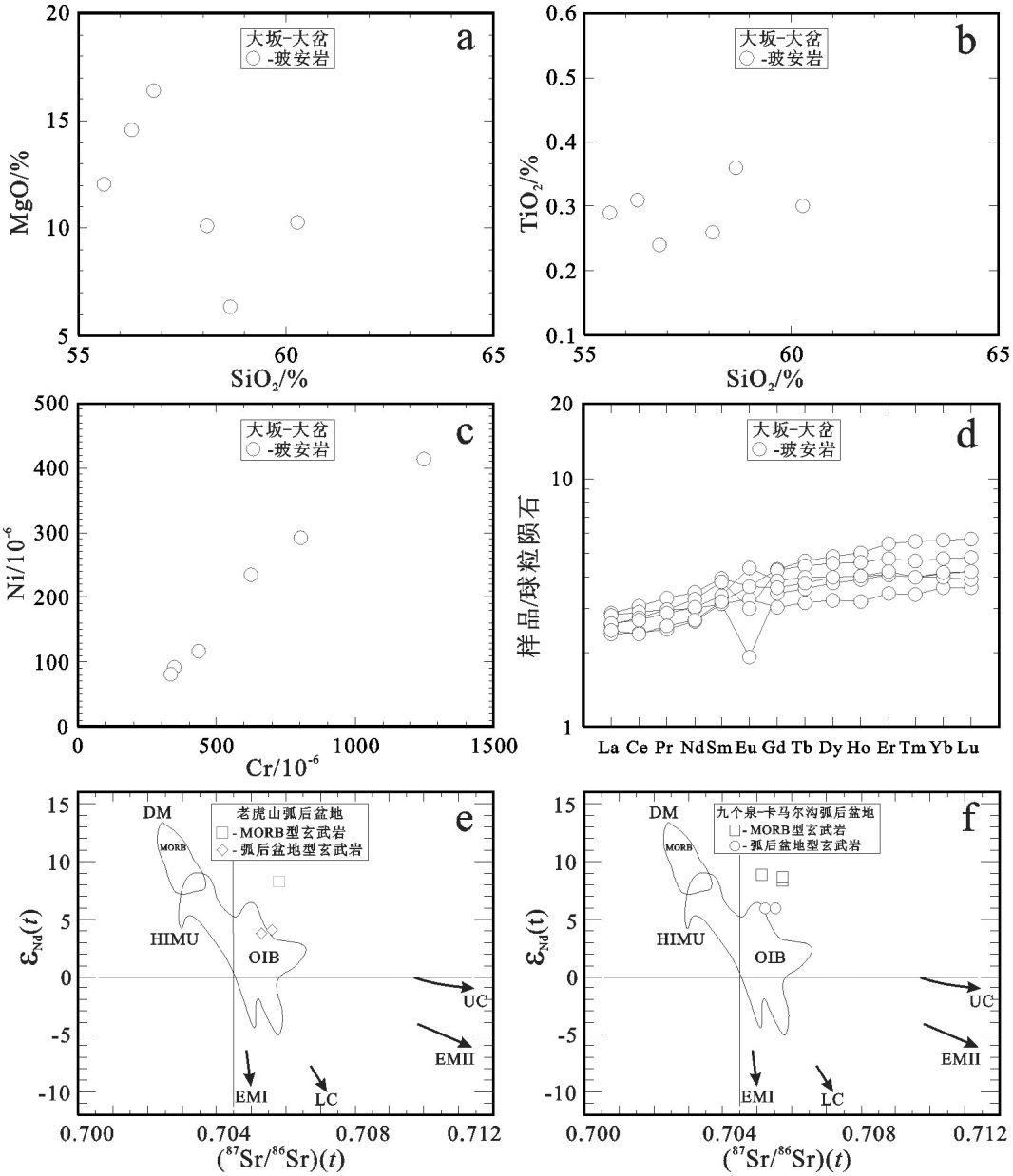

图22 北祁连山大坂—大岔地区玻安岩的a—MgO − SiO_2 图解, b—TiO_2 −SiO_2 图解, c—Ni−Cr 图解和d—REE球粒陨石(据 [201])标准化蛛网图; e和f—老虎山和九个泉—卡马尔沟弧后盆地中玄武岩的$\varepsilon_{Nd}(t)$−$^{87}Sr/^{86}Sr(t)$图解, 图解据[185]

UC—上地壳; LC—下地壳; EM I和EM II—富集地幔源I和II; HIMU—高μ地幔源; DM—亏损地幔源数据来源同图18和图20

Fig. 22 a−MgO versus SiO_2 diagram, b−TiO_2 versus SiO_2 diagram, c−Ni versus Cr diagram and d−Chondrite (after reference [201]) normalized spider diagram for the boninites in the Daban−Dacha area from the North Qilian Mountain; e and f−Plots of $\varepsilon_{Nd}(t)$ versus $^{87}Sr/^{86}Sr(t)$ for the basalts in the Laohushan and the Jiugequan−Kamargou back−arc basins (diagrams after [185])

UC−Upper crust; LC−Lower crust; EM I and EM II−Enriched mantle I and II sources; HIMU−High−μ mantle source; DM−Depleted mantle source

Data sources as for Fig. 18 and Fig. 20

带, 沿着距肃南县城南西方向约20 km的摆浪河延伸20 km左右。该低级蓝片岩带代表了被折返的北祁连弧后扩张海底的次级俯冲带[19]。

此处, 我们可以利用图23解释北祁连弧后盆地形成过程中地幔对流方式和熔体产生作用的变化。在一个没有发生裂谷化的岛弧中, 岛弧岩浆是通过地幔流底辟上升。但是, 在通过岛弧裂谷化形成弧后盆地的早期阶段, 这些熔体从岛弧转向了附

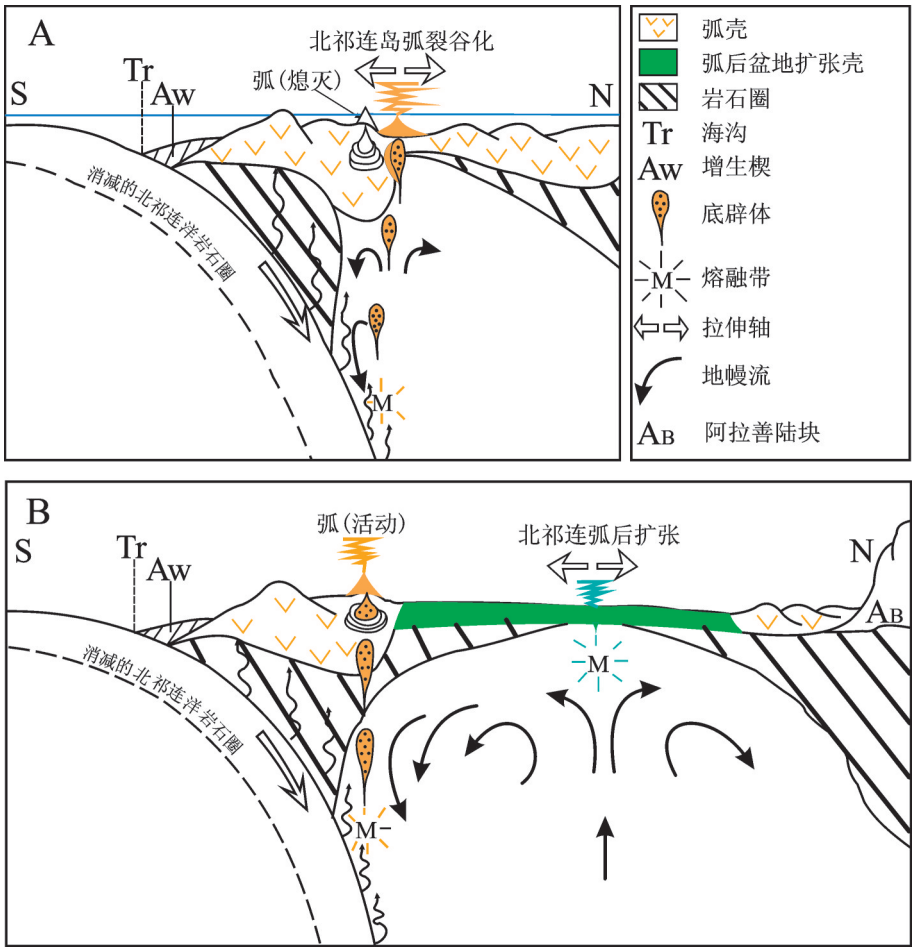

图23 北祁连山弧后盆地构造演化示意图
(显示地幔对流方式和熔体产生过程的变化, 据[20]修编)

A—早期的岛弧裂谷化没有扰乱地幔中岛弧岩浆生成的正常过程, 悬浮的底辟体克服周围地幔由于消减板片俯冲引起的下沉而上升, 产生岛弧熔体, 这些熔体从岛弧转向附近的裂谷区; B—弧后海底扩张体制的建立反映弧后盆地扩张脊之下地幔的上隆, 从而导致近于绝热状态的柱状地幔发生减压熔融, 这一过程和正常洋中脊处发生的作用相似。随着底辟体克服周围下沉的地幔流上升, 继续产生岛弧岩浆, 但是, 此时弧后拉伸轴已与岛弧火山前峰分离, 从而发育正常岩浆弧

Fig. 23 Schematic representation of tectonics showing changing patterns of mantle convection and processes of melt generation associated with the evolving back−arc basin now preserved in the North Qilian Mountain (modified after reference [20])

A−Early island−arc rifting did not disturb normal processes of arc magmagenesis in the mantle. Arc melts resulted from the rise of buoyant diapirs at a rate that allowed these to overcome the ambient mantle down flow induced by the subducting slab. These melts were diverted from the arc to the nearby rift axis; B−Establishment of a seafloor−spreading regime reflects establishment of a zone of mantle upwelling beneath the spreading ridge in the back−arc basin, resulting in decompression melting of a nearly adiabatic mantle column indistinguishable from that of normal mid−ocean ridges. Arc magmas continued to be generated and to diapirically ascend against ambient downward mantle flow, but the separation of the extension axis and the arc volcanic front allowed development of a normal magmatic arc

近的裂谷轴(图23−A)[20]。只要被俯冲板片引起的地幔下沉(downwelling)持续于裂谷轴之下, 就不可能造成产生似MORB减压熔融体所必需的地幔上涌(upwelling)。然而, 随着弧后拉伸继续, 裂谷轴逐渐离开岛弧火山前峰, 且随着弧后盆地变宽, 裂谷轴离开岛弧岩浆流的距离也逐渐增大。最终, 裂谷轴和弧下地幔沉降带之间的距离增大得足以造成弧后盆地扩张脊之下的幔上涌, 产生一个类似于洋中脊的减压熔融系统(图23−B)[20]。由于该弧后地幔上涌带逐渐地与俯冲板片的源的水源分开, 从而导致部分熔融程度逐渐降低。此时, 由于弧后地幔的上涌, 造成弧壳大幅度减薄, 从而引发真正意义上的弧后海底扩张, 并相应在弧后盆地和海底扩张区中建立起一个独立的岩浆系统−弧后盆地岩浆系统[20]。

综上所述, 北祁连山早古生代岛弧和弧后盆地熔岩的研究揭示, 在弧后盆地形成过程中, 岩浆的源成分和产生方式发生了系统变化。在整个弧后拉伸过程中, 从初始的岛弧裂谷化演变到弧后海底扩张, 相伴的火山喷发产物呈现规律性变化。从早期岛弧裂谷熔岩(与正常的岛弧熔岩无区别)到弧后盆地扩张中心之下地幔上涌导致减压熔融所产的弧后扩张脊熔岩, 在地球化学成分上显示出一种逐渐过渡。这种过渡反映了演化中的弧后盆地之下地幔对流体制的重组: 从初始岛弧裂谷之下由消减板片俯冲引起的地幔下沉, 转变为弧后扩张带之下地幔的上涌。当弧后扩张中心靠近海沟时, 俯冲板片源流体必然会影响弧后火山岩的化学成分。然而, 随着弧后扩张作用的进行, 弧后扩张中心逐渐远离海沟, 俯冲板片源流体的影响就会逐渐减弱。随着弧后盆地演化, 在岛弧–弧后盆地岩浆系统中发生的最重要的变化并非是岛弧火成活动的结束, 因为岛弧岩浆仍在地幔楔中恒定地产生。其最重要的改变是在岛弧发生初始裂谷化之后, 在弧后盆地和海底扩张区之中逐渐地建立起一个独立的岩浆系统——弧后盆地岩浆系统[20]。

3.3.3 南祁连寒武纪至奥陶纪(542~486 Ma)岛弧和弧后盆地火山岩

寒武纪至奥陶纪(542~486 Ma; 表1)滩涧山群火山岩带分布于柴北缘高压–超高压变质带的北东侧, 主要出露于吉绿素、绿樑山、锡铁山和乌兰等地(图2)。新元古代早期的达肯大坂群构成滩涧山群火山岩系的下伏基底, 泥盆纪—新生代地层呈角度不整合覆盖于该火山岩系之上[58]。

滩涧山群火山岩系以赋含滩涧山式Pb–Zn块状硫化物矿床而闻名[17]。对于这套火山岩的岩石成因和构造属性, 研究者们曾提出过3种不同的解释。第一种意见认为滩涧山群火山岩由洋中脊火山岩组合(拉斑系列)、洋岛(海山)火山岩组合(碱性系列)和岛弧火山岩组合(钙碱系列和拉斑系列)构成, 是存在柴北缘奥陶纪洋盆(也就是本文中所指的南祁连洋盆)的重要证据[205]。第二种意见由赵凤清等[56]提出, 他们将滩涧山群火山岩当作是大陆裂谷火山作用的产物。第三种意见主张滩涧山群火山岩为岛弧火山岩系[57, 58]。

我们的综合研究结果揭示:

(1)寒武纪至早奥陶世(542~486 Ma)滩涧山群火山岩系产出于祁连陆块的南缘(图2; 表1)。该火山岩系主要由厚层中性熔岩组成, 其次为玄武质和长英质熔岩、火山碎屑岩和同时代的次火山岩脉(图18–c)。大多数玄武质岩石样品属拉斑系列, 某些中性和长英质岩石样品属钙碱系列, 还有一些玄武质岩石样品具有很高的含碱量, 属橄榄玄粗岩系列(shoshonitic series)(图18–c, d)。

(2)从图19–c, d可见: 滩涧山群火山岩具有岛弧、弧后盆地和洋中脊等多重信号, 表明它们应当是形成于岛弧和弧后盆地环境。前已述及, 在北祁连山西部, 可以清楚地观察到岛弧带和弧后盆地带之间的过渡关系。然而, 在南祁连山, 却观察不到岛弧带和弧后盆地带之间的原始接触关系, 这是因为这种原始的过渡关系可能已被碰撞后的构造事件所破坏。

(3)在南祁连造山带中也广泛地分布有与弧火山岩同时代的弧花岗岩类侵入体(图3)。地质年代学研究揭示, 这些花岗岩类侵入体形成于南祁连洋壳俯冲时期(从大约514 Ma至约440 Ma)[8, 95–97]。一些研究得较为详细的规模较大的侵入体有: ①嗷唠山花岗岩体[95](473 Ma; 表3), ②团鱼山花岗岩–花岗闪长岩体[97](470~444 Ma; 表3), ③赛什腾山花岗岩体[97](465 Ma, 表3), ④柴达木山花岗岩体[95, 96](446 Ma; 表3)。

南祁连造山带中, 柴北缘高压–超高压变质杂岩带和滩涧山群岛弧–弧后盆地火山岩带自南西向北东的分布(图2), 意味着早古生代南祁连大洋岩石圈是向着北东方向俯冲。滩涧山群岛弧–弧后盆地火山岩的年龄数据(542~486 Ma; 表1)和南祁连大洋岩石圈俯冲过程中的峰期高压变质(也就是进化变质作用)年龄(476~446 Ma; 表4; 图4)标示着: 自542 Ma至446 Ma的年龄范围可能反映了南祁连洋俯冲的时间。

3.4 祁连陆块中部拉脊山寒武纪至奥陶纪裂谷火山岩

拉脊山寒武纪至奥陶纪火山岩呈北西方向主要分布于祁连陆块东部的拉脊山地区(图2), 此外, 在祁连陆块的西部还出露有一些研究程度很低的同时代火山岩(图2)。古元古代湟源群和中元古代湟中群构成拉脊山火山岩系下伏结晶基底。拉脊山火山岩系主要由厚层玄武质熔岩组成, 其次有中

性和酸性熔岩, 并含有大量沉积岩和火山碎屑岩夹层[14, 206]。近20年间, 对于拉脊山火山岩的岩石成因和产出的构造环境一直有很大的争议。一些研究者曾认为这套火山岩具有洋岛和岛弧火山岩的性质[14]; 另一些研究者则提出, 拉脊山地区在寒武纪至奥陶纪期间, 曾经历过从大陆裂谷经陆间裂谷(小洋盆)和火山弧到造山带的构造演化[206]; 最近, Song et al. [10]则推断: 拉脊山火山岩系由525 Ma的蛇绿岩和460~442 Ma的洋内弧火山岩构成, 认为其可能是指示了祁连—柴达木消减系的最终缝合带。

我们的综合研究结果揭示:

(1)火山岩系主要发育于拉脊山地区(图2)。火山岩的成分变很大, 从玄武质至流纹质皆有发育(图24−a)。大部分属拉斑系列, 仅少数样品属钙碱系列和碱性系列(图24−a, b)。

(2)根据Ti/Y比值, 拉脊山寒武纪至奥陶纪玄武质熔岩可以被划分为高Ti/Y(HT, Ti/Y ≥ 500)和低Ti/Y (LT, Ti/Y < 500)等2个主要岩浆类型。根据Nb/La比值, LT熔岩又可进一步被划分为LT1 (Nb/La > 0.8) 和LT2 (Nb/La < 0.8) 熔岩等2个亚类(图24−c)。

(3)因为大陆岩石圈物质通常具有高La/Nb、Ba/

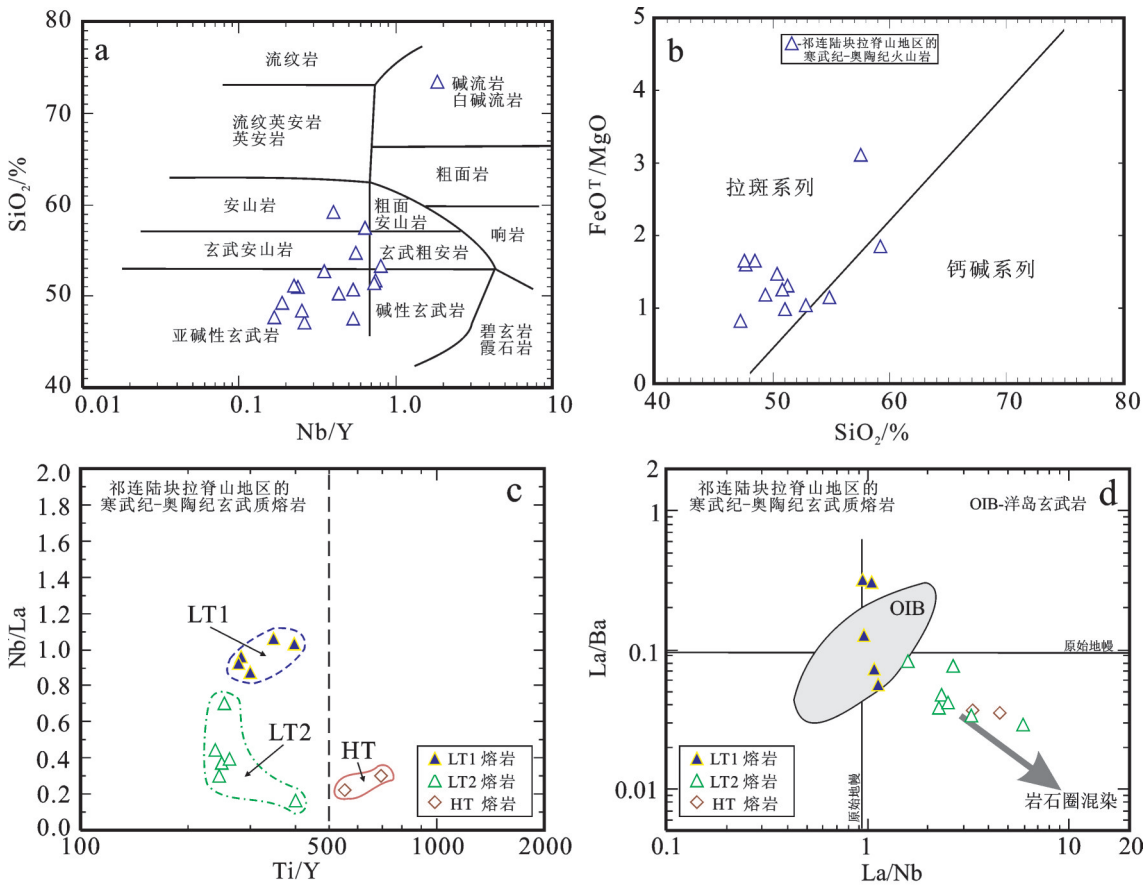

图24 祁连陆块拉脊山地区寒武纪—奥陶纪火山岩的a—SiO_2 − Nb/Y 图解 (图解据 [154])和b—FeO^T/MgO − SiO_2 图解 (图解据 [155]); 祁连陆块拉脊山地区寒武纪−奥陶纪玄武质熔岩的c—Nb/La − Ti/Y 图解 和d—La/Ba − La/Nb图解

图24–b适用于图24–a中的亚碱性火山岩

数据来源: [14, 206]

Fig. 24 a−SiO_2 versus Nb/Y diagram (after reference [154]) and b−FeOT/MgO versus SiO_2 diagram (after reference [155]) for Cambrian to Ordovician volcanic rocks in the Lajishan area of the Qilian Block; c−Nb/La versus Ti/Y diagram and d−La/Ba versus La/Nb diagram for Cambrian to Ordovician basaltic lavas in the Lajishan area of the Qilian Block

Fig. 24 b shows the sub−alkaline volcanic rocks as plotted in Fig. 24−a

Data sources: references [14, 206]

Nb和低La/Ba的特点[207, 208], 所以, 如果玄武质岩浆遭受了大陆岩石圈物质产混染, 其不相容元素如La或Ba的含量相对于Nb的含量就会增高。图24−d显示了拉脊山寒武纪至奥陶纪玄武质熔岩的La/Nb比值相对于La/Ba比值的变化, 并和OIB的成分域[158, 159]加以对比。HT和LT2熔岩具有较高的La/Nb比值和较低的La/Ba比值, 表明它们曾遭受了地壳或/和陆下岩石圈组分的混染。

(4)没有遭受混染的地幔柱成因的玄武质岩石通常具有平坦型REE分配型式或LREE富集型REE分配型式, 并缺乏Nb、Ta和Ti负异常[164, 165, 209, 210]。Nb/La比值是地壳混染的可靠微量元素标志[211, 212]。Saunders et al. [213]也曾提出: 地幔柱组分是以Nb/La比值大于1或近于1为特征。LT1熔岩具有高的Nb/La比值(> 0.80), 表明它们并未遭受地壳(或岩石圈)混染, 或者只是受到了地壳(或岩石圈)的轻微混染(图24−c)。此外, LT1熔岩具有与洋岛玄武岩(OIB)成分域相重叠的元素比值(图24−d), 并显示“隆起状”原始地幔标准化不相容微量元素分配型式(图25−a)。然而, 受到大陆岩石圈混染的玄武质熔岩(如HT和LT2熔岩)则具有明显的Nb、Ta和Ti负异常(图25−b), 但其不相容微量元素的浓度却是明显地高于消减带玄武岩(图25−b), 这一点明显地不同于弧玄武岩。因此, 没有遭受混染的熔岩(即LT1熔岩)的确是形成于板内环境, 而受到混染的熔岩(也就是HT和LT2熔岩)也只是遭受了大陆岩石圈混染的大陆玄武岩, 并不是弧玄武岩。

(5)当我们利用不使用Nb、Ta或Ti作为判别因子的Zr/Y−Zr图解时, 可以发现, 所有拉脊山玄武质熔岩的成分点均落在板内玄武岩(WPB)的成分域内(图25−c)。相反, 当利用使用Nb、Ta或Ti作为判别因子的构造环境地球化学判别图解(如图25−d, e)时, 可以发现, 未遭受混染的样品(即LT1熔岩)的成分点仍然落在WPB成分域或者大陆拉斑玄武岩(CT)成分域内, 但其他遭受了岩石圈混染的样品(也就是HT和LT2熔岩)的成分点, 却向着低Nb、低Ta或低Ti方向迁移, 落入到岛弧和陆缘弧玄武岩的成分域内。在这种情况下, 我们当然不能将HT和LT2熔岩当作是弧玄武岩, 它们乃是遭受了岩石圈混染的大陆板内玄武岩。

综上所述, 拉脊山寒武纪至奥陶纪火山岩的地球化学特点证明: 它们是形成于大陆板内裂谷拉伸环境, 不是形成于弧环境。

3.5 祁连陆块北缘的晚奥陶世至早志留世(445~428 Ma)碰撞后裂谷火山岩

3.5.1 北祁连洋和南祁连洋最终闭合的时间

前已述及, 由页岩、板岩、砂岩和砾岩组成的志留纪初始磨拉石在祁连山地区广泛分布, 它们不整合覆盖在前志留纪地层之上(图2, 图17)。我们采纳这样的意见, 即该不整合发育的时间大约是444 Ma, 代表了北祁连洋和南祁连洋闭合的时间。该推断与最年轻的蛇绿岩的年龄以及北祁连高压变质带和柴北缘高压−超高压变质带中保存的与早期大洋俯冲有关的峰期高压变质年龄相一致。

例如: 从图2和表1可见, 出露于北祁连弧后盆地东部最年轻的老虎山蛇绿岩套中的辉长岩具有(448.5 ± 4.7) Ma的锆石SHRIMP U−Pb年龄[9], 表明其是形成于晚奥陶世; 同样, 最年轻的白银岛弧流纹岩具(446 ± 3) Ma的锆石SHRIMP U−Pb年龄[72], 也是形成于晚奥陶世。

众所周知, 区域性HP−LT变质作用的时间构成了一个造山带最好的碰撞标志。北祁连高压变质带的峰期HP−LT变质作用的年龄(489~446 Ma)[11, 64, 71, 83−85](图4; 表2)表明: 北祁连洋极有可能是在445 Ma时关闭的。柴北缘高压—超高压变质带的峰期高压变质作用(与大洋俯冲有关)年龄和峰期超高压变质作用(与大陆俯冲有关)年龄分别为476~442 Ma和440~421 Ma[10, 11, 29, 31, 33−35, 37, 39−43, 45, 46, 48−52, 55, 64](图4; 表4), 意味着: 南祁连洋是在441 Ma时闭合的。

此外, 卢欣祥等[100]还获得了祁连陆块南缘塔塔楞环斑花岗岩侵入体的SHRIMP U−Pb锆石年龄值为(440±14)Ma(图3; 表3), 这同样也标示: 南祁连洋在奥陶纪末已经闭合。

根据上述证据, 我们有理由推断: 北祁连洋和南祁连的最终闭合分别发生于445 Ma和441 Ma。

3.5.2 祁连陆块北缘的晚奥陶世至早志留世(445~428 Ma)碰撞后裂谷火山岩

晚奥陶世—早志留世火山岩系零星地分布于祁连陆块北缘的祁连县冰沟、门源县红沟和压浪县葫芦河等地[16](图2)。该火山岩系主要由玄武质熔岩组成, 其次有中性和酸性熔岩, 夹含火山碎屑岩和大量陆缘碎屑岩(包括有砾岩、砂岩、粉砂岩和板

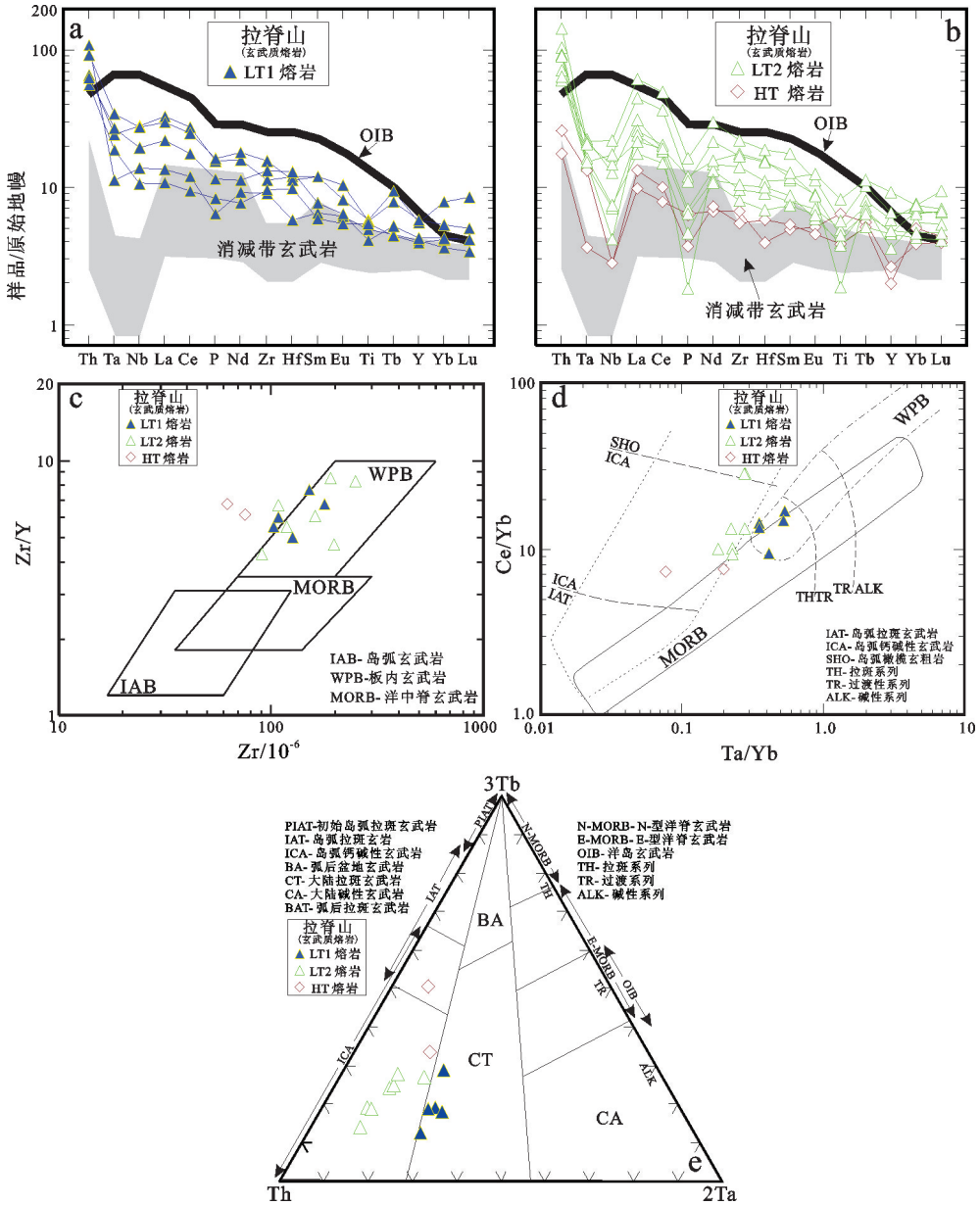

图25 a, b—祁连陆块拉脊山地区寒武纪—奥陶纪玄武质熔岩的不相容微量元素原始地幔 (据[156]) 标准化蛛网图; 祁连陆块拉脊山地区寒武纪—奥陶纪裂谷玄武质熔岩形成的构造环境判别图解: c—Zr/Y − Zr diagram (图解据 [160]); d—Ce/Yb − Ta/Yb 图解 (图解据[161]); e—3Tb–Th–2Ta 图解 (图解据[193])

图25−a, b中, 洋岛玄武岩(OIB)据 [156]; 图中阴影区表示消减带玄武岩的成分范围, 其上限和下限分别由高−K玄武岩和低−K玄武岩的平均值(据[157])限定

数据来源同图24

Fig. 25 a, b−Primitive mantle (after reference [156]) normalized incompatible trace−element spider diagrams for Cambrian to Ordovician basaltic lavas in the Lajishan area of the Qilian Block. Tectonic setting of Cambrian to Ordovician rift−related basaltic lavas in the Lajishan area of the Qilian Block. c−Zr/Y versus Zr diagram (after reference [160]); d−Ce/Yb versus Ta/Yb diagram (after reference [161]); e−3Tb–Th–2Ta diagram (after reference [193])

In Fig. 25−a, b, the patterns for oceanic island basalts (OIB) are after reference [156]; the shaded area shows the range for subduction−zone basalts, with the lower and upper limits being defined by “average” low−K and high−K basalts, respectively (after reference [193])

Data sources as for Fig. 24

岩, 代表了碰撞后初始磨拉石建造)。

已发表2组有关该火山岩系的地质年代学数据: 葫芦河地区玄武岩的Sm−Nd等时线年龄: 445~428 Ma[16](表1); 红沟地区玄武岩的LA−ICP−MS锆石U−Pb年龄: (443.2 ± 1.2) Ma[80]。

这套火山岩系的成分变化很宽, 从玄武质到流纹质均有发育(图26−a), 基性和中性火山岩石包含拉斑和碱性等2个系列, 酸性火山岩属钙碱系列(图26−a, b)。

根据Ti/Y比值, 该火山岩系的玄武质熔岩可以被划分为高Ti/Y (HT, Ti/Y ⩾ 500) 和低Ti/Y (LT, Ti/Y < 500)等2个岩浆系列; 按照Nb/La比值, LT熔岩又可以进一步被划分为LT1 (Nb/La > 1.0)和LT2 (Nb/La < 1.0)等2个亚类(图26−c)。

LT1和HT熔岩具有高Nb/La比值 (>1.0)的特点, 表明它们没有遭受过大陆岩石圈的混染(图26−c)。在图26−d中可以见到, LT1和HT熔岩具有和洋岛玄武岩(OIB)相似的元素比值(即成分域)。LT1和HT熔岩强烈富集不相容微量元素, 具有与洋岛玄武岩(OIB)相似的典型“大隆起”式原始地幔标准化不相容微量元素分配型式(图26−e)。

LT2熔岩具有较高的La/Nb比值和较低的La/Ba比值, 表明其形成过程中曾遭受过地壳或陆下岩石圈组分的混染(图26−d)。虽然LT2熔岩具有十分明显的负Nb、Ta和Ti的异常(图26−f), 但其不相容微量元素的浓度明显地高于消减带玄武岩的不相容微量元素的浓度(图26−f)。因此, LT2熔岩并不是消减带玄武岩, 它们应当是遭受过大陆岩石圈混染的大陆板内玄武岩。

此类445~228 Ma玄武质熔岩的$\varepsilon_{Nd}(t)$值的变化, 与它们遭受地壳或大陆岩石圈混染的程度密切相关。如图27−e所示: (1)没有遭受过混染的岩石样品(即LT1和HT熔岩)恒定地具有正的$\varepsilon_{Nd}(t)$值(+0.2至+2); (2)受到混染的岩石样品(即LT2熔岩)则以具有负的$\varepsilon_{Nd}(t)$值(− 0.5 至 − 9.5)为特征。此特征表明LT2熔岩乃是遭受了古老大陆岩石圈混染的大陆板内玄武岩[165]。应当指出, 虽然大陆岩石圈的混染作用和俯冲板片源流体和/或熔体的作用, 都可以导致受到作用的岩石具有低的Nb/La比值, 但是, 只有古老大陆岩石圈的混染作用才能导致产生很低的负$\varepsilon_{Nd}(t)$值[126, 164, 165]。

Zr/Y−Zr图解(图27−a)显示: 所有445~228 Ma玄武质熔岩的成分点全部落在板内玄武岩(WPB)成分域内。当利用其他使用Nb、Ta或Ti作为判别因子构造环境判别地球化学图解(图27−b~d)时, 可以发现, 没有遭受大陆岩石圈混染的岩石样品(也就是HT和LT1熔岩)的成分点, 仍然落在板内玄武岩(WPB)成分域内, 但是, 所有其他受到大陆岩石圈混染的岩石样品(即LT2熔岩)的成分点, 均向着低Nb、低Ta或低Ti的方向迁移, 进入到弧玄武岩成分域。在这种情况下, 受到大陆岩石圈混染的玄武岩是不应当被当做是火山弧玄武岩的。

此外, 多年的地质工作业已查明, 这套445~428 Ma火山岩系中赋存有红沟型Cu−Fe块状硫化物矿床[17]。

综上所述, 产于祁连陆块北缘的晚奥陶世—早志留世(445~428 Ma)火山岩乃是大陆板内裂谷火山岩。

上述445~428 Ma火山岩及与其同时代的花岗岩侵入体, 如: 熬油沟奥长花岗岩侵入体[93](438 Ma); 金佛寺二长花岗岩侵入体[88](424 Ma); 老虎山石英闪长岩侵入体[92](424 Ma), 乃是碰撞后岩浆作用的产物(图2, 图3; 表3)。

此外, 还应当提及的是, 在祁连陆块南部分布的厚大志留纪沉积岩系中也含有少量火山岩(图2), 这套志留系沉积(含火山岩)建造曾被认为是冒地槽建造[214]。极有可能, 这套志留纪沉积岩石乃是堆积于南祁连造山带前陆盆地系中的初始磨拉石建造。与这套志留纪初始磨拉石共生的火山岩也应当是碰撞后火山作用的产物。

4 祁连山新元古代中—晚期至早古生代构造岩浆演化历史的重建

基于对祁连山新元古代中—晚期至早古生代火山岩性质、时、空变化特点和区域地质资料的综合分析, 笔者提出祁连山新元古代中—晚期至早古生代构造岩浆演化历史经历了如下5个阶段(图28)。

4.1 880~500 Ma: Rodinia超大陆裂谷化和裂解及北祁连洋和南祁连洋的开启和扩张

中国的一些古陆块(包括塔里木、阿拉善、祁连、柴达木和华南等古陆块)上的新元古代中—晚期裂谷岩浆作用是Rodinia超大陆裂谷化—裂解过程中发生的全球性裂谷岩浆作用组成部分[126, 177]。全球

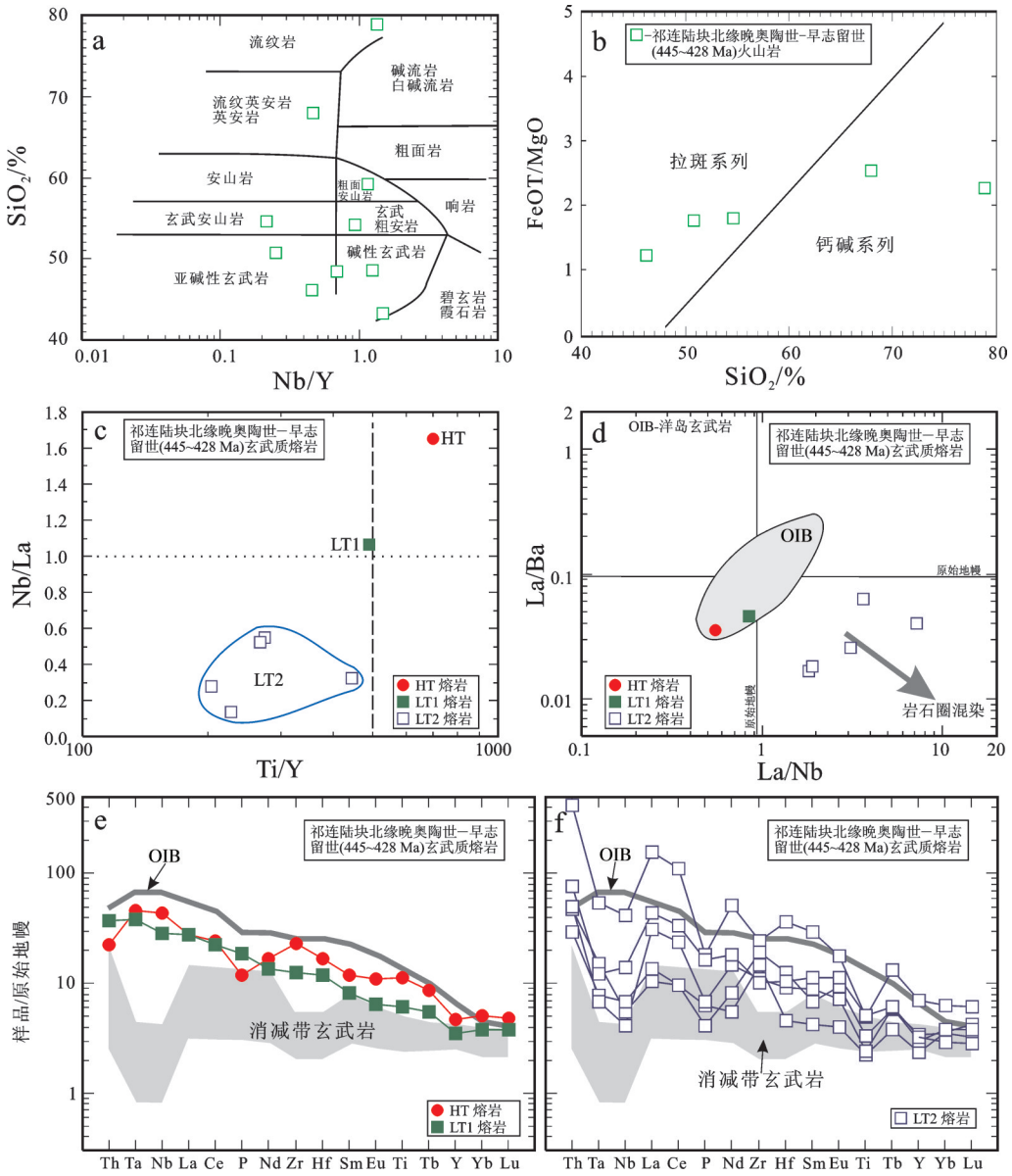

图26 祁连陆块北缘晚奥陶世—早志留世(445~428 Ma)火山岩的a—SiO_2 − Nb/Y 图解 (图解据 [154])和b—FeO^T/MgO − SiO_2 图解 (图解据[155]); 祁连陆块北缘晚奥陶世—早志留世(445~428 Ma)玄武质熔岩的c—Nb/La − Ti/Y 图解, d—La/Ba − La/Nb 图解, 和e, f—不相容微量元素原始地幔(据 [156])标准化蛛网图

图26–b适用于图26–a中的亚碱性火山岩; 图26–d中, 岩石圈混染效应导致成分点向高La/Nb 和低La/Ba方向迁移; 洋岛玄武岩(OIB)的成分范围据[158, 159]; 图26–e, f中, 洋岛玄武岩(OIB)据Sun & McDonough (1989); 图中阴影区表示消减带玄武岩的成分范围, 其上限和下限分别由高−K玄武岩和低−K玄武岩的平均值(据 [157])限定

数据来源: [16, 17]

Fig.26 a−SiO_2 versus Nb/Y diagram (after reference [154]) and b−FeOT/MgO versus SiO_2 diagram (after reference [155]) for Late Ordovician−Early Silurian (445−428 Ma) volcanic rocks on the northern margin of the Qilian Block; c−Nb/La versus Ti/Y diagram, (d−La/Ba versus La/Nb diagram; and e, f−Primitive mantle (after [156]) normalized incompatible trace−element spider diagrams for Late Ordovician−Early Silurian (445−428 Ma) basaltic lavas on the northern margin of the Qilian Block

Fig. 26−b shows the sub−alkaline volcanic rocks as plotted in Fig. 26−a. In Fig. 26−d, the dispersion to higher La/Nb and lower La/Ba ratios may represent the effects of lithospheric contamination. Field for oceanic island basalts (OIB) is after references [158, 159]. Patterns for oceanic island basalts (OIB) are from reference [156]. In Fig. 26−e, f, the shaded area shows the range for subduction−zone basalts, with the lower and upper limits being defined by "average" low−K and high−K basalts, respectively (after reference [157])

Data sources: references [16, 17]

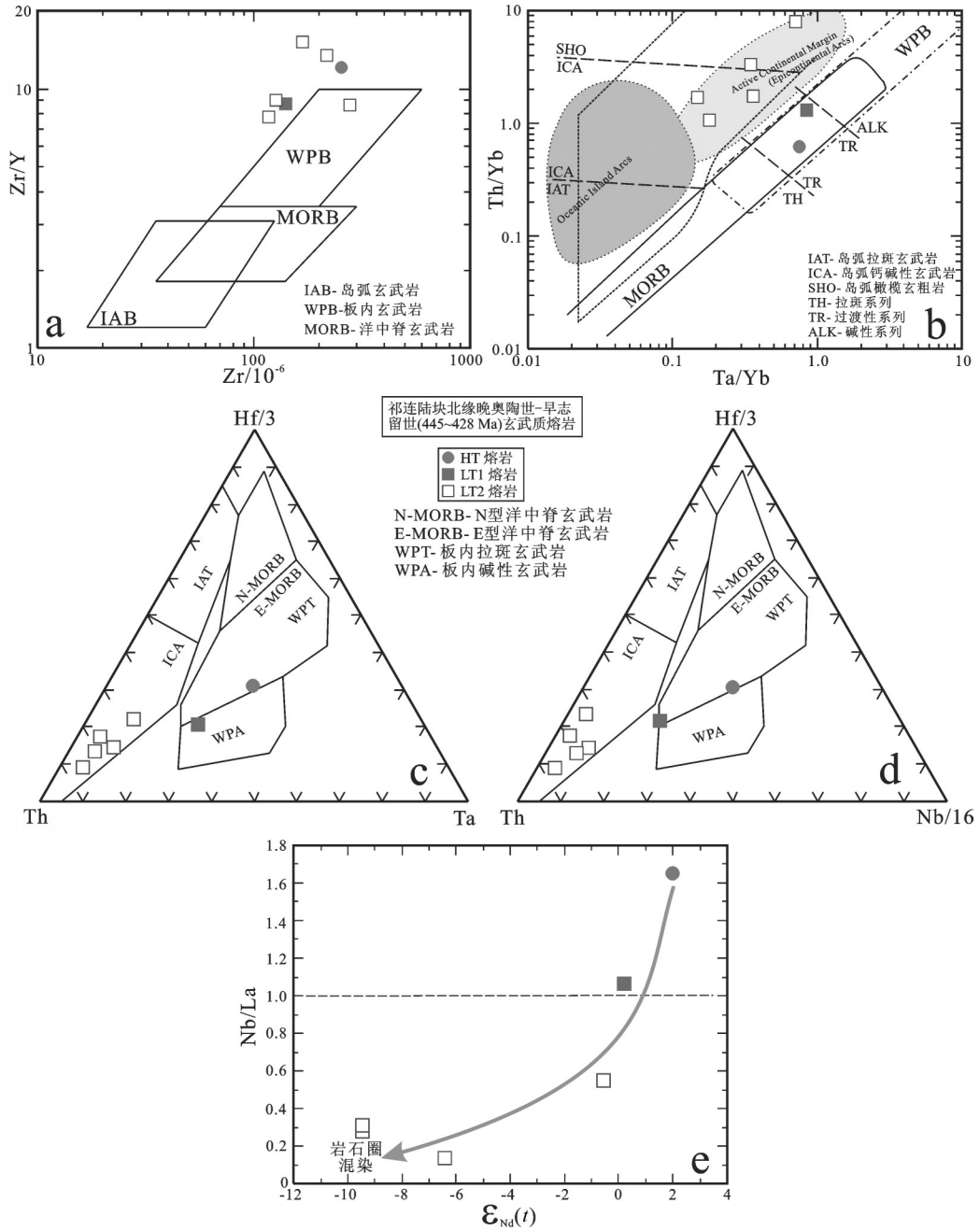

图27祁连陆块北缘晚奥陶世—早志留世(445~428 Ma)玄武质熔岩形成的构造环境判别图解

a—Zr/Y−Zr图解 (据[160]); b—Th/Yb−Ta/Yb图解 (据 [161]); c—Hf/3–Th–Ta 图解 (据 [162]); d—Hf/3–Th–Nb/16 图解 (据 [162]); e—祁连陆块北缘晚奥陶世—早志留世(445~428 Ma)玄武质熔岩的Nb/La − $\varepsilon_{Nd}(t)$图解

数据来源同图26

Fig.27 Tectonic setting of Late Ordovician−Early Silurian (445−428 Ma) basaltic lavas on the northern margin of the Qilian Block

a−Zr/Y versus Zr diagram (after reference [160]); b−Th/Yb versus Ta/Yb diagram (after reference [161]); c−Hf/3–Th–Ta diagram (after reference [162]); d−Hf/3–Th–Nb/16 diagram (after reference [162]); e−Nb/La versus $\varepsilon_{Nd}(t)$ diagram for Late Ordovician−Early Silurian (445−428 Ma) basaltic lavas on the northern margin of the Qilian Block

Data sources as for Fig. 26

性新元古代中—晚期裂谷火山作用也是全球性早古生代大洋开启的先兆[126](图10)。北祁连洋和南祁连洋可能是全球性早古生代大洋的2个分支(图28-A)。Rodinia超大陆的裂解是穿时发生的[177]。新元古代中期之末(660~630 Ma)的裂谷火山活动, 在时间上, 与澳大利亚—东南极、华南、柴达木、祁连和劳仑等古陆间的裂离相一致。早寒武世裂谷火山作用被解释成是发生于澳大利亚和塔里木古陆间分离的过程之中[126, 177]。鉴于499 Ma扎马什河蛇绿岩[70](表1)是北祁连造山带中已被识别出的最年轻的仰冲早古生代洋壳的残片。因此, 有理由推断, 北祁连洋的海底扩张可能一直可以延续到约500 Ma。而柴北缘高压—超高压变质带中的516 Ma沙柳河蛇绿岩[39](表4)则是意味着: 南祁连洋的海底扩张可以延续至大约510 Ma。

应当指出, 全球性早古生代大洋曾被称为"Iapetus"洋[177, 215, 216]。该全球性早古生代大洋是在新元古代由于Rodinia超大陆的裂解而被打开。该大洋在早古生代末的闭合和最终碰撞, 形成了北美的阿巴拉契亚(Appalachian)造山带、欧洲的加里东(Caledonian)造山带和中国的中央造山带。

4.2 630~446 Ma: 大洋俯冲和岛弧-弧后盆地对的发育

4.2.1 大洋俯冲和弧岩浆作用

祁连陆块和阿拉善陆块碰撞之前, 北祁连大洋岩石圈是向北或北东方向俯冲到阿拉善陆块之下[6-8, 11, 13-22](图28-B)。与此同时, 在柴达木陆块和祁连陆块碰撞之前, 南祁连大洋岩石圈是向北俯冲到祁连陆块之下[6-8](图28-B)。

经地质年代学研究查明, 大坂—大岔弧后盆地蛇绿岩套中的辉长岩具有(517 ± 4) Ma的锆石SHRIMP U-Pb年龄[78](表1); 该年龄值指示了北祁连弧后盆地构造环境中最早的岩浆作用。据此, 可以推断: 北祁连大洋岩石圈的俯冲可能是开始于520 Ma之前。此外, 南祁连最老的滩涧山群岛弧玄武岩具有约(542±13)Ma的TIMS U-Pb锆石年龄[57](表1), 该年龄值意味着: 南祁连大洋岩石圈的俯冲可能是开始于540 Ma之前。

Wilson[217]曾指出: 洋壳俯冲过程中, 随着压力和温度的增加, 发生进化变质反应, 洋壳的玄武质组分逐渐经绿片岩相和角闪岩相转变成榴辉岩相; 此种进化变质作用的实际效果, 是将初始的含水矿物组合脱水, 从而释放出独立的流体相-H_2O; 随着俯冲深度的增大, 在更大的深处, 榴辉岩发生含水部分熔融, 从而产生富H_2O的中性和酸性部分熔融体, 尔后, 这些部分熔融体上升进入上覆的地幔楔; 此类俯冲板片源流体(包括含水流体和部分熔融体)有效地降低了地幔楔的固相线, 由此促使其发生部分熔融, 从而引发岛弧岩浆作用。

在此, 还应当提及的是, 有一些研究者(如: 吴才来等[89, 96])根据柯柯里斜长花岗岩(512 Ma)和窑沟花岗闪长岩(463 Ma)(表3)分别产出于祁连陆块北缘和北祁连弧后盆地带之北(图3)的产状特点, 从而提出北祁连洋的早古生代消减作用可能具有双向俯冲的特点(即: 柯柯里斜长花岗质岩浆作用是由北祁连洋壳的向南俯冲所引起; 窑沟花岗闪长质岩浆活动是由北祁连洋壳的向北俯冲作用所引起)。

4.2.2 岛弧和弧后盆地对的产生

大约在早寒武世(520 Ma左右)时, 低角度向北俯冲的北祁连大洋板片和南祁连大洋板片发生陡角度回转(图28-C), 诱使岛弧后方的软流圈上涌, 从而引发弧后岩石圈伸展, 形成北祁连弧后盆地和南祁连弧后盆地, 并导致在这2个弧后盆地中产生早寒武世至晚奥陶世(520~445 Ma)弧后盆地火山作用。与此同时, 由于俯冲大洋板片的重力拖拽, 不仅使得板块的汇聚速率增大, 还开始将与南祁连大洋岩石圈相连的柴达木大陆岩石圈向深处拖拽(图28-C)。

值得提及的是, 地球上的俯冲-消减系并非总是以弧后拉伸为特征。例如: 东太平洋俯冲-消减系就是以大洋板片呈低角度(约30º)俯冲, 弧后呈挤压性构造为特征; 相反, 西太平洋俯冲-消减系, 却是具有大洋板片呈高角度俯冲, 弧后呈张性构造的特征[217]。据此, 可以推断: 祁连山早古生代俯冲-消减系的俯冲-消减角度应当是较为陡峻(>30º)。

4.2.3 拉脊山火山岩系形成于陆内裂谷拉伸环境

如前所述, 对于祁连陆块东部拉脊山地区的寒武纪—奥陶纪(525~442 Ma)火山岩系的岩石成因和产出环境有着许多不同的解释, 例如: 洋岛和岛弧[14]、从大陆裂谷经小洋盆和火山弧至造山带[205]和"是祁连-柴达木消减系的最终缝合带"[10]等。笔者的综合研究结果证明: 拉脊山火山岩系是形成于陆内裂谷伸展环境(图28-C)。此外, 根据最新的研究

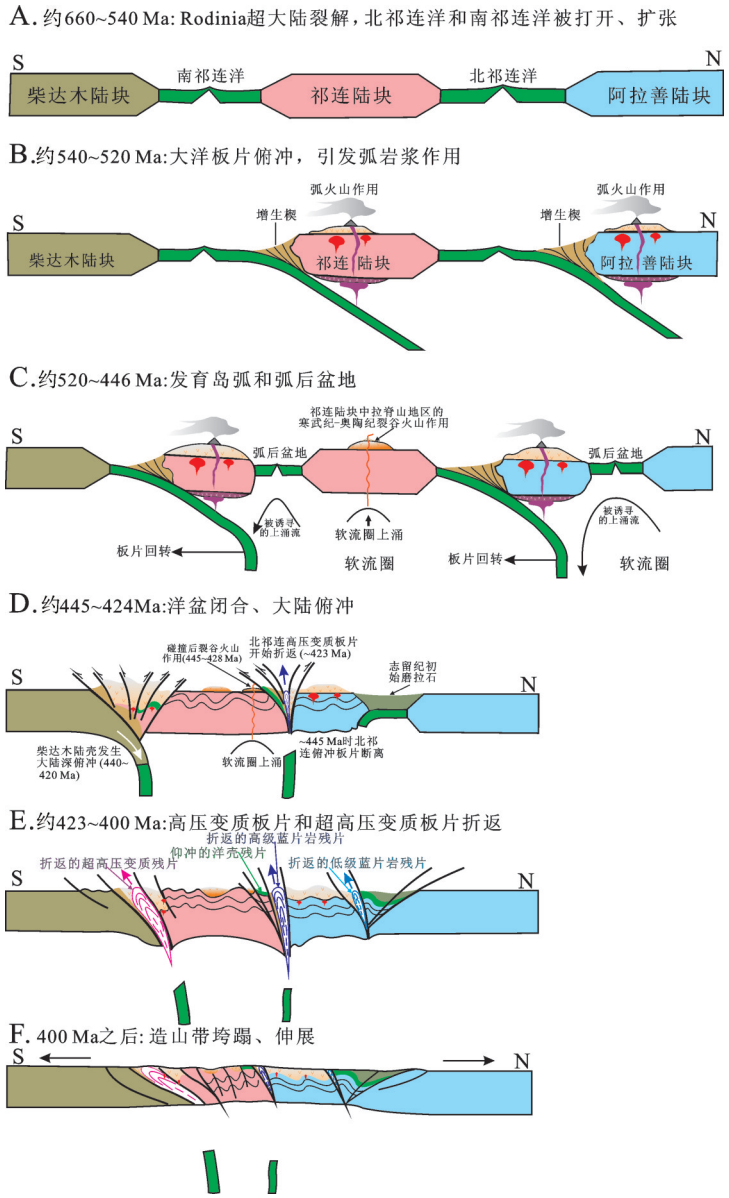

图28 祁连山新元古代—古生代构造岩浆演化阶段示意图

A—新元古代, Rodinia超大陆裂解导致全球性早古生代大洋(包括北祁连洋和南祁连洋)打开；B—早古生代大洋岩石圈以低角度向北俯冲−消减, 导致弧火山作用；C—大约自早寒武世(约520 Ma)起, 北祁连和南祁连大洋板片回转, 相伴发生软流圈上涌, 导致弧后岩石圈伸展和弧后盆地火山作用；与此同时(525~442 Ma), 包括拉脊山和化隆地区在内的祁连陆块的中部, 则是处于陆内裂谷环境；D—北祁连洋和南祁连洋的最终闭合分别发生于445 Ma和441 Ma；大约在445 Ma, 北祁连大洋板片断离, 诱使软流圈上涌, 导致在祁连陆块北缘发生445~428 Ma的碰撞后裂谷火山活动；大约自440 Ma始, 柴达木大陆岩石圈开始深俯冲；E—大约自423 Ma始, 俯冲的北祁连洋壳开始折返；大约在420~400 Ma, 南祁连板片断离, 致使俯冲的南祁连板片折返, 形成柴北缘高压−超高压变质带；F—晚泥盆世, 祁连造山系开始垮塌；在大约400~370 Ma期间, 连续的岩石圈伸展和拆沉, 致使发生地壳熔融和强烈的岩浆活动, 形成许多碰撞后花岗质侵入体

Fig.28 Sketch map showing the stages of Qilian Mountain Neoproterozoic−Paleozoic tectonomagmatic evolution

A−The global Early Paleozoic Ocean, including the North Qilian Ocean and the South Qilian Ocean, was opened in the Neoproterozoic as the consequence of breakup of supercontinent Rodinia. B−Carton, showing the north−dipping, low−angle subduction of the Early Paleozoic oceanic lithosphere, which resulted in the arc volcanism. C−Carton: illustrating the back−arc lithospheric extension and back−arc basin volcanism in both North Qilian and South Qilian back−arc basins that occurred as a result of upwelling of asthenosphere accompanied by roll−back of the North Qilian and South Qilian oceanic slabs since early Cambrian (about 520 Ma). In the meantime (525−442 Ma), the central part of the Qilian Block, including the Lajishan and the Hualong areas, was in an intracontinental rift−related setting. D−The final closure of the North Qilian Ocean and the South Qilian Ocean took place at 445 Ma and 441 Ma, respectively. The break−off of the North Qilian oceanic slab at about 445 Ma induced an upwelling of asthenosphere, which gave rise to the 445−428 Ma post−collisional rift−related volcanism on the north margin of the Qilian Block. At about 440 Ma, the Qaidam continental deep subduction started. E−At about 423 Ma, the subduced North Qilian oceanic crust started to exhume. The subducted South Qilian slab started to exhume, forming the North Qaidam HPM−UHPM belt, as a result of South Qilian slab break off at 420−400 Ma. F−In the late Devonian, the Qilian orogenic system started to collapse; continuous lithosphere extension and delamination resulted in crust melting and strong magmatic activity and formed a number of post−collisional granitic intrusions with the ages of 400−370 Ma

报道[218], 一些年龄为455~436 Ma的赋含Ni−Cu硫化物矿床的镁铁质−超镁铁质侵入体产出于拉脊山地区之南的化隆地区。这同样也证明: 祁连陆块的中部(包括拉脊山和化隆等地区), 在早古生代时, 的确是处于陆内裂谷伸展环境。

4.3 445~420 Ma: 洋盆闭合、大陆深俯冲和志留纪初始磨拉石建造

一系列证据表明, 北祁连洋和南祁连洋的最终闭合分别发生于445 Ma和441 Ma。这些证据有: (1)北祁连造山带中最晚的弧火山岩是形成于晚奥陶世, 具有(446 ± 3) Ma的锆石SHRIMP U−Pb年龄[72](表1; 图2); (2)北祁连高级蓝片岩带中多硅白云母的Ar−Ar坪年龄为454~446 Ma[84, 85](表2; 图4); (3)柴北缘高压—超高压变质带的峰期高压变质作用(即石英稳定的榴辉岩相前进变质作用)年龄为476~442 Ma[10, 11, 29, 31, 34, 40−43, 49, 50, 55, 64, 101](表4; 图4); (4)祁连山地区广泛分布着由页岩、板岩、砂岩和砾岩构成的志留纪初始磨拉石, 其不整合覆盖在前志留纪地质体之上[14, 16, 19, 153, 219](图2, 图17)。

奥陶纪末(大约445 Ma), 因弧−陆碰撞, 北祁连大洋板片与祁连大陆岩石圈脱离(图28−D)。约445 Ma时, 北祁连大洋板片的断离诱使软流圈上涌, 进而在祁连陆块北缘诱发产生445~428 Ma碰撞后裂谷火山活动[16, 80](图2, 图28−D; 表1)。

与此同时, 在洋盆闭合的最后阶段, 北祁连大洋板片的极小一部分逃脱了在俯冲−消减带被毁灭的命运, 被仰冲到碰撞大陆的前陆(也就是祁连陆块的北缘)之上, 形成新元古代晚期—寒武纪(550~497 Ma)洋壳(蛇绿岩)的仰冲岩片(图2, 图28−D, E)。

由于下插的南祁连大洋板片的拖拽[220]或是上驮板块的向下推挤[221], 大约自440 Ma始, 柴达木大陆岩石圈开始发生大陆深俯冲(图28−D)。由变泥质岩和榴辉岩中的含柯石英锆石和石榴子石橄榄岩中的含金刚石锆石所约束的峰期超高压变质年龄值: 约440~421 Ma[10, 11, 28, 33, 34, 37, 39, 40−43, 45, 46, 48−52, 55, 64, 101] (表4; 图4), 标示了大陆深俯冲至100~200 km深处的时间[9, 10]。

4.4 420~400 Ma: 俯冲岩片折返和造山作用

北祁连低级和高级蓝片岩的423~411 Ma Ar−Ar退变质年龄[71, 86](表2)和北祁连高压变质带中锆石的退变质年龄424~404 Ma[64](表2)标示: 自424 Ma始, 北祁连俯冲大洋板片断离, 导致一小部分俯冲的北祁连洋壳开始沿着逆冲断裂折返, 形成北祁连高压变质带(图28−D, E)。

柴北缘高压—超高压变质带中, 榴辉岩的多硅白云母和角闪石及花岗片麻岩中白云母的409~402 Ma Ar−Ar退变质年龄[11, 31](表4)和榴辉岩中锆石的退变质年龄409~403 Ma[11, 40, 182](表4)同样也标示: 南祁连俯冲板片可能在420~400 Ma发生了断离, 其一小部分也开始折返, 形成柴北缘高压−超高压变质带(图28−E)。

晚志留世至早泥盆世(420~400 Ma), 发生强烈造山作用, 导致山脉形成, 并于早泥盆世, 堆积磨拉石建造[9, 10, 16, 19, 20](图28−E)。

4.5 <400 Ma: 造山期后伸展和剥蚀

晚泥盆世, 祁连造山系开始垮塌; 连续地岩石圈伸展(图28−F)和拆沉作用引起地壳熔融和强烈的岩浆活动, 形成许多年龄为400~370 Ma的闪长岩−花岗闪长岩−花岗岩侵入体[87, 90, 95−97, 100](表3; 图3)。石炭纪时, 造山运动完全终止, 祁连山地区的所有杂岩均被海相和海−陆交互相沉积层所覆盖。喜马拉雅期以来, 由于印度−亚洲的碰撞, 作为特提斯—喜马拉雅造山带后陆地区的祁连造山系, 遭受了古近纪以来的再造山作用, 形成大量逆冲推覆构造, 并使得早期构造重新活化, 伴随产生新生代的山前及山间磨拉石盆地, 山体再次隆升, 形成现今的祁连山链[9, 10, 19, 222]。

5 结　语

祁连山新元古代中—晚期至早古生代火山作用是祁连山构造演化的火山响应。随着祁连山构造演化从Rodinia超大陆裂谷化和裂解, 经早古生代大洋打开和扩张、大洋板片俯冲、弧后拉伸和洋盆闭合, 直至弧−陆碰撞和陆−陆碰撞, 火山作用也逐渐地从大陆裂谷和大陆溢流玄武质, 转变为MORB型、岛弧和弧后盆地型, 直至碰撞后裂谷喷发。与此同时, 火山作用也显示规律性的时、空迁移: 850~604 Ma, 主要发生于祁连陆块和柴达木陆块; 550~446 Ma, 发生于北祁连和南祁连洋−沟−弧−盆系; 522~442 Ma, 同样也发育于祁连陆块中部; 445 Ma至428 Ma, 发生于祁连陆块北缘。祁连山新元古代中—晚期至早古生代火山作用系统的时、空变化对形成广袤祁连山的深部地球动力学过程提供了重

要约束。该过程包括有: (1)地幔柱或超级地幔柱上涌, 导致Rodinia超大陆裂谷化和裂解、早古生代大洋打开−扩张和俯冲, 从而产生岛弧; (2)俯冲大洋板片回转, 在岛弧后方发生弧后拉伸, 进而形成弧后盆地; (3)洋盆闭合、俯冲板片断离, 导致软流圈上涌, 诱发在祁连陆块北缘发生碰撞后裂谷火山活动。晚志留世至早泥盆世(420~400 Ma), 山体隆升, 前期俯冲的壳体(包括洋壳和陆壳)折返。400 Ma之后, 祁连造山系拆沉、伸展−垮塌, 同时伴随有碰撞后花岗质侵入活动。

致谢: 审稿专家对论文提出了宝贵修改意见, 在此致以诚挚的谢意!

参考文献 (References):

[1] Santosh M, Zhao G. Supercontinent dynamics [J]. Gondwana Res. , 2009, 15: 225−227.

[2] Santosh M. A synopsis of recent conceptual models on supercontinent tectonics in relation to mantle dynamics, life evolution and surface environment [J]. J. Geodyn. , 2010, 50 (3−4): 116−133.

[3] Yoshida M, Santosh M. Supercontinent, mantle dynamics and plate tectonics: A perspective based on conceptual vs. numerical models [J]. Earth Sci. Rev. , 2011, 105: 1−24.

[4] Santosh M, Maruyama S, Yamamoto S. The making and breaking of supercontinents: Some speculations based on superplumes, super downwelling and the role of tectosphere [J]. Gondwana Res. , 2009, 15: 324−341.

[5] 姜春发, 王宗起, 李锦轶, 等. 中央造山带开合构造 [M]. 北京: 地质出版社, 2000.
Jiang Chunfa, Wang Zongqi, Li Jinyi, et al. Opening Closing Tectonics of Central Orogenic Belt [M]. Beijing: Geological Publishing House, 2000 (in Chinese).

[6] Yang J S, Xu Z Q, Song S G, et al. Subduction of continental crust in the early palaeozoic North Qaidam ultrahigh− pressure metamorphic belt, NW China: evidence from the discovery of coesite in the belt [J]. Acta Geol. Sin. Engl. Ed. , 2002, 76: 63−68.

[7] Yang J S, Xu Z Q, Zhang J X, et al. Early Palaeozoic North Qaidam UHP metamorphic belt on the north−eastern Tibetan plateau and a paired subduction model [J]. Terra Nova, 2002, 14: 397−404.

[8] Xu Z Q, Yang J S, Wu C L, et al. Timing and mechanism of formation and exhumation of the Northern Qaidam ultrahigh−pressure metamorphic belt [J]. J. Asian Earth Sci. , 2006, 28: 160−173.

[9] Song S G, Niu Y L, Su L, et al. Tectonics of the North Qilian orogen, NW China [J]. Gondwana Res. , 2013, 23: 1378−1401.

[10] Song S G, Niu Y L, Su L, et al. Continental orogenesis from ocean subduction, continental collision/subduction, to orogen collapse, and recycling: The example of the North Qaidam UHPM belt, NW China [J]. Earth Sci. Rev. , 2014, 129: 59−84.

[11] Song S G, Zhang L F, Niu Y L, et al. Evolution from oceanic subduction to continental collision: a case study of the Northern Tibetan Plateau inferred from geochemical and geochronological data [J]. J. Petrol. , 2006, 47: 435−455.

[12] Gehrels G E, Yin A, Wang X F. Detrital−zircon geochronology of the northeastern Tibetan plateau [J]. Geol. Soc. Am. Bull. , 2003, 115 (7): 881−896.

[13] 夏林圻, 夏祖春, 彭礼贵, 等. 北祁连山石灰沟奥陶纪岛弧火山岩系岩浆性质的确定 [J]. 岩石矿物学杂志, 1991, 10(1): 1−10.
Xia Linqi, Xia Zuchun, Peng Ligui, et al. Determination of nature of Ordovician island−arc volcanic series at Shihuigou area from Northern Qilian Mountains [J]. Acta Petrol. Mineral., 1991, 10 (1): 1−10 (in Chinese with English abstract).

[14] 夏林圻, 夏祖春, 任有祥, 等. 祁连、秦岭山系海相火山岩 [M]. 武汉: 中国地质大学出版社, 1991.
Xia Linqi, Xia Zuchun, Ren Youxiang, et al. Marine Volcanic Rocks from Qilian and Qinling Mountains [M]. Wuhan: China University of Geosciences Press, 1991 (in Chinese with English abstract).

[15] 夏林圻, 夏祖春, 徐学义. 北祁连山构造−火山岩浆演化动力学 [J]. 西北地质科学, 1995, 16(1): 1−28.
Xia Linqi, Xia Zuchun, Xu Xueyi. Dynamics of tectono−volcano−magmatic evolution from North Qilian Mountains, China [J]. Northwest Geoscience, 1995, 16(1): 1− 28 (in Chinese with English abstract).

[16] 夏林圻, 夏祖春, 徐学义. 北祁连山海相火山岩岩石成因 [M]. 北京: 地质出版社, 1996.
Xia Linqi, Xia Zuchun, Xu Xueyi. Petrogenesis of Marine Volcanic Rocks from Northern Qilian Mountains [M]. Beijing: Geological Publishing House, 1996 (in Chinese).

[17] 夏林圻, 夏祖春, 任有祥, 等. 祁连山及邻区火山作用与成矿 [M]. 北京: 地质出版社, 1998.
Xia Linqi, Xia Zuchun, Ren Youxiang, et al. Volcanism and mineralization in Qilian Mountains and its adjacent area [M]. Beijing: Geological Publishing House, 1998 (in Chinese).

[18] 夏林圻, 夏祖春, 徐学义. 北祁连山早古生代洋脊−洋岛和弧后盆地火山作用 [J]. 地质学报, 1998, 72(4): 301−312.
Xia Linqi, Xia Zuchun, Xu Xueyi. Early Paleozoic mid−ocean ridge−ocean island and back−arc basin volcanism in the North Qilian Mountains [J]. Acta Geol. Sin. , 1998, 72(4): 301−312 (in Chinese with English abstract).

[19] 夏林圻, 夏祖春, 任有祥, 等. 北祁连山构造−火山岩浆−成矿动力学 [M]. 北京: 中国大地出版社, 2001.
Xia Linqi, Xia Zuchun, Ren Youxiang, et al. Tectonics−Volcanic Magmatism− Mineralization Dynamics of North Qilian

Mountains [M]. Beijing: China Land Press, , 2001 (in Chinese).

[20] Xia L Q, Xia Z C, Xu X Y. Magmagenesis in the Ordovician backarc basins of the Northern Qilian Mountains, China [J]. Geol. Soc. Am. Bull. , 2003, 115: 1510−1522.

[21] 许志琴, 徐惠芬, 张建新, 等. 北祁连走廊南山加里东俯冲杂岩增生地体及其动力学 [J]. 地质学报, 1994, 68(1): 1−15.
Xu Zhiqin, Xu Huifen, Zhang Jianxin, et al. The Zhoulangnanshan Caledonian subduction complex in the Northern Qilian Mountains and its dynamics [J]. Acta Geol. Sin. , 1994, 68 (1): 1−15 (in Chinese with English abstract).

[22] 冯益民, 何世平. 祁连山大地构造与造山作用 [M]. 北京: 地质出版社, 1996.
Feng Yimin, He Shiping. Geotectonics and Orogeny of the Qilian Mountains [M]. Beijing: Geological Publishing House, 1996 (in Chinese).

[23] 杨建军, 朱红, 邓晋福, 等. 柴达木北缘石榴石橄榄岩的发现及其意义 [J]. 岩石矿物学杂志, 1994, 13: 97−105.
Yang Jianjun, Zhu Hong, Deng Jinfu, et al. Discovery of garnet−peridotite at the northern margin of the Qaidam Basin and its significance [J]. Acta Petrol. Mineral. , 1994, 13: 97− 105 (in Chinese with English abstract).

[24] Yang J S, Xu Z Q, Li H B, et al. Discovery of eclogite at northern margin of Qaidam basin, NW China [J]. Chin. Sci. Bull. , 1998, 43: 1755−1760.

[25] Yang J S, Xu Z Q, Song S G, et al. Brunel, M. Discovery of coesite in the North Qaidam Early Palaeozoic ultrahigh pressure (UHP) metamorphic belt, NW China [J]. C. R. Acad. Sci. II Fascicule Sci. Terre Planets, 2001, 333: 719−724.

[26] Song S G, Yang J S, Xu Z Q, et al. Metamorphic evolution of coesite− bearing UHP terrane in the North Qaidam, northern Tibet, NW China [J]. J. Metamorph. Geol. , 2003, 21: 631−644.

[27] Song S G, Yang J S, Liou J G, et al. Petrology, geochemistry and isotopic ages of eclogites in the Dulan UHPM terrane, the North Qaidam, NW China [J]. Lithos, 2003, 70 (3−4): 195−211.

[28] Song S G, Zhang L F, Niu Y L. Ultra− deep origin of garnet peridotite from the North Qaidam ultrahigh− pressure belt, Northern Tibetan Plateau, NW China [J]. American Mineral. , 2004, 89: 1330−1336.

[29] Song S G, Zhang L F, Niu Y L, et al. Geochronology of diamond−bearing zircons from garnet− peridotite in the North Qaidam UHPM belt, North Tibetan Plateau: a record of complex histories associated with continental collision [J]. Earth. Planet. Sci. Lett. , 2005, 234: 99−118.

[30] 宋述光, 牛耀龄, 张立飞, 等. 大陆造山运动: 从大洋俯冲到大陆俯冲、碰撞、折返的时限——以北祁连山、柴北缘为例 [J]. 岩石学报, 2009, 25(9): 2067−2077.
Song Shuguang, Niu Yaoling, Zhang Lifei, et al. Time constraints on orogenesis from oceanic subduction to continental subduction, collision, and exhumation: An example from North Qilian and North Qaidam HP−UHP belts [J]. Acta Petrol. Sin. , 2009, 25 (9): 2067−2077 (in Chinese with English abstract).

[31] Zhang J X, Yang J S, Mattinson C G, et al. Two constrasting eclogite cooling histories, North Qaidam HP/UHP terrane, western China: Petrological and isotopic constraints [J]. Lithos, 2005, 84: 51−76.

[32] 张贵宾, 宋述光, 张立飞, 等. 柴北缘超高压变质带沙柳河蛇绿岩型地慢橄榄岩及其意义 [J]. 岩石学报, 2005, 21: 1049−1058.
Zhang Guibin, Song Shuguang, Zhang Lifei, et al. Ophiolite−type mantle peridotite from Shaliuhe, North Qaidam UHPM belt, NW China and its tectonic implications [J]. Acta Petrol. Sin. , 2005, 21: 1049−1058 (in Chinese with English abstract).

[33] 马旭东, 陈丹玲. 柴达木盆地北缘超高压变质岩的围岩长英质片麻岩LA−ICP−MS锆石U−Pb定年 [J]. 地质通报, 2006, 25: 99−103.
Ma Xudong, and Chen Danling. LA− ICP− MS zircon U− Pb dating of quartz− feldspathic gneisses: the country rocks of ultrahigh−pressure metamorphic rocks on the northern margin of the Qaidam basin, Northwest China [J]. Geol. Bull. China, 2006, 25: 99−103 (in Chinese with English abstract).

[34] Mattinson C G, Wooden J L, Liou J G, et al. Age and duration of eclogite− facies metamorphism, North Qaidam HP/UHP terrane, western China [J]. American J. Sci. , 2006, 306: 683−711.

[35] Mattinson C G, Wooden J L, Liou J G, et al. Geochronology and tectonic significance of Middle Proterozoic granitic orthogneiss, North Qaidam HP/UHP terrane, Western China [J]. Mineral. Petrol. , 2006, 88: 227−241.

[36] Mattinson C G, Menold C A, Zhang J X, et al. High− and ultrahigh− pressure metamorphism in the North Qaidam and South Altyn Terranes, western China [J]. Int. Geol. Rev. , 2007, 49: 969−995.

[37] Mattinson C G, Wooden J L, Zhang J X, et al. Paragneiss zircon geochronology and trace element geochemistry, North Qaidam HP/UHP terrane, western China [J]. J. Asian Earth Sci. , 2009, 35: 298−309.

[38] Zhang J X, Yang J S, Meng F C, et al. U−Pb isotopic studies of eclogites and their host gneisses in the Xitieshan area of the North Qaidam Mountains, western China: new evidence for an early Paleozoic HP− UHPmetamorphic belt [J]. J. Asian Earth Sci. , 2006, 28: 143−150.

[39] Zhang G B, Song S G, Zhang L F, et al. The subducted oceanic crust within continental−type UHP metamorphic belt in the North Qaidam, NW China: Evidence from petrology, geochemistry and geochronology [J]. Lithos, 2008, 104: 99−108.

[40] Zhang J X, Mattinson C G, Meng F C, et al. Polyphase tectonothermal history recorded in granulitized gneisses from the North Qaidam HP／UHP metamorphic terrane, Western China: evidence fromzircon U− Pb geochronology [J]. Geol. Soc. Am. Bull. , 2008, 120: 732−749.

[41] Zhang J X, Mattinson C G, Yu S Y, et al. U− Pb zircon geochronology of coesite− bearing eclogites from the southern Dulan area of the North Qaidam UHP terrane, northwestern China: spatially and temporally extensive UHP metamorphism during continental subduction [J]. J. Metamorph. Geol. , 2010, 28: 955−978.

[42] Zhang C, Zhang L F, Roermund H V, et al. Petrology and SHRIMP U−Pb dating of the eclogite in the Xitieshan area of the North Qaidam HP−UHP metamorphic belt, Western China [J]. J. Asian Earth Sci. , 2011, 42: 752−767.

[43] Zhang C, Van Roermund H, Zhang L F, et al. A polyphase metamorphic evolution for the Xitieshan paragneiss of the north Qaidam UHP metamorphic belt, western China: In− situ EMP monazite− and U− Pb zircon SHRIMP dating [J]. Lithos, 2012, 136: 27−45.

[44] 张贵宾, 张立飞, 宋述光. 柴北缘超高压变质带: 从大洋到大陆的深俯冲过程 [J]. 高校地质学报, 2012, 18: 28−40.
Zhang Guibin, Zhang Lifei, Song Shuguang. An overview of the tectonic evolution of North Qaidam UHPM belt: from oceanic subduction to continental collision [J]. Geol. J. China Univ. , 2012, 18: 28−40 (in Chinese with English abstract).

[45] Chen D L, Sun Y, Liu L. In situ LA−ICP−MS zircon U−Pb age of ultrahigh− pressure eclogites in the Yukahe area, northern margin of the Qaidam basin [J]. Sci. China (Ser. D), 2007, 37 (Supp.): 279−287.

[46] Chen D L, Liu L, Sun Y, et al. Geochemistry and zircon U− Pb dating and its implications of the Yukahe HP/UHP terrane, the North Qaidam, NW China [J]. J. Asian Earth Sci. , 2009, 35: 259−272.

[47] Chen N S, Gong S L, Sun M, et al. Precambrian evolution of the Quanji Block, northeastern margin of Tibet: insights from zircon U−Pb and Lu−Hf isotope compositions [J]. J. Asian Earth Sci. , 2009, 35: 367−376.

[48] 陈丹玲, 孙勇, 刘良. 柴北缘鱼卡河榴辉岩围岩的变质时代及其地质意义 [J]. 地学前缘, 2007, 14(1): 108−116.
Chen Danling, Sun Yong, Liu Liang. The metamorphic ages of the country rock of the Yukahe eclogites in the North Qaidam and its geological significance [J]. Earth Sci. Front. , 2007, 14(1): 108−116 (in Chinese with English abstract).

[49] 陈丹玲, 孙勇, 刘良. 柴北缘野马滩超高压榴辉岩中副片麻岩夹层的锆石U−Pb定年及其地质意义[J]. 岩石学报, 2008, 24(5): 1059−1067.
Chen Danling, Sun Yong, Liu Liang. Zircon U− Pb dating of paragneiss interbed in the UHP eclogite from Yematan area, the North Qaidam UHP terrane, NW China [J]. Acta Petrol. Sin. , 2008, 24 (5): 1059−1067 (in Chinese with English abstract).

[50] 陈丹玲, 孙勇, 刘良, 等. 柴北缘野马滩超高压地体的成因——年代学研究结果的约束 [J]. 西北大学学报(自然科学版), 2009, 39(4): 631−638.
Chen Danling, Sun Yong, Liu Liang, et al. Formation mechanism of the Yematan UHP terrane, the North Qaidam: constrains from zircon U− Pb dating [J]. J. Northwest Univ. (Natur. Sci. Ed.), 2009, 39 (4): 631−638 (in Chinese with English abstract).

[51] Song S G, Su Li, Li X H, et al. Tracing the 850−Ma continental flood basalts from a piece of subducted continental crust in the North Qaidam UHPM belt, NW China [J]. Precambrian Res. , 2010, 183: 805−816.

[52] 宋述光, 张聪, 李献华, 等. 柴北缘超高压带中锡铁山榴辉岩的变质时代 [J]. 岩石学报, 2011, 27(4): 1191−1197.
Song Shuguang, Zhang Cong, Li Xianhua, et al. HP/UHP metamorphic time of eclogite in the Xitieshan terrane, North Qaidam UHPM belt, NW China [J]. Acta Petrol. Sin. , 2011, 27 (4): 1191−1197 (in Chinese with English abstract).

[53] Song S G, Su L, Li X H, et al. Grenville− age orogenesis in the Qaidam− Qilian block: the link between South China and Tarim [J]. Precambrian Res. , 2012, 220: 9−22.

[54] Liu X C, Wu Y B, Gao S, et al. First record and timing of UHP metamorphism from zircon in the Xitieshan terrane: implications for the evolution of the entire North Qaidam metamorphic belt [J]. Am. Mineral. , 2012, 97: 1083−1093.

[55] Zhang J X, Mattinson G G, Meng F C, et al. U−Pb geochronology of paragneisses and metabasite in the Xitieshan area, north Qaidam Mountains, western China: Constraints on the exhumation of HP/UHP metamorphic rocks [J]. J. Asian Earth Sci. , 2009, 35: 245−258.

[56] 赵风清, 郭进京, 李怀坤. 青海锡铁山地区滩间山群的地质特征及同位素年代学 [J]. 地质通报, 2003, 22: 28−31.
Zhao Fengqing, Guo Jinjing, Li Huaikun. Geological characteristics and isotopic age of Tanjianshan Group along northern margin of Qaidam basin [J]. Geol. Bull. China, 2003, 22: 28−31 (in Chinese with English abstract).

[57] 王惠初, 陆松年, 袁桂邦, 等. 柴达木盆地北缘滩间山群的构造属性及形成时代[J]. 地质通报, 2003, 22(7): 487−493.
Wang Huichu, Lu Songnian, Yuan Guibang. et al. Tectonic setting and age of the Tanjianshan Group on the northern margin of the Qaidam basin [J]. Geol. Bull. China, 2003, 22 (7): 487− 493 (in Chinese with English abstract).

[58] 史仁灯, 杨经绥, 吴才来, 等. 柴达木北缘超高压变质带中的岛弧火山岩 [J]. 地质学报, 2004, 78: 52−64.
Shi Rendeng, Yang Jingsui, Wu Cailai, et al. Island arc volcanic rocks in the North Qaidam UHP metamorphic belt [J]. Acta Geol. Sin. , 2004, 78: 52−64 (in Chinese with English abstract).

[59] Liu L, Che Z C, Luo J H, et al. Determination of eclogite in the west segment of Altun mountains and its geological significance [J]. Chin. Sci. Bull. , 1996, 41: 1458−1488.

[60] Zhang J X, Zhang Z M, Xu, Z. Q. , et al. Petrology and geochrology of eclogite from the western segment of the Altyn Tagh, northwestern China [J]. Lithos, 2001, 56: 187−206.

[61] 许志琴, 杨经绥, 张建新, 等. 阿尔金断裂两侧构造单元的对比及岩石圈剪切机制 [J]. 地质学报, 1999, 73: 193−205.
Xu Zhiqin, Yang Jingsui, Zhang Jianxin, et al. A comparison between the tectonic units on the two sides of the Altyn Tagh sinistral strike− slip fault and the mechanism of lithospheric shearing [J]. Acta Geol. Sin. , 1999, 73: 193−205 (in Chinese with English abstract).

[62] 李怀坤, 陆松年, 王惠初, 等. 青海柴北缘新元古代超大陆裂解的地质记录——全吉群 [J]. 地质调查与研究, 2003, 26(1): 27−37.
Li Huaikun, Lu Songnian, Wang Huichu, et al. Geological records of break− up of Neoproterozoic supercontinent from northern margin of the Qaidam Block, Qinghai Province [J]. Geol. Sur. Res. , 2003, 26 (1): 27−37 (in Chinese).

[63] 徐学义, 王洪亮, 陈隽璐, 等. 中祁连东段兴隆山群基性火山岩锆石 U−Pb 定年及岩石成因研究 [J]. 岩石学报, 2008, 24(4): 827−840.
Xu Xueyi, Wang Hongliang, Chen Junlu, et al. Zircon U− Pb dating and petrogenesis of Xinglongshan Group basic volcanic rocks at eastern segment of Middle Qilian Mts [J]. Acta Petrol. Sin. , 2008, 24(4): 827−840 (in Chinese with English abstract).

[64] Zhang J X, Meng F C, Wan Y S. A cold Early Paleozoic subduction zone in the North Qilian Mountains, NW China: petrological and U− Pb geochronological constraints [J]. J. Metamor. Geol. , 2007, 25: 285−304.

[65] Mao J W, Zhang Z C, Yang J M. Dating of single−grain zircon for Precambrican strata in western part of from North Qilian Mountains [J]. Chin. Sci. Bull. , 1997, 42: 1414−1417.

[66] 史仁灯, 杨经绥, 吴才来, 等. 北祁连玉石沟蛇绿岩形成于晚震旦世的SHRIMP年龄证据 [J]. 地质学报, 2004, 78: 649−657.
Shi Rendeng, Yang Jingsui, Wu Cailai, et al. First SHRIMP dating for the formation of the Late Sinian Yushigou ophiolite, North Qilian Mountains [J]. Acta Geol. Sin. , 2004, 78: 649− 657 ((in Chinese with English abstract).

[67] Tseng C Y, Yang H J, Yang H Y, et al. The Dongcaohe ophiolite from the North Qilian Mountains: a fossil oceanic crust of the Paleo−Qilian ocean [J]. Chin. Sci. Bull. , 2007, 52: 2390−2401.

[68] 相振群, 陆松年, 李怀坤, 等. 北祁连西段熬油沟辉长岩的锆石 SHRIMP U−Pb 年龄及地质意义 [J]. 地质通报, 2007, 26: 1686−1691.
Xiang Zhenqun, Lu Songnian, Li Huaikun, et al. SHRIMP U−Pb zircom age of gabbro in Aoyougou in the western segment of the North Qilian Mountains, China and its geological implications [J]. Geol. Bull. China, 2007, 26: 1686−1691 (in Chinese with English abstract).

[69] 夏小洪, 孙楠, 宋述光, 等. 北祁连西段熬油沟—二只哈拉达坂蛇绿岩的形成环境和时代 [J]. 北京大学学报(自然科学版), 2012, 48(5): 757−769.
Xia Xiaohong, Sun Nan, Song Shuguang, et al. Age and tectonic setting of the Aoyougou−Erzhihaladaban ophiolite in the Western North Qilian Mountains, NW China [J]. Acta Sci. Natura. Univ. Pekin., 2012, 48 (5): 757−769 (in Chinese with English abstract).

[70] 武鹏, 李向民, 徐学义, 等. 北祁连山扎麻什地区东沟蛇绿岩 LA−ICP−MS 锆石 U−Pb 测年及其地球化学特征 [J]. 地质通报, 2012, 31(6): 896−906.
Wupeng, Li Xiangmin, Xu Xueyi, et al. LA−ICP−MS zircon U−Pb dating and geochemical characteristics of Donggou ophiolites in Zamashi area of northern Qilian Mountains [J]. Geol. Bull. China, 2012, 31 (6): 896−906 (in Chinese with English abstract).

[71] 张建新, 许志琴, 陈文, 等. 北祁连中段俯冲−增生杂岩/火山弧的时代探讨 [J]. 岩石矿物学杂志, 1997, 16: 112−119.
Zhang Jianxin, Xu Zhiqin, Chen Wen, et al. A tentative discussion on the ages of the subduction−accretionary complex/volcanic arcs in the middle sector of North Qilian Mountains [J]. Acta Petrol. Minerl., 1997, 16: 112−119 (in Chinese with English abstract).

[72] Wang C Y, Zhang Q, Qian Q, et al. Geochemistry of the Early Paleozoic Baiyin volcanic rocks (NW China): implications for the tectonic evolution of the North Qilian Orogenic Belt [J]. J. Geol. , 2005, 113: 83−94.

[73] 何世平, 王洪亮, 陈隽璐, 等. 甘肃白银矿田变酸性火山岩锆石 LA−ICP−MS 测年——白银式块状硫化物矿床形成时代新证据 [J]. 矿床地质, 2006, 25: 401−411.
He Shipin, Wang Hongliang, Chen Junlu, et al. A LA−ICP−MS U−Pb chronological study of zircons from meta−acdic volcanics in Baiyin orefield, Gansu Province: new evidence for metallogenic age of Baiyin type massive sulfide deposits [J]. Mineral Deposits, 2006, 25: 401− 411 (in Chinese with English abstract).

[74] 李向民, 马中平, 孙吉明, 等. 甘肃白银矿田基性火山岩的 LA−ICP−MS 同位素年代学 [J]. 地质通报, 2009, 28: 901−906.
Li Xiangmin, Ma Zhongping, Sun Jiming, et al. A LA−ICP−MS chronological study of basic volcanics in Baiyin orefield, Gansu, China [J]. Geol. Bull. China, 2009, 28: 901−906 (in Chinese with English abstract).

[75] 余吉远, 李向民, 马中平, 等. 青海省祁连县清水沟—白柳沟矿田含矿火山岩系年代学研究 [J]. 地球科学进展, 2010, 25(1): 55−60.
Yu Jiyuan, Li Xiangmin, Ma Zhongping, et al. Chronological study of mata− acidic volcanics in Qingshuigou− Bailiugou orefield, Qilian County of Qinghai Province [J]. Advance Earth Sci. , 2010, 25 (1): 55−60 (in Chinese with English abstract).

[76] 余吉远, 李向民, 马中平, 等. 北祁连构造带冷龙岭地区火山岩地球化学特征及年代学 [J]. 地质科技情报, 2010, 29(4): 6−13.
Yu Jiyuan, Li Xiangmin, Ma Zhongping, et al. 2010. Geochemical characters and LA− ICP− MS zircon U− Pb dating of the Lenglongling volcanic rocks from the North Qilian tectonic belt [J]. Geol. Sci. Technol. Inform. , 2010, 29 (4): 6− 13 (in Chinese with English abstract).

[77] Xia X H, and Song S G. Forming age and tectono−petrogenesis of the Jiugequan ophiolite in the North Qilian Mountains, NW China [J]. Chin. Sci. Bull. , 2010, 55: 1899−1907.

[78] Xia X H, Song S G, Niu Y L. Tholeiite−Boninite terrane in the North Qilian suture zone: Implications for subduction initiation and back− arc basin development [J]. Chem. Geol. , 2012, 328: 259−277.

[79] 孟繁聪, 张建新, 郭春满, 等. 大岔大坂MOR型和SSZ型蛇绿岩对北祁连洋演化的制约 [J]. 岩石矿物学杂志, 2010, 29(5): 453−466.
Meng Fancong, Zhang Jianxin, Guo Chunman, et al. Constraints on the evolution of the North Qilian ocean basin: MOR−type and SSZ−type ophiolites from Dachadaban [J]. Acta Petrol. Mineral. , 2010, 29 (5): 453−466 (in Chinese with English abstract).

[80] 王国强, 李向民, 徐学义, 等. 青海门源地区红沟铜矿床含矿基性火山岩LA−ICP−MS锆石U−Pb年龄 [J]. 地质通报, 2011, 30 (7): 1060−1065.
Wang Guoqiang, Li Xiangmin, Xu Xueyi. LA− ICP− MS U− Pb dating of zircons from basic volcanic rocks in the Honggou copper polymetallic deposit, Menyuan area, Qinghai [J]. Geol. Bull. China, 2011, 30 (7): 1060− 1065 (in Chinese with English abstract).

[81] Li X H, Su L, Song B, et al. SHRIMP U− Pb zircon age of the Jinchuan ultramafic intrusion and its geological significance [J]. Chin. Sci. Bull. , 2004, 49: 420−422.

[82] Li X H, Su L, Chung S L, et al. Formation of the Jinchuan ultramafic intrusion and the world's third largest Ni− Cu sulfide deposit: associated with the similar to 825 Ma south China mantle plume? [J]. Geochemistry, Geophysics, Seosystems, 2005, 6: Q11004, doi: 10. 1029/2005GC001006.

[83] Song S G, Zhang L F, Niu Y L, et al. Zircon U−Pb SHRIMP ages of eclogites from the North Qilian Mountains, NW China and their tectonic implication [J]. Chin. Sci. Bull. , 2004, 49: 848−852.

[84] Liou J G, Wang X, Coleman R G. Blueschists in major suture zones of China [J]. Tectonics, 1989, 8: 609−619.

[85] Liu Y J, Neubauer F, Takasu A, et al. $^{40}Ar/^{39}Ar$ ages of blueschist facies politic schists from Qingshuigou in the Northern Qilian Mountains, western China [J]. Island Arc, 2006, 15: 187−198.

[86] Lin Y H, Zhang L F, Ji J Q, et al. $^{40}Ar/^{39}Ar$ age of Jiugequan lawsonite− blueschists in northern Qilian Mountains and its petrologic significance [J]. Chin. Sci. Bull. , 2010, 55: 2021−2027.

[87] 胡能高, 许安东, 杨家喜. 龙首山直沟门岩体特征及构造环境 [J]. 地球科学与环境学报, 2005, 27: 5−11.
Hu Nenggao, Xu Andong, Yang Jiaxi. Characteristics and ctectonic environment of Zhigoumen pluton in Longshoushan area [J]. J. Earth Sci. Environ. , 2005, 27: 5−11 (in Chinese with English abstract).

[88] 吴才来, 徐学义, 高前明, 等. 北祁连早古生花岗质岩浆作用及构造演化 [J]. 岩石学报, 2010, 26: 1027−1044.
Wu Cailai, Xu Xueyi, Gao Qianming, et al. Early Palaeozoic granitoid magmatism and tectonic evolution in North Qilian, NW China [J]. Acta Petrol. Sin. , 2010, 26: 1027− 1044 (in Chinese with English abstract).

[89] 吴才来, 姚尚志, 杨经绥, 等. 北祁连洋早古生代双向俯冲的花岗岩证据 [J]. 中国地质, 2006, 33(6): 1197−1208.
Wu Cailai, Yao Shangzhi, Yang Jingsui. et al. Doubel subduction of the Early Paleozoic North Qilian oceanic plate: evidence from granites in the central segment of North Qilian, NW China [J]. Geology in China, 2006, 33 (6): 1197− 1208 (in Chinese with English abstract).

[90] 吴才来, 杨经绥, 杨宏仪, 等. 北祁连东部两类I型花岗岩定年及其地质意义 [J]. 岩石学报, 2004, 20(3): 425−432.
Wu Cailai, Yang Jingsui, Yang Hongyi. 2004 Two types of I−type granite dating and geological significance from North Qilian, NW China [J]. Acta Petrol. Sin. , 2004, 20 (3): 425− 432 (in Chinese with Enmglish abstract).

[91] Tseng C Y, Yang H J, Yang H Y, et al. Continuity of the North Qilian and North Qinling orogenic belts, Central Orogenic System of China: evidence from newly discovered Paleozoic adakitic rocks [J]. Gondwana Res. , 2009, 16: 285−293.

[92] 钱青, 王岳明, 李惠民, 等. 甘肃老虎山闪长岩的地球化学特征及其成因 [J]. 岩石学报, 1998, 14: 520−528.
Qian Qing, Wang Yueming, Li Huimin, et al. Geochemical characteristics and genesis of diorites from Laohushan, Gasu Province [J]. Acta Petrl. Sin. , 1998, 14: 520−28 (in Chinese with English abstract).

[93] Chen Y X, Song S G, Xia X H. Petrogenesis of Aoyougou high−silica adakite in the western sector of Noth Qilian Mountains, NW China: evidence for decompression melting of oceanic slab [J]. Sci. China (Ser. D), 2012, 57: 2072−2085.

[94] 秦海鹏, 吴才来, 王次松, 等. 北祁连下古城花岗岩体LA−ICP−MS锆石U−Pb年代学及岩石化学特征 [J]. 地质学报, 2014, 88 (10): 1832−1842.
Qin Haipeng, Wu Cailai, Wang Cisong, et al. LA− ICP− MS zircon U− Pb characteristical of Xiagucheng granite in North Qilian [J]. Acta Geol. Sin. , 2014, 88 (10): 1832−1842 (in Chinese with English abstract).

[95] 吴才来, 杨经绥, 许志琴 等. 柴达木盆地北缘古生代超高压带中花岗质岩浆作用 [J]. 地质学报, 2004, 78(5): 658−674.
Wu Cailai, Yang Jingsui, Xu Zhiqin, et al. 2004. Granitic magmatism on the Early Paleozoic UHP belt of Northern Qaidam, NW China. Acta Geol. Sin. 78 (5): 658− 674. (in Chinese with English abstract).

[96] 吴才来, 郜源红, 吴锁平, 等. 柴达木盆地北缘大柴旦地区古生代花岗岩锆石SHRIMP定年 [J]. 岩石学报, 2007, 23(8): 1861−1875.

Wu Cailai, Gao Yuanhong, Wu Suoping, et al. Zircon SHRIMP U− Pb dating of granites from the Daqaidam area in the north margin of Qaidam basin, NW China [J]. Acta Petrol. Sin. , 2007, 23 (8): 1861−1875 (in Chinese with English abstract).

[97] Wu C L, Wooden J L, Robinson P T. , et al. Geochemistry and zircon SHRIMP U−Pb dating of granitoids from the west segment in the North Qaidam [J]. Sci. China (Ser. D), 2009, 52: 1771−1790.

[98] 孟繁聪, 张建新, 杨经绥. 柴北缘锡铁山早古生代HP/UHP变质作用后的构造热事件: 花岗岩和片麻岩的同位素与岩石地球化学证据 [J]. 岩石学报, 2005, 21(1): 45−56.
Meng Fancong, Zhang Jianxin, Yang Jingsui. Tectono− thermal event of post− HP/UHP metamorphism in the Xitieshan area of the North Qaidam Mountains, western China: isotopic and geochemical evidence of granite and gneiss [J]. Acta Petrol. Sin. , 2005, 21 (1): 45−56 (in Chinese with English abstract).

[99] 卢欣祥, 孙延贵, 张雪亭, 等. 柴达木盆地北缘塔塔楞环斑花岗岩的SHRIMP年龄 [J]. 地质学报, 2007, 81(5): 626−634.
Lu Xinxiang, Sun Yangui, Zhang Xueting, et al. The SHRIMP age of Tatalin rapakivi granite at the north margin of Qaidam basin [J]. Acta Geol. Sin. , 2007, 81 (5): 626− 634 (in Chinese with English abstract).

[100] Wu C L, Gao Y H, Li Z L, et al. Zircon SHRIMP U−Pb dating of granites from Dulan and the chronological framework of the North Qaidam UHP belt, NW China [J]. Sci. China (Ser. D), 2014. 57 (12): 2945−2965.

[101] Xiong Q, Zheng J P, Griffin W L, et al. Zircons in the Shenglikou ultrahigh− pressure garnet peridotite massif and its country rocks from the north qaidam terrane (western China): Meso− Neoproterozoic crust− mantle coupling and early Paleozoic convergent plate− margin processes [J]. Precambrian Res. , 2011, 187, 33−57.

[102] 赵国春. 华北克拉通基底主要构造单元变质作用演化及其若干问题讨论 [J]. 岩石学报, 2009, 25: 1772−1792.
Zhao Guochun. Metamorphic evolution of major tectonic units in the basement of the North China Craton: key issues and discussion [J]. Acta Petrol. Sin. , 2009, 25: 1772− 1792 (in Chinese with English abstract).

[103] Zhai M G, Santosh M. The early Precambrian odyssey of the North China Craton: a synoptic overview [J]. Gondwana Res. , 2011, 20, 6−25.

[104] 修群业, 于海峰, 李铨, 等. 龙首山岩群成岩时代探讨 [J]. 地质学报, 2004, 78: 366−373.
Xiu Qunye, Yu Haifeng, Li Quan, et al. Discussion on the petrogenic time of Longshoushan Group, Gansu Province [J]. Acta Geol. Sin. , 2004, 78: 366− 373 (in Chinese with English abstract).

[105] 宁夏地质矿产局. 宁夏区域地质志. 中华人民共和国地质矿产部地质专报 [M]. 北京: 地质出版社, 1990.
NBGMR (Ningxia Bureau of Geology and Mineral Resources). Regional Geology of Ningxia Hui Autonomous Region. Geological Memoirs of Ministry of Geology and Mineral Resources of People's Republic of China [M]. Beijing: Geological Publishing House, 1990 (in Chinese).

[106] 耿元生, 王新社, 沈其韩, 等. 内蒙古阿拉善地区前寒武纪变质基底阿拉善群的再厘定 [J]. 中国地质, 2006, 33: 138−145.
Geng Yuansheng, Wang Xinshe, Shen Qihan, et al. Redefinition of the Alxa Group− complex (Precambrian metamorphic basement) in the Alxa area, Inner Mongolia [J]. Geology in China, 2006, 33: 138−145 (in Chinese with English abstract).

[107] 耿元生, 王新社, 沈其韩, 等. 内蒙古阿拉善地区前寒武纪变质岩系形成时代的初步研究 [J]. 中国地质, 2007, 34: 251−261.
Geng Yuansheng, Wang Xinshe, Shen Qihan, et al. Chronology of the Precambrian metamorphic series in the Alxa area, Inner Mogolia [J]. Geology in China, 2007, 34: 251−261 (in Chinese with English abstract).

[108] Tung K A, Yang H Y, Liu D Y. SHRIMP U−Pb geochronology of detrital zircons from the Longshoushan Group and its tectonic significance [J]. Chin. Sci. Bull. , 2007, 52: 1414−1425.

[109] 万渝生, 许志琴, 杨经绥. 祁连山带及邻区前寒武纪深变质基底的时代和组成 [J]. 地质学报, 2001, 75: 375−384.
Wan Yusheng, Xu Zhiqin, Yang Jingsui. Ages and compositions of the Precambrian highgrade basement of the Qilian terrance and its adjacent areas [J]. Acta Geol. Sin. , 2001, 75: 375− 384 (in Chinese with English abstract).

[110] 耿元生, 王新社, 沈其韩, 等. 阿拉善地区新元古代晋宁期变形花岗岩的发现及其地质意义 [J]. 矿物岩石学杂志, 2002, 21: 412−420.
Geng Yuansheng, Wang Xinshe, Shen Qihan, et al. The discovery of Neoproterozoic Jinningian deformed granites in Alax area and its significance [J]. Mineral. Petrogi. Acta, 2002, 21: 412−420 (in Chinese with English abstract).

[111] Dan W, Li X H, Guo J, Liu, et al. Paleoproterozoic evolution of the eastern Alxa Block, westernmost North China: evidence from in situ zircon U− Pb dating and Hf− O isotopes [J]. Gondwana Res. , 2012, 21: 838−864.

[112] 陆松年. 青藏高原北部前寒武纪地质初探 [M]. 北京: 地质出版社, 2002.
Lu Songnian. Preliminary Study of Precambrian Geology in the North Tibet− Qinghai Plateau [M]. Beijing: Geological Publishing House, 2002 (in Chinese).

[113] Wang Q Y, Pan Y M, Chen N S, et al. Proterozoic polymetamorphism in the Quanji Block, northwestern China: evidence from microtextures, garnet compositions and monazite CHIME ages [J]. J. Asian Earth Sci. , 2009, 34: 686−698.

[114] 郭进京, 赵凤清, 李怀坤. 中祁连东段晋宁期碰撞型花岗岩及其地质意义 [J]. 地球学报, 1999, 20: 10−15.
Guo Jinjing, Zhao Fengqing, Li Huaikun. Jinningian collisional

granite belt in the eastern sector of the Central Qilian Massif and its implication [J]. Acta Geosci. Sin. , 1999, 20: 10− 15 (in Chinese with English abstract).

[115] Tung K A, Yang H J, Yang H Y, et al. SHRIMP U− Pb geochronology of the zircons from the Precambrian basement of the Qilian Block and its geological significances [J]. Chin. Sci. Bull. , 2007, 52: 2687−2701.

[116] Xia L Q, Xia Z C, Zhao J T, et al. Determination of properties of Proterozoic continental flood basalts of western part from North Qilian Mountains [J]. Sci. China (Ser. D), 1999, 42: 506−514.

[117] Darby B J, Gehrels G. Detrital zircon reference for the North China block [J]. J. Asian Earth Sci. , 2006, 26: 637−648.

[118] 王惠初, 袁桂邦, 辛后田, 等. 柴达木盆地北缘鱼卡河岩群的地质特征和时代[J]. 地质通报, 2004, 23: 314−321.
Wang Huichu, Yuan Guibang, Xin Houtian. Geological characteristic and age of the Iqe River Group− complex on the northern margin of the Qaidam basin [J]. Geol. Bull. China, 2004, 23: 314−321 (in Chinese with English abstract).

[119] 高振家, 王务严, 彭昌文, 等. 新疆震旦系 [M]. 乌鲁木齐: 新疆人民出版社, 1985.
Gao Zhenjia, Wang Wuyan, Peng Changwen, et al. Sinian System in Xinjiang, China [M]. Urumqi: Xinjiang People’s Publishing House, 1985 (in Chinese with English abstract).

[120] 高振家, 陈晋镳, 陆松年, 等. 新疆北部前寒武系 [M]. 北京: 地质出版社, 1993.
Gaozhenjia, Chenjinbiao, Lu Songnian, et al. The Precambrian Geology in Northern Xinjiang [M]. Beijing: Geological Publishing House, 1993 (in Chinese with English abstract).

[121] 高振家, 陈克强. 新疆的南华系及我国南华系的几个地质问题——纪念恩师王曰伦先生诞辰一百年 [J]. 地质调查与研究, 2003, 26 (1): 8−14.
Gao Zhenjia, Chen Keqiang. The Nanhua System of Xinjiang and some geological issues of Nanhua System in China [J]. Geological Survey and Research, 2003, 26 (1): 8−14 (in Chinese with English abstract).

[122] Xu B, Jian H, Zou H, et al. U− Pb zircon geochronology and geochemistry of Neoproterozoic volcanic rocks in the Tarim Block of northwestern China: implications for the breakup of Rodinia supercontinent and Neoproterozoic glaciations [J]. Precambrian Res. , 2005, 136: 107−23.

[123] 姜常义, 吴文奎, 李良辰, 等. 南天山东段显生宙构造演化 [M]. 北京: 地质出版社, 2001.
Jiang Changyi, Wu Wenkui, Li Liangchen, et al. The Phanerozoic Tectonic Evolution in Eastern Segment of South Tianshan [M]. Beijing: Geological Publishing House, 2001 (in Chinese).

[124] 夏林圻, 张国伟, 夏祖春, 等. 天山古生代洋盆开启、闭合时限的岩石学约束——来自震旦纪、石炭纪火山岩的证据 [J]. 地质通报, 2002, 21(2): 55−62.
Xia Linqi, Zhang Guowei, Xia Zuchun, et al. Constraints on the timing of opening and closing of the Tianshan Paleozoic oceanic basin: evidence from Sinian and Carboniferous volcanic rocks [J]. Geological Bulletin of China, 2002, 21(2): 55−2 (in Chinese with English abstract).

[125] 夏林圻, 夏祖春, 徐学义, 等. 天山岩浆作用 [M]. 北京: 中国大地出版社, 2007.
Xia Linqi, Xia Zuchun, Xu Xueyi , et al. 2007. Magmatism in the Tianshan [M]. Beijing: China Land Press, 2007 (in Chinese).

[126] Xia L Q, Xia Z C, Xu X Y, et al. Mid−late−Neoproterozoic rift−related volcanic rocks in China: Geological records of rifting and break−up of Rodinia [J]. Geosci. Front. , 2012, 3: 375−399.

[127] 王飞, 王博, 舒良树. 塔里木西北缘阿克苏地区大陆拉斑玄武岩对新元古代裂解事件的制约 [J]. 岩石学报, 2010, 26(2): 547−558.
Wangfei, Wangbo, Shuliangshu. Continental tholeiitic basalt of the Akesu area (NW China) and its implication for the Neoproterozoic rifting in the north Tarim [J]. Acta Petrol. Sin. , 2010, 26 (2): 547−558 (in Chinese with English abstract).

[128] 朱杰辰, 孙文鹏. 新疆天山地区震旦系同位素地质研究 [J]. 新疆地质, 1987, 5(1): 55−61.
Zhujiechen, Sunwenpeng. Geochronology study of Sinian system for Tianshan region, Xinjiang [J]. Xinjiang Geol. , 1987, 5 (1): 55−61 (in Chinese with English abstract).

[129] Xu B, Xiao S H, Zou H B, et al. SHRIMP zircon U− Pb age constraints on Neoproterozoic Qurugtagh diamictites in NW China [J]. Precambrian Res. , 2009, 168: 247−258.

[130] 朱杰辰, 孙文鹏. 中天山变质岩系的成岩时代及演化探讨 [J]. 新疆地质, 1986, 4(4): 47−52.
Zhujiechen, Sunwenpeng. Approach of deagenetic age and evolution of metamorphic rocks of middle Tianshan [J]. Xinjiang Geol. , 1986, 4(4): 47−52 (in Chinese with English abstract).

[131] Chen Y, Xu B, Zhan S, et al. First mid− Neoproterozoic paleomagnetic results from the Tarim Basin (NW China) and their geodynamic implications [J]. Precambrian Res. , 2004, 133: 271−281.

[132] Zhang C L, Li Z X, Li X H, Ye, et al. Neoproterozoic mafic dyke swarms at the northern margin of the Tarim Block, NW China: age, geochemistry, petrogenesis and tectonic implications [J]. J. Asian Earth Sci. , 2009, 35: 167−179.

[133] Zhu W B, Zheng B H, Shu L S, et al. Geochemistry and SHRIMP U− Pb zircon geochronology of Korla mafic dykes: constrains on the Neoproterozoic continental breakup in the Tarim Block, northwest China [J]. J. Asian Earth Sci. , 2011, 42: 791−804.

[134] 李曰俊, 贾承造, 胡世玲, 等. 塔里木盆地瓦基里塔格辉长岩 $^{40}Ar-^{39}Ar$年龄及其意义 [J]. 岩石学报, 1999, 15: 594−599.
Liyuejun, Jiachengzao, Hushiling, et al. The $^{40}Ar-^{39}Ar$ isotopic age of Wajilitag gabbro in Tarim basin and its geological

significance [J]. Acta Petrologica Sinica, 1999, 15: 594−599 (in Chinese with English abstract).

[135] Zhang C L, Li X H, Li Z X, et al. Neoproterozoic ultramafic−mafic− carbonatite complex and granitoids in Quruqtagh of northeastern Tarim Block, western China: geochronology, geochemistry and tectonic implications [J]. Precambrian Res. , 2007, 152: 149−169.

[136] Zhang C L, Yang D S, Wang H Y, et al. Neoproterozoic mafic−ultramafic layered intrusion in Quruqtagh of northeastern Tarim Block, NW China: two phases of mafic igneous activity with different mantle sources [J]. Gondwana Res. , 2011, 19: 177−190.

[137] Guo ZJ, Yin A, Bobinson A, et al. Geochronology and geochemistry of deep−drill−core samples from the basement of the central Tarim basin [J]. J. Asian Earth Sci. , 2005, 25: 45−56.

[138] Zhang C L, Yang D S, Wang H Y, et al. Neoproterozoic mafic dykes and basalts in the southern margin of Tarim, northwest China: age, geochemistry and geodynamic implications [J]. Acta Geol. Sin. , 2010, 84: 549−562.

[139] 王剑. 华南新元古代裂谷盆地演化—兼论与Rodinia解体的关系 [M]. 北京: 地质出版社, 2000.
Wangjian. Neoproterozoic Rifting History of South China: Significance to Rodinia Breakup [M]. Beijing: Geological Publishing House, 2000 (in Chinese with English abstract).

[140] Wang J, Li Z X. History of Neoproterozoic rift basins in South China: implications for Rodinia break− up [J]. Precambrian Res. , 2003, 122: 141−158.

[141] 李献华, 周汉文, 李正祥, 等. 川西新元古代双峰式火山岩成因的微量元素和Sm−Nd同位素制约及其大地构造意义 [J]. 地质科学, 2002, 37(3): 264−276.
Li Xianhua, Zhouhanwen, Lizhengxiang, et al. Petrogenesis of Neoproterozoic bimodal volcanics in western Sichuan and its tectonic implications: geochemical and Sm− Nd isotopic constraints [J]. Chin. J. Geol. , 2002, 37(3): 264−276 (in Chinese with English abstract).

[142] Li X H, Li Z X, Zhou H, et al. U− Pb zircon geochronology, geochemistry and Nd isotopic study of Neoproterozoic bimodal volcanic rocks in the Kangdian Rift of South China: implications for the initial rifting of Rodinia [J]. Precambrian Res. , 2002, 113: 135−154.

[143] Li X H, Li Z X, Sinclair J A, et al. Revisiting the "Yanbian Terrane": implications for Neoproterozoic tectonic evolution of the western Yangtze Block, South China [J]. Precambrian Res. , 2006, 151: 14−30.

[144] Li X H, Li W X, Li Z X, Lo, et al. Amalgamation between the Yangtze and Cathaysia Blocks in South China: constraints from SHRIMP U−Pb zircon ages, geochemistry and Nd−Hf isotopes of the Shuangxiwu volcanic rocks [J]. Precambrian Res. , 2009, 174: 117−128.

[145] Ye M F, Li X H, Li W X, et al. SHRIMP zircon U− Pb geochronological and whole−rock geochemical evidence for an early Neoproterozoic Sibaaoan magmatic arc along the southeastern margin of the Yangtze Block [J]. Gondwana Res. , 2007, 12: 144−156.

[146] 高林志, 杨明桂, 丁孝忠, 等. 华南双桥山群及河上镇群凝灰岩中的锆石SHRIMP U−Pb年龄——对江南新元古代造山带地质演化的制约 [J]. 地质通报, 2008, 27(10): 1744−1758.
Gaolinzhi, Yangminggui, Dingxiaozhong, et al. SHRIMP U−Pb zircon dating of tuff in the Shuangqiaoshan and Heshangzhen groups in South China: constraints on the evolution of the Jiangnan Neoproterozoic Orogenic Belt [J]. Geol. Bull. China, 2008, 27(10): 1744−1758 (in Chinese with English abstract).

[147] 高林志, 戴传固, 刘燕学, 等. 黔东南—桂北地区四堡群凝灰岩锆石SHRIMP U−Pb年龄及其地层学意义 [J]. 地质通报, 2010, 29(9): 1259−1267.
Gaolinzhi, Daichuangu, Liuyanxue, et al. Zircon SHRIMP U−Pb dating of tuff bed of the Sibao Group in southern Guizhou−northern Guangxi area, China and its stratigraphic implication [J]. Geol. Bull. China, 2010, 29(29): 1259− 1267 (inChinese with English abstract).

[148] 高林志, 陈峻, 丁孝忠, 等. 湘东北岳阳地区冷家溪群及板溪群凝灰岩SHRIMP锆石U−Pb年龄——对武陵运动的制约 [J]. 地质通报, 2011, 30(9): 1001−1008.
Gaolinzhi, Chenjun, Dingxiaozhong, et al. Zircon SHRIMP U−Pb dating of the tuff bed of Lengjiaxi and Banxi groups, northeastern Hunan: constraints on the Wuling Movement [J]. Geol. Bull. China, 2011, 30 (9): 1001− 1008 (in Chinese with English abstract).

[149] 周金城, 王孝磊, 邱检生. 江南造山带新元古代构造−岩浆演化 [M]. 北京: 科学出版社, 2014.
Zhoujinchen, Wangxiaolei X L, Qiu J S. Neoproterozoic Tectono− Magmatic Evolution of the Jiangnan Orogen [M]. Beijing: Science Press, 2014 (in Chinese).

[150] Qiu Y M, Gao S, McNaughton N J, et al. First evidence of >3. 2 Ga continental crust in the Yangtze craton of South China and its implications for Archean crustal evolution and Phanerozoic tectonics [J]. Geology, 2000, 28: 11−14.

[151] Li X H. Timing of the Cathaysia block formation: constraints from SHRIMP U−Pb zircon geochronology [J]. Episodes, 1997, 20: 188−192.

[152] Li Z X, Li X H. Formation of the 1300 km− wide intra−continental orogen and post− orogenic magmatic province in Mesozoic South China: a flat− slab subduction model [J]. Geology, 2007, 35: 179−182.

[153] 甘肃省地质矿产局. 甘肃省区域地质志. 中华人民共和国地质矿产部地质专报 [M]. 北京: 地质出版社, 1989.
GBGMR (Gansu Bureau of Geology and Mineral Resources). Regional Geology of Gansu Province. Geological Memoirs of

Ministry of Geology and Mineral Resources of People's Republic of China [M]. Beijing: Geological Publishing House, 1989 (in Chinese).

[154] Winchester J A, Floyd P A. Geochemical discrimination of different magma series and their differentiation products using immobile elements [J]. Chem. Geol. , 1977, 20: 325−343.

[155] Miyashiro A. Classification, characteristics and origin of ophiolites [J]. J. Geol. , 1975, 83: 249−281.

[156] Sun S S, McDonough W F. Chemical and isotopic systematics of oceanic basalts: implications for mantle composition and processes [C]//Saunders A D, Norry M J(eds.). Magmatism in the Ocean Basins [D]. Geological Society, London, Special Publications, 1989, 42: pp. 313−346.

[157] Tatsumi Y, Eggins S M. Subduction Zone Magmatism [M]. Cambridge: Blackwell Science, 1995.

[158] Fitton J G. Coupled molybdenum and niobium depletion in continental basalts [J]. Earth Planet. Sci. Lett. , 1995, 136: 715−721.

[159] Fitton J G, James D, Leeman W P. Basic magmatism associated with the late Cenozoic extension in the western United States: compositional variations in space and time [J]. J. Geophys. Res. , 1991, 96: 13693−13711.

[160] Pearce J A. and Norry M J. Petrogenetic implications of Ti, Zr, Y and Nb variations in volcanic rocks [J]. Contrib. Mineral. Petrol. , 1979, 69, 33−47.

[161] Pearce, J A. Trace element characteristics of lavas from destructive plate boundaries [C]//Thorps R S(ed.). Andesites. New York: John Wiley and Sons, 1982: 525−548.

[162] Wood D A. The application of a Th−Hf−Ta diagram to problems of tectonomagmatic classification and to establishing the nature of crustal contamination of basaltic lavas of British Tertialy volcanic province [J]. Earth Planet. Sci. Lett. , 1980, 50: 11−30.

[163] 李怀坤, 陆松年, 相振群, 等. 北祁连山西段北大河岩群碎屑锆石 SHRIMP U−Pb 年代学研究 [J]. 地质论评, 2007, 53: 132−140.
Li Huaikun, Lu Songnian, Xiang Zhenqun, et al. SHRIMP U−Pb geochronological research on detrital zircons from the Beidahe complex− Group in the western segment of the North Qilian Mountains, Northwest China [J]. Geol. Rev. , 2007, 53: 132−140 (in Chinese with English abstract).

[164] 夏林圻, 夏祖春, 徐学义, 等. 利用地球化学方法判别大陆玄武岩和岛弧玄武岩 [J]. 岩石矿物学杂志, 2007, 26(1): 77−89.
Xia Linqi, Xia Zuchun, Xu Xueyi, et al. The discrimination between continental basalt and island arc basalt based on geochemical method [J]. Acta Petrol. Mineral. 2007, 26 (1): 77−89 (in Chinese with English abstract).

[165] Xia L Q. The geochemical criteria to distinguish continental basalts from arc related ones [J]. Earth Sci. Rev. , 2014, 139: 195−212.

[166] Condie K C, Incompatible element ratios in oceanic basalts and komatites: tracking deep mantle sources and continental growth rates with time[J]. Geochemistry Geophysics Geosystems, 2003, 4 (1): 1005.

[167] Condie K C. High field strength element ratios in Archean basalts: a window to evolving sources of mantle plumes?[J]. Lithos, 2005, 79: 491−504.

[168] Zhao J X, McCulloch M T, Korsch R J. Characterisation of a plume− related approximately 800 Ma magmatic event and its implications for basin formation in central− southern Australia [J]. Earth Planet. Sci. Lett. , 1994, 121: 349−367.

[169] Wingate M T D, Campbell I H, Compston W, et al. Ion microprobe U−Pb ages for Neoproterozoic basaltic magmatism in south− central Australia and implications for the breakup of Rodinia [J]. Precambrian Res. , 1998, 87: 135−159.

[170] Radhakrishna T, Mathew J. Late Precambrian (850− 800 Ma) palaeo− magnetic pole for the south Indian shield from the Harohalli alkaline dykes: geotectonic implications for Gondwana reconstructions [J]. Precambrian Res. , 1996, 80: 77−87.

[171] Frimmel H E, Zartman R, Späth E. The Richtersveld igneous complex, South Africa: U−Pb zircon and geochemical evidence for the beginning of Neoproterozoic continental breakup [J]. J. Geol. , 2001, 109: 493−508.

[172] Stein M, Goldstein S L. From plume head to continental lithosphere in the Arabiane Nubian shield [J]. Nature, 1996, 382: 773−778.

[173] Teklay M, Kröner A. Mezger, K. Enrichment from plume interaction in the generation of Neoproterozoic arc rocks in northern Eritrea: implications for crustal accretion in the southern Arabiane−Nubian Shield [J]. Chem. Geol. , 2002, 184: 167−184.

[174] Su Q, Golberg S A, Fullagar P D. Precise U−Pb zircon ages of Neoproterozoic plutons in the southern Appalachian Blue Ridge and their implications for the initial rifting of Laurentia [J]. Precambrian Res. , 1994, 68: 81−95.

[175] Aleinikoff J N, Zartman R E, Walter M. et al. U− Pb ages of metarhyolites of the Catoctin and Mount Rogers formations Central and Southern Appalachians: evidence for two pulses of Lapetan rifting [J]. Am. J. Sci. , 1995, 295: 428−454.

[176] Fetter A H, Goldberg S A. Age and geochemical characteristics of bimodal magmatism in the Neoproterozoic Grandfather Mountain Rift Basin [J]. J. Geol. , 1995, 103: 313−326.

[177] Li Z X, Bogdanova S V, Collins A S, et al. Assembly, configuration, and breakup history of Rodinia: a synthesis [J]. Precambrian Res. , 2008, 168: 179−210.

[178] Li Z X, Zhang L, Powell C M. Positions of the East Asian cratons in the Neoproterozoic supercontinent Rodinia [J]. Australian J. Earth Sci. , 1996, 43: 593−604.

[179] Evins L Z, Jourdan F, Phillips D. The Cambrian Kalkarindji

Large Igneous Province: extend and characteristics based on new $^{40}Ar/^{39}Ar$ and geochemical data [J]. Lithos, 2009, 110: 294−304.

[180] 冯益民, 何世平. 北祁连蛇绿岩的地质地球化学研究 [J]. 岩石学报, 1995, 11 (增刊): 125−146.
Feng Yimin, He Shiping. Research for geology and geochemistry of several ophiolites in the North Qilian Mountains, China [J]. Acta Petrol. Sin. , 1995, 11(Supp.): 125−146 (in Chinese with English abstract).

[181] Hou Q Y, Zhao Z D, Zhang H F, et al. Indian Ocean−MORB−type isotopic signature of Yushigou Ophiolite in north Qilian Mountains and its implications [J]. Sci. China. (Ser. D), 2006, 49 (6): 561−572.

[182] 张聪, 张立飞, 张贵宾, 等. 柴北缘锡铁山一带榴辉岩的岩石学特征及其退变PT轨迹 [J]. 岩石学报, 2009, 25: 2247−2259.
Zhang Cong, Zhang Lifei, Zhang Guibin, et al. Petrology and calculation of retrograde PT path of eclogites from Xitieshan, North Qaidam, China [J]. Acta Petrol. Sin. , 2009, 25: 2247−2259 (in Chinese with English abstract).

[183] Meschede M. A method of discriminating between different type of mid− ocean ridge basalt and continental tholeiites with the Nb−Zr−Y diagram [J]. Chem. Geol. , 1986, 56: 207−218.

[184] Pearce J A. and Cann J R. Tectonic setting of basic volcanic rocks determined using trace element analyses [J]. Earth Planet. Sci. Lett. , 1973, 19, 290−300.

[185] Zindler A, Hart S R. Chemical geodynamics [J]. Annu. Rev. Earth Planet. Sci. , 1986, 14: 493−571.

[186] Yogodzinski G M, Naumann T R, Smith E I, et al. Crustal assimilation by alkalic basalt, and the evolution of a mafic volcanic field in the central Great Basin, south− central Nevada [J]. J. Geophys. Res. , 1996, 101: 17425−17445.

[187] Gehrels G, Kapp P, DeCelles P, et al. Detrital zircon geochronology of pre−Tertiary strata in the Tibetan−Himalayan orogen [J]. Tectonics, 2011, 30: TC5016−TC.

[188] Sengör A M C. The cimmeride orogenic system and the tectonics of Eurasia [J]. Geol. Soc. Am. Special paper, 1984, 195; 82 pp.

[189] Metcalfe I. Gondwanaland dispersion, Asian accretion and evolution of Eastern Tethys [J]. Australian J. Earth Sci. , 1996, 43 (6): 605−623.

[190] Peccerillo A. and Taylor S R. Geochemistry of Eocene calc alkaline volcanic rocks from Kastamonu area, North Turkey [J]. Contrib. Miner. Petrol. , 1976, 58: 63−81.

[191] 张旗, 孙晓猛, 周德进, 等. 北祁连蛇绿岩的特征、形成环境及其构造意义 [J]. 地球科学进展, 1997, 12: 366−393.
Zhang Qi, Sun Xiaomeng, Zhou Dejin, et al. The characteristics of North Qilian ophiolites, forming settings and their tectonic significance [J]. Advance in Earth Sci. , 1997, 12: 366−393 (in Chinese with English abstract).

[192] Zhang Q, Chen Y, Zhou D J, et al. Geochemical characteristics and genesis of Dacha−Daban ophiolite in North Qilian area [J]. Sci. China (Ser. D), 1998, 41: 277−281.

[193] Cabanis P B, et Thiéblemont D. La discrimination des tholéiites continentals et des basalts arrière−arc. Proposition d'un nouveau diagramme, le triangle Th−3Tb−2Ta [J]. Bull. Soc. Géol. Fr. , 1988, IV(6): 927−935.

[194] Holm P E. The geochemical fingerprints of different tectonomagmatic environments using hygromagmatophile element abundances of tholeiitic basalts and basaltic andesites [J]. Chem. Geol. , 1985, 51: 303−323.

[195] 张旗, 王岳明, 钱青, 等. 甘肃景泰县老虎山地区蛇绿岩及其上覆岩系中枕状熔岩的地球化学特征 [J]. 岩石学报, 1997, 13 (1): 92−99.
Zhang Qi, Wang Yuemin, Qian Qin, et al. Geochemical characteritics of pillow lavas in ophiolite and its overlying rock sequence in the Laohushan area from Jingtai county, Gansu province [J]. Acta Petrol. Sin. , 1997, 13 (1): 92−99 (in Chinese with English abstract).

[196] 周德进, 陈雨, 张旗, 等. 北祁连山南侧阿拉斯加型岩体的发现及地质意义 [J]. 地质科学, 1997, 32: 122−127.
Zhou Dejin, Chen Yu, Zhang Qi, et al. The finding of Alaska−type mafic− ultramafic complex from Qilian County and constraints on Qilian Mountain tectonic evolusion [J]. Sci. Geol. Sin. , 1997, 32: 122−127 (in Chinese with English abstract).

[197] Gehrels G E, Yin A. Magmatic history of the northeastern Tibetan Plateau [J]. J. Geophys. Res. , 2003, 108 (B9): 2423.

[198] Yin A, Manning C E, Lovera O, et al. Early Paleozoic tectonic and thermomechanical evolution of ultrahigh− pressure (UHP) metamorphic rocks in the Northern Tibetan Plateau, Northwest China [J]. Int. Geol. Rev. , 2007, 49: 681−716.

[199] Xiao W J, Windley B F, Yong Y, et al. Early Paleozoic to Devonian multiple−accretionary model for the Qilian Shan, NW China [J]. J. Asian Earth Sci. , 2009, 35: 323−333.

[200] 左国朝, 刘寄陈. 北祁连山早古生代大地构造演化 [J]. 地质科学, 1987, 63: 14−24.
Zuo Guochao, Liu Jichen. 1987. The evolution of tectonics of Early Paleozoic in North Qilian Range. China [J]. Sci. Geol. Sin. , 1987, 63: 14−24 (in Chinese with English abstract).

[201] Boynton W V. Cosmochemistry of the Rare Earth Elements: Meteorite Studies [C]//Henderson P (ed.). Rare Earth Element Geochemistry, 1984: 63−114.

[202] Crawford A J, Beccaluva L, Serri G. Tectono− magmatic evolution of the west Philippine−Mariana region and the origin of boninites [J]. Earth Planet. Sci. Lett. , 1981, 54: 346−356.

[203] Wu H Q, Feng Y M, Song S G. Metamorphism and deformation of blueschist belts and their tectonic implications, North Qilian Mountains, China [J]. J. Metamor. Geol. , 1993, 11: 523−36.

[204] 宋述光. 北祁连山俯冲杂岩带的构造演化 [J]. 地球科学进展, 1997, 12: 351−365.
Song Shuguang. Tectonic evolution of subductive complex belts

in the North Qilian Mountains [J]. Advance in Earth Siences, 1997, 12: 351−365 (in Chinese with English abstract).

[205] 赖绍聪, 邓晋福, 赵海玲. 柴达木北缘奥陶纪火山作用与构造机制 [J]. 西安地质学院学报, 1996, 18: 9−14.
Lai Shaocong, Deng Jinfu, Zhao Hailing. Volcanism and tectonic setting during Ordovician period on north margin of Qaidam [J]. J. Xi'an College Geol. , 1996, 18: 9− 14 (in Chinese with English abstract).

[206] 邱家骧, 曾广策, 王思源, 等. 拉脊山早古生代海相火山岩与成矿[M]. 武汉: 中国地质大学出版社, 1996.
Qiu Jiaxiang, Zeng Guangce, Wang Siyuan, et al. Early Paleozoic marine volcanic rocks and mineralization in Laji Mountains [M]. Wuhan: China University of Geosciences Press, 1996 (in Chinese with English abstract).

[207] Weaver B L, Tarney J. Empirical approach to estimating the composition of the continental crust [J]. Nature, 1984, 310: 575−577.

[208] Wedepohl K H. The composition of the continental crust [J]. Geochim. Cosmochim. Acta, 1995, 59: 1217−1232.

[209] Campbell I H. Identification of ancient mantle plumes [A]. In: Ernst, R. E. , Buchan, K. L. (Eds.), Mantle Plumes: Their Identification Through Times [D]. Geol. Soc. Am. Spec. Pap. , 2001, 352: 5−21.

[210] Ernst R E, Buchan K L, Campbell I H. Frontiers in large igneous province research [J]. Lithos, 2005, 79: 271−297.

[211] Condie K C. Mantle Plumes and Their Record in Earth History [M]. Oxford. UK: Cambridge University Press, 2001.

[212] Kieffer B, Arndt N, Lapierre H, et al. Flood and shield basalts from Ethiopia: magmas from the African superswell [J]. J. Petrol. , 2004, 45: 793−834.

[213] Saunders A D, Storey M, Kent R W, et al. Consequences of plume− lithosphere interactions [C]//Storey B C, Alabaster T, Pankhurst R J(eds.). Magmatism and the Causes of Continental Breakup. Geological Society of London Special Publication, London, 1992, 68: 41−60.

[214] 任纪舜, 姜春发, 张振坤. 中国大地构造及其演化 [M]. 北京: 科学出版社, 1980.
Ren Jishun, Jiang Chunfa, Zhang Zhenkun. Geotectonics and Evolution of China [M]. Beijing: Science Press, 1980 (in Chinese).

[215] Meert J G. A synopsis of events related to the assembly of eastern Gondwana [J]. Tectonophysics, 2003, 362: 1−40.

[216] Torsvik T H. The Rodinia jigsaw puzzle [J]. Science, 2003, 300: 1379−1381.

[217] Wilson M. Igneous Petrogenesis [M]. London: Unwin Hyman, 1989.

[218] 张照伟, 李文渊, 王亚磊, 等. 南祁连化隆地区镁铁−超镁铁质侵入岩地质、地球化学特征与铜镍成矿 [J]. 地质学报, 2015, 89: 632−644.
Zhang Zhaowei, Li Wenyuan, Wang Yalei, et al. Geological and geochemical characteristics of mafic−ultramafic intrusions in the Hualong area, southern Qilian Mountains and its Ni− Cu mineralization [J]. Acta. Geol. Sin. , 2015, 89: 632− 644 (in Chinese with English abstract).

[219] 青海省地质矿产局. 青海省区域地质志. 中华人民共和国地质矿产部地质专报 [M]. 北京: 地质出版社, 1991.
QBGMR (Qinghai Bureau of Geology and Mineral Resources). Regional Geology of Qinghai Province. Geological Memoirs of Ministry of Geology and Mineral Resources of People's Republic of China [M]. Beijing: Geological Publishing House, 1991 (in Chinese).

[220] Wortel M J R, Spakman W. Subduction and slab detachment in the Mediterranean− Carpathian region [J]. Science, 2000, 290: 1910−1917.

[221] Doglioni C, Carminati E, Cuffaro M, et al. Subduction kinematics and dynamic constraints [J]. Earth Sci. Rev. , 2007, 83: 125−175.

[222] 许志琴, 张建新, 许惠芬, 等. 中国主要大陆山链韧性剪切带及动力学 [M]. 北京: 地质出版社, 1997.
Xu Zhiqin, Zhang Jianxin, Xu Huifen, et al. Ductile Shear Zones in the Main Continental Mountain Chains of China and Their Dynamics [M]. Beijing: Geological Publishing House, 1997 (in Chinese with English abstract).